UNIVERSITY OF CALGARY

Designing Novel Peptidic Inhibitors of Beta Amyloid Oligomerization

by

Samir Roy

A THESIS

SUBMITTED TO THE FACULTY OF GRADUATE STUDIES

IN PARTIAL FULFILLMENT OF THE REQUIREMENTS FOR THE

DEGREE OF DOCTOR OF PHILOSOPHY

DEPARTMENT OF CHEMISTRY

CALGARY, ALBERTA

Jan, 2010

UNIVERSITY OF
CALGARY

ABSTRACT

Alzheimers Disease (AD) is the most commonly diagnosed cause of progressive dementia in the 65 and over age group. No currently approved, or experimental, drug has been shown to have a disease modifying effect in human AD. Hypotheses on the etiology of AD have revolved around the excessive production of β amyloid, resulting in amyloid plaques, or *tau*, resulting in neurofibrillary tangles. Recent experiments with transgenic animal models of AD suggest that soluble oligomers of β amyloid initiate a series of events, including increase in soluble tau, that result in neuronal dysfunction and death. However the major known risk factors for late onset AD in humans are associated with vascular dysfunction. A new hypothesis, known as ABSENT, factors the combined effects of β amyloid on neurons and the vascular system. The hypothesis, as outlined in Chapter 2, creates a biologically unified and chemically feasible framework for integrating our current understanding of the various facets of AD. The use of computer assisted drug design can speed up the process of drug discovery, however the flexible nature of β amyloid and peptidic ligands that block its oligomerization necessitate development of new techniques (and protocols) to handle such atypical receptor-ligand systems. Chapter 3 describes the creation of a β amyloid receptor model, as well as techniques and protocols to dock peptidic ligands. The results demonstrate that it is possible to model experimentally derived structure activity relationships, and is the basis for the design of novel classes of ligands as described in Chapter 4. Four classes, based on the chirality of residues and predicted mode of binding are also explored in that chapter. Initial synthesis and basic experimental characterization of a few novel ligands are described in Chapter 5. The results of Thioflavin T and Western Blot assays show that the new ligands are superior to existing ligands at blocking β amyloid fibrillization and oligomerization. Circular Dichroism is also used to demonstrate binding of the ligands to β amyloid. Chapter 6 describes future experiments for more thorough characterization of novel designed ligands.

ACKNOWLEDGEMENTS

I would like to acknowledge the support of Dr. Arvi Rauk (my supervisor), and past/ present members of our research group.

Dr. Dave Schriemer is acknowledged for letting me to use his lab facilities for performing the Thioflavin T assay. I would also like to acknowledge Dr. Hans Vogel for allowing me to use his lab facilities to perform Circular Dichroism measurements. Past and present members of both research groups are also acknowledged for their assistance.

My extensive discussions with Dr. Graham Moore, were helpful in making decisions on peptidic ligand design. Dr. Miklos Feher involvement in development of the ‘analysis_dock.svl’ script is also acknowledged.

The research project was funded through grants by NSERC and Alzheimer Society of Canada.

TABLE OF CONTENTS

LIST OF TABLES

LIST OF FIGURES

LIST OF ABBREVIATIONS

ABSENT	Amyloid Beta Synergistic Endothelial & Neuronal Toxicity
AD	Alzheimers Disease
ADME	Absorption Distribution Metabolism Excretion
AGE	Advanced Glycation Endproduct
AFM	Atomic Force Microscopy
ApoE4	Apolipoprotein E4
APP	Amyloid Precursor Protein
BBB	Blood Brain Barrier
CADD	Computer Assisted Drug Design
CBF	Cerebral Blood Flow
CCAP	Cerebral Capillary Amyloid Angiopathy
CD	Circular Dichroism
CG	Conjugate Gradient
CVA	Cerebro-Vascular Event (“stroke”)
DDD	Distance Dependent Dielectric
DMD	Disease Modifying Drugs
EM	Electron Microscopy
E_bind	Binding Energy (Approximate)
FTD	Fronto-Temporal Dementia
FTIR	Fourier Transform Infrared
GB/SA	Generalized Born/ Surface Area
GPCR	G-Protein Coupled Receptor
HB	Hydrogen Bond (Salt Bridge)
HMW	High Molecular Weight
I5mer	Ac-K-(me)L-V-(me)F-F-NH_2
LBD	Lewy Body dementia
LMW	Low Molecular Weight
MALDI-TOF	Matrix Assisted Laser Desorption/ Ionization – Time of Flight
MCI	Mild Cognitive Impairment
MOE	Molecular Operating Environment

m-SG1	Myristoyl-dab-O-(me)L-F-(me)F-L-P-bA-COOH
NFT	Neuro-Fibrillar Tangles
NMDA	N-Methyl D-Aspartate
NMR	Nuclear Magnetic Resonance
PD	Parkinson’s Disease
PSEN	Presenilin
RB	Receptor Buriedness
RNA	Ribonucleic Acid
SAR	Structure Activity Relationship
SD	Steepest Descent
SDS	Sodium Dodecyl Sulfate
SG1	Ac-dab-O-(me)L-F-(me)F-L-P-bA-COOH
SG2	Ac-dab-O-(me)L-V-(me)F-F-A-E-NH_2
SOD	Superoxide Dismutase
STEM	Scanning Tunnel Electron Microscopy
SVL	Scientific Vector Language
TIA	Transient Ischemic Attack (“mini-stroke”)
TN	Truncated Newton
VaD	Vascular Dementia

CHAPTER I: GENERAL INTRODUCTION

1.1 Introduction

Alzheimer's disease (AD) is the most common diagnosed cause of progressive dementia in people age 65 and older. The number of people diagnosed with AD will increase over the next 15–20 years, primarily due to the rapid growth in that demographic group. Patients with AD can currently expect to survive 5 –10 years after diagnosis.[1, 2]

The increasing incidence of AD today, and in the near future, is a consequence of two synergistic demographic factors. A majority of people born in developed countries since the 1930's will reach the age of 65 years. The average remaining life expectancy after 65 years, currently over 19 years, has also increased since the 1940's.[3, 4] Therefore a historically unprecedented number (and percentage) of the population will soon be in an age group with the highest susceptibility to late-onset* idiopathic† AD, which accounts for over 90% of new AD cases.

The current annual cost of caring for AD patients in the US is estimated to be well over 100 billion dollars per year.[5] AD also causes a substantial increase in age-related mortality. Women are more likely to develop AD, primarily because of their longer average life span. A secondary factor for this gender discrepancy might be that higher testosterone levels in men decrease the incidence and progression of AD.[6, 7, 8] There are currently no approved drugs to halt or reverse the course of this progressive illness. Currently approved drug therapy for AD is mainly symptomatic and, at best, results in a 6-18 month delay in the progression of disease symptoms.[9, 10, 11] Atypical anti-psychotics, benzodiazepines and similar drugs are often used to make AD patients more manageable, though this practice has become controversial of late.[12]

---

* > 65 years old
† No known cause or strong predisposition

The rest of this chapter provides background information on various facets of AD relevant to the subject matter of this thesis, starting with history of AD and current theories about its etiology. The basic introduction is followed by a discussion on the current state of knowledge about structures of β amyloid oligomers and fibrils. A discussion on known peptidic inhibitors of β amyloid oligomerization along with a brief review of currently approved, and experimental drug therapy for AD will conclude this chapter.

1.2 Senile dementia through human history

The extensive deterioration of mental faculties such as memory, cognition and self-awareness in some elderly people has been common knowledge throughout history. Ancient Indian, Chinese, Greek and Egyptian medical texts do describe disease conditions that would today be diagnosed as AD.[13] Presumptive diagnosis of AD based on historical accounts is however complicated by lack of modern medical tests (especially postmortem histology) and insufficient evidence to rule out other causes of dementia. Widespread use of lead, mercury and arsenic compounds in pre-20th century medicine is another reason to question any definitive diagnosis of AD based, purely, on historical accounts.

One of the best descriptions of AD in pre-modern literature is found in the character of King Lear in William Shakespeare's play of the same name. At the beginning of this play, the aging King Lear divides his kingdom in a manner that seems to defy logic, which might today be seen as the mild cognitive impairment (MCI). As the play unfolds, Lear's decision-making skills start to deteriorate and he experiences flares of strong emotion, which is another sign of early stage AD. Towards the end of the play, which describes events a couple of years after those described in the beginning, Lear is lost and found wandering by his daughter's troops. The following paragraph in the play is particularly descriptive.

“Now, by my life, old fools are babes again,
Pray, do not mock me, I am a very foolish fond old man;
Fourscore and upward, not an hour more nor less,
And, to deal plainly, I fear I am not in my perfect mind.
Me thinks I should know you, and know this man,
Yet I am doubtful for I am mainly ignorant.
What place this is; and all the skill I have remembers not these garments;
Nor I know not where I did lodge last night.
Do not laugh at me for, as I am a man,
I think this lady to be my child Cordelia."

(William Shakespeare (1605) King Lear, Act IV, Scene 7)[14]

If the above paragraph (translated into contemporary English) were a patient’s description of his symptoms to a doctor, a diagnosis of early stage idiopathic AD would be the preliminary and most likely final diagnosis. Such a diagnosis would be further bolstered by considerations such as his age (>80 years), lack of other serious neurological conditions and the *sequence* and *speed* of progressive deterioration of mental faculties. It therefore appears that people from previous ages were aware of the sequence of progressive deterioration in mental faculties that we today ascribe to AD. However lacking modern diagnostic concepts and tools, they did not see it as a disease, but rather as a somewhat inevitable part of getting old. Today we know that AD, or any other form of senile dementia, is a disease and not a ‘natural outcome’ of getting old any more than dying of a stroke or myocardial infarction. Indeed, people who reach extreme old age are usually quite healthy and often have little evidence of such disease processes. [15]

Throughout most of post-enlightenment medicine, senile dementia was believed to be caused by cerebrovascular problems, mainly due to the numerous vascular abnormalities seen in autopsies of patients with senile dementia. Any observable changes in brain tissue, such as atrophy or necrosis, were attributed to poor

perfusion or infarction of brain tissue. Histological methods to identify inclusion bodies, plaques and neurofibrillary tangles were not developed until the last 2 decades of the 19th century. Discoveries by scientists such as Pick, Alzheimer and Lewy, in the late 19th and early 20th century started a process of reevaluation of theories about senile dementia.[16, 17, 18]

It soon became obvious that histopathological changes seen in patient with *presenile* dementias, could also be found in many patients with senile dementia. The old vascular hypothesis of senile dementia was gradually supplanted by a belief that each subclass of senile dementia was caused by one particular (and identifiable) neurodegenerative process. The current histopathological classification of senile dementias is based on studies of *presenile* dementias with a significant genetic component. Most patients with late onset AD, Parkinson's disease (PD), Lewy body dementia (LBD), Fronto-Temporal dementia (FTD) do not have a strong genetic predisposition to these conditions.

1.3 Alois Alzheimer's discovery

A quick discussion of events surrounding the first clear diagnostic and histological description of AD might seem out of place in a thesis primarily concerned with modeling the Structure Activity Relationship (SAR) of known β amyloid aggregation inhibitors. However these events, which are not widely known, have an important implication for the original definition of AD as opposed to its widely understood current definition. The changing criteria for diagnosing AD have consequences on our current understanding of mature-onset idiopathic AD, and are discussed at some length in Chapter 2. An understanding of the etiology of late-onset idiopathic AD, which accounts for over 90% of AD diagnoses, is vital to designing Disease Modifying Drugs (DMDs) for AD.

The first of the two patients, whose case history would give rise to the publications that ultimately defined AD, was a woman known as 'Auguste D' (see Figure 1.1).

Her real name was Auguste Deter and she is best known from one unflattering sepia toned photo of her face, after hospitalization in 1901. She was hospitalized in the Municipal Mental Asylum in Frankfurt at the age of 51 by her family, after a couple of years of progressive mental deterioration. Alois Alzheimer (see Figure 1.1) was the doctor assigned to make a detailed clinical evaluation of her case. The course of her mental deterioration was progressive and mirrored that seen in early-onset AD today. She died of an infection caused by her prolonged bed ridden status in 1906. Histological staining of brain sections by the Bielchowsky method revealed abundant extracellular amyloid plaque, thickened neurofibrils and neurofibrillar tangles (NFTs) (see Figure 1.1). Alzheimer also realized that these abnormal neurofibrils could be stained with dyes that did not stain neurofibrils in normal brains. Neither the entorhinal cortex nor the hippocampus of Auguste D (and Johann F), which are the regions of the brain first affected by AD, were examined microscopically. Initially Alzheimer only reported these findings as a case of presenile dementia with unusual clinical and histopathological features.[22]

'Johann F' was the other patient whose case file and autopsy results formed the basis of the original diagnostic definition of AD. He started developing symptoms of progressive dementia in his mid 50s, and was admitted to the same hospital, as 'Auguste D', in 1903. It is interesting to note that Johann F's AD was of the uncommon 'amyloid plaque only' type, and NFTs were almost absent in brain sections. Subsequent reexamination of the original sections has confirmed the lack of NFTs noted in the publication. [19] A study of the kin and descendants of 'Johann F' have also shown a high incidence of early onset dementia and some of his descendants have mutations known to predispose to early onset AD. [20] In late1903 Alzheimer moved to the Anatomical Laboratory of the Royal Psychiatric Clinic at Munich University, headed by Emil Kraepelin.

Emil Kraepelin (see Figure 1.1) was already well known for his innovative work in the field of classifying mental disorders. It was from the brain sections of 'Auguste D' and 'Johann F' that Emil Kraepelin later created the concept of a disease

condition characterized by progressive *presenile* dementia with amyloid plaques and neurofibrillary tangles (NFTs). Kraepelin started using the term ‘Alzheimer’s Disease’ in manuscripts of a textbook he was writing at that time, and later convinced a reluctant Alzheimer to name the disease condition “Alzheimersche Krankheit” (Alzheimer’s Disease) in his famous 1911 publication. [21]

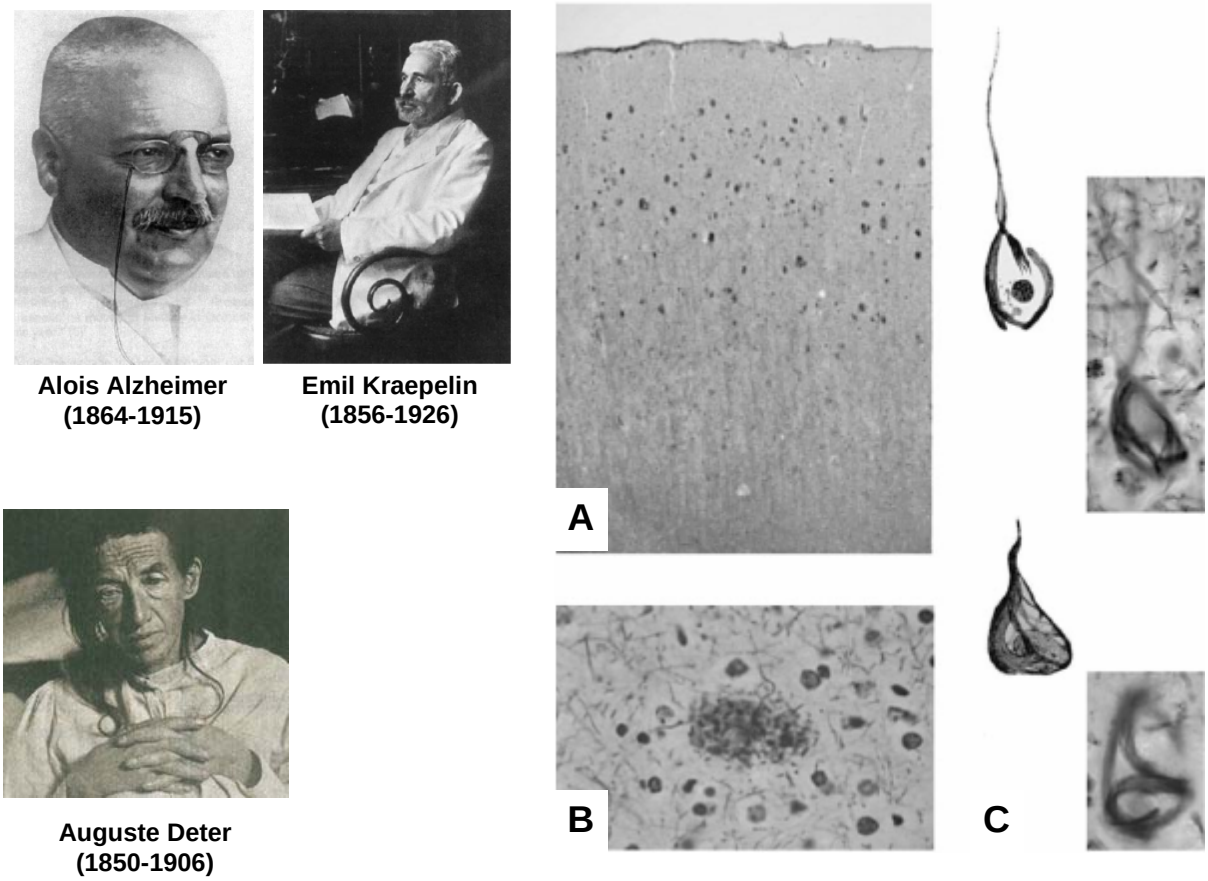

Figure 1.1 *A visual synopsis of the discovery of AD as a disease entity. Alois Alzheimer observed and described the characteristic changes in Auguste Deter’s brain, but Emil Kraepelin recognized it as an independent disease entity. Tissue sections from Auguste Deter’s original brain sections, rediscovered in the mid 1990s, show (A, B) amyloid plaques and (C) neurofibrillary tangles in the cerebral cortex.*[22] *Copyrighted parts reproduced with permission from Eur Arch Psychiatry Clin Neurosc, 249, 1999, Suppl 3: 10-3, Figure 1: With kind permission of Springer Science & Business Media.*

It should be noted that both amyloid plaques and NFTs had been previously observed by other researchers in brains of middle aged people with epilepsy, and the concept of senile dementia was already well understood. Moreover other researchers had also discovered amyloid plaques in middle-aged patients with progressive dementia. [23] However Emil Kraepelin had the insight to make the connection between a clinical presentation of presenile dementia and histopathological findings of amyloid plaques (and NFTs). AD was thus originally defined as *presenile* dementia with amyloid plaques, and NFTs. Less than 10% of currently diagnosed cases of AD would qualify as AD under its original definition. The changes that led to the current definitions of AD are one of better examples of 'definition creep' in the history of medicine[24], and are discussed at some length in Chapter 2.

1.4 Theories on the etiology of AD & transgenic animal models

The two main histopathological characteristics of AD, apart from extensive neuronal death, are the presence of amyloid plaques and neurofibrillary tangles (NFTs).[25] Amyloid plaques have peptidic and non-peptidic components; however they are unique in possessing large amounts of a group of amyloidogenic peptides, known as β amyloid. [26] These amyloidogenic peptides are between 39-43 (usually 40 or 42) amino acid residues long with an identical 1-39 sequence. The longer versions have a few extra hydrophobic residues at the C-terminal end. NFTs are the hyperphosphorylated and insoluble deposits of a microtubule associated protein known as *tau*.[27]

The most well known hypotheses on the etiology of AD are based on either β amyloid or *tau*. [28] These two camps have humorously called themselves 'Baptists' (β amyloid) [29] and 'Tauists' (*tau* protein) [30, 31] and offered their own version of AD etiology. Of late, there has been a growing realization that both camps were partially correct in that excessive soluble β amyloid oligomers do

seem to start the process triggering a series of events, including abnormal *tau* phosphorylation, ultimately resulting in widespread neuronal dysfunction and death. [32, 33] A significant body of evidence and interpretation, in favor of or against each hypothesis, already exists and reviewing them in detail is beyond the scope (and length) of this thesis. The remainder of this section will therefore concentrate on studies of mutations found in early onset familial AD in humans and transgenic animal models of AD based on them.

The vast majority of early onset familial AD cases, in humans, are related to mutations in four protein complexes.[34, 35] They are amyloid precursor protein (APP), Presenilin I (PSEN1) complex [γ secretase complex], Presenilin II complex (an isoform of PSEN 1) and Apolipoprotein E Type 4 ($ApoE_4$). Mutations in the first three proteins result in increased splicing of β amyloid from its precursor (APP mutations), increased amyloidogenicity of mutant β amyloid (APP mutations) or increased alternate splicing of APP to produce β amyloid (PSEN1 and PSEN2). $ApoE_4$ seems to be a better facilitator of β amyloid oligomerization than other isoforms of ApoE.[36]

A brief summary of relevant information on current animal models of AD based on early-onset familial AD, is shown in Table 1.1. The five major types of models can be divided into three main etiological categories, namely *β* amyloid only, *tau* only and mixed models (β amyloid and *tau*).

As seen in Table 1.1, only the more recent animal models come close to replicating the full sequence and range of pathology seen in human AD. Most β amyloid only (APP-, PSEN- and APP/PSEN- based) transgenic animal models of AD utilize known mutations, found in human APP or PSEN.[37, 38] The earliest semi-successful transgenic animal (mouse) model of AD was created by overexpression of mutant human APP. [39]

Table 1.1 *Summary of major transgenic animal models of AD. Each class of animal model is accompanied with a brief description of the pathological changes, behavioral alterations and comparison to human AD.*

Model	Relevance to AD		Role in AD research and drug discovery	Disadvantages
	Pathophysiological level	Behavioral level		
Transgenic models				
APP-based (e.g Tg2576)	▪Aβ pathology ▪Neurodegeneration ▪Neurotransmitter & synaptic dysfunction ▪Inflammation	•Cognitive decline •Behavioral alterations	▪Confirmed role of APP & Aβ ▪Target identification ▪Preclinical evaluation of drugs	▪No development of NFTs
PSEN-based	▪Increased $A\beta_{42}/A\beta_{40}$ ratio is some models.	▪Few cognitive or behavioral abnormalities	▪Basis for double tg APP/PSEN models	▪No development of NFTs ▪No Aβ pathology
Tau-based (e.g rTg4510).	▪NFT pathology ▪Neuronal Loss	▪Cognitive Decline ▪Behavioral alterations	▪Increased knowledge of Tau pathology ▪Basis for tg APP/tau models	▪No Aβ pathology
Double transgenic models (e.g PSAPP, APP/*tau*))	▪Accelerated Aβ pathology in APP/PSEN versus APP-only model ▪Accelerated Tau pathology in APP/Tau models ▪Neuronal loss and Inflammation	▪Cognitive decline ▪Behavioral alterations	▪APP/PSEN models support modifying role of PSEN ▪APP/Tau models support hypothesis with Aβ pathology mediating Tau pathology ▪Preclinical evaluation of drugs	▪No NFT pathology in APP/PSEN models ▪Aβ pathology progression is different from human AD.
Triple transgenic Models (e.g 3xTgAD)	▪Aβ pathology ▪NFT formation ▪Neurodegeneration, neuronal loss and Inflammation	▪Cognitive decline ▪Behavioral alterations	▪Supports amyloid cascade hypothesis ▪AD relevant spatial and temporal symptoms ▪Preclinical evaluation of drugs	▪Modeling higher cognitive functions in rodents. ▪No resemblance to late onset idiopathic human AD

One of the most popular transgenic mouse models for testing new AD therapies, Tg2576, is based on the K670M/N671L double APP mutation.[40] It seems to recapitulate many of the symptoms and changes seen in human Mild Cognitive Impairment (MCI) and early stages of AD. However Tg2576 and other APP- only models fail to recreate the extensive neuronal loss or NFTs seen in later stages of human AD. [41] Mutant PSEN-only animal models have elevated CSF levels of β amyloid peptides, but do not exhibit memory impairment, amyloid plaque formation or other AD related pathology. [42] Transgenic animals overexpressing *normal*

human APP do not suffer from substantial memory impairment, amyloid plaques or measurable neuron loss.[43]

Combining PSEN mutations with APP mutations in one animal has a synergistic effect on the disease process and is the basis of the popular PSAPP transgenic mouse model. [44, 45] These double transgenic, β amyloid only, animal models exhibit accelerated disease pathology and more neuronal loss than seen in single transgenic, APP- only, models. However, they still do not exhibit NFT pathology or extensive neuron loss.

The observation that mutations in *tau* are not associated with familial (or idiopathic) AD in humans is the major reason behind loss of support for a '*tau* only' hypothesis of AD. Moreover, a wide range of neuropathology (including motor/ sensory dysfunction) is seen in transgenic mice expressing various *tau* mutations. [46] The t*au* model with the most similarity to human AD is rTg4510(P301L). [47] Familial forms of FrontoTemporal Dementia (FTD) have been shown to be associated with *tau* overexpression and mutations. [48, 49]

The possibility of synergy between *tau* and β amyloid has been investigated and shown considerable promise. The initial experiments involved injection of β amyloid in transgenic *tau* animal models and resulted in amplification of NFT formation and increased neuron loss.[50] The first animal model to implement a transgenic APP/ *tau* combination did demonstrate a synergistic effect on neuronal dysfunction and loss.[51, 52] A subsequent APP/ *tau* model with a different *tau* mutation proved to be very successful and is considered to be the first transgenic animal model to reproduce core features of early onset human AD. Another unexpected feature of this model was that onset of pathology was earlier and more aggressive in female mice, mirroring known human AD epidemiology.[53]

The latest transgenic AD animal models combine APP, PSEN and *tau* mutations into one animal. [54] The triple transgenic (3xTgAD) mouse model reproduces the

sequence of events seen in early onset familial AD better than any other APP/ *tau* model. In 3xTgAD mice, the initial increase in β amyloid formation is manifested at around 6 months of age as an increase in soluble β amyloid, localized inflammation and some cognitive deficits, which are then followed by amyloid plaque formation. The first increase in soluble *tau* and NFTs occurs after a few more months, starting with the hippocampus and spreading into the cortex. An increase in soluble t*au* levels (and NFTs) is associated with a further increase in the rate and extent of cognitive decline. Female 3xTgAD mice have an earlier onset and more aggressive form of the disease, once again mirroring human epidemiology.

Recent studies in 3xTgAD animals with monoclonal antibodies, that block β amyloid oligomerization, have provided some interesting insights into AD pathology.[55] The use of monoclonal antibodies at an early stage in the 3xTgAD model, seems to decrease soluble β amyloid (and plaque) levels and stop the disease process. It also decreases or blocks subsequent increase in soluble *tau* levels and NFT burden. If the disease is allowed to progress untreated past a point, some changes such as NFTs become irreversible. However chronic administration of monoclonal antibodies to older and previously untreated animals causes a reduction in β amyloid (soluble and plaque) levels, soluble *tau* levels and seems to normalize cognitive function. It therefore seems likely that significant cognitive impairment and neuron loss are correlated to an increase in soluble β amyloid and (induced) soluble *tau* levels. NFTs, like β amyloid fibrils, might therefore be a marker of excess *tau* production and not the cause of neuronal death.

It should be noted that 3xTgAD animals are otherwise healthy and without co-morbidities such as old age, hypertension, vascular disease or Type II Diabetes Mellitus. They are therefore a good reproduction of the pathology seen in early onset familial AD, as opposed to late onset idiopathic AD. While 3xTgAD, and similar double and triple transgenic models, might be the best available models to test the efficacy of various disease modifying therapies, positive results in these

models may not translate into therapeutic activity for human AD. Indeed based on the positive results of some experimental drugs in animal models of AD, we should already have been able to successfully reverse human AD. The data from studies of mutations found in early onset human AD and animal models merely suggests that β amyloid is the best candidate for initiation of a sequence of events leading to full blown AD. The next three sections of this chapter review existent information about production and oligomerization of β amyloid into soluble oligomers and fibrils.

1.5 Amyloid precursor protein (APP) and it's processing

β amyloid, like most other endogenous peptides, is derived through enzymatic cleavage of a larger precursor protein. There are two major pathways for APP processing, namely the non-amyloidogenic pathway and the amyloidogenic pathway (see Figure1.2) The protein that gives rise to β amyloid peptides is known as Amyloid Precursor Protein (APP). APP is the best known member of a widely expressed family of Type I transmembrane glycoproteins. The most common isoforms of APP in the brain are APP_{695}, APP_{751} and APP_{770}. These isoforms are named based upon the number of amino acids residues in each isoform. [56] APP_{695} is the predominant form expressed on neurons. The hippocampus and cerebellum have the highest expression levels for all APP isoforms. The hippocampus is also the first major area of the brain affected by AD and damage to it results in the first symptoms of AD.

The precise biological functions of APP are still unclear, however its expression is increased during the formation of new synapses and neuronal repair.[57] Roles in cell signaling, long-term potentiation and cell adhesion have been proposed, based on animal studies.[58] APP knockout animals show deficits in grip strength, reduced locomotor activity, impaired learning and memory.[59] APP knockout mice are, however, viable and do not have any severe cognitive deficits or evidence of significant neuron loss. Acute down-regulation of APP gene activity by antisense

RNA probes suggests that APP is involved in the formation/ consolidation of memory, new neuronal synapses and neurogenesis in the brain.[60]

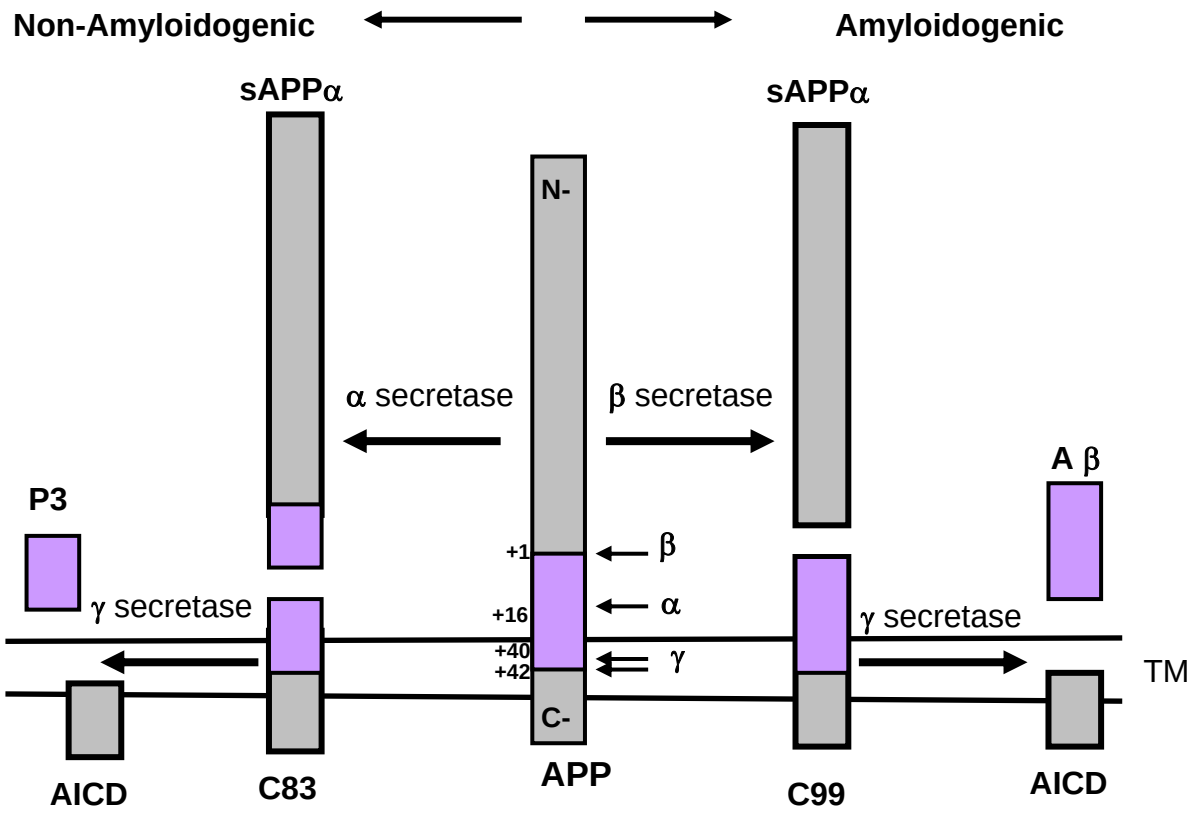

Figure 1.2 *Processing pathways for Amyloid Precursor Protein (APP). A schematic illustration of non-amyloidogenic (α secretase dominant) and amyloidogenic processing (β secretase dominant) of Amyloid Precursor Protein.*

A high quality structure of nascent β amyloid monomers, under physiological conditions, may never be obtained as nascent β amyloid monomers appear to lack a defined secondary structure and probably exist as an ensemble of structures. FTIR and CD studies of freshly prepared monomeric β amyloid suggest the lack of defined secondary structure. [61, 62] Incubation of monomers, under physiological conditions, initiates oligomer formation with a concurrent increase in β strand content.[63, 64] The formation of a salt bridge between two AA residues (D_{23} and

K_{28}) in β amyloid, to create a hairpin turn, appears to be the first definitive step in oligomerization. Covalently linking the two residues (D_{23} and K_{28}) has been shown to speed up oligomerization by over a thousand fold. [65] The formation of this salt bridge seems to facilitate subsequent backbone amide and sidechain interactions between residues on either side of the hairpin turn and probably leads to the formation of a hairpin-like monomer.

The next step involves recognition of one hairpin-like monomer by another to form species such as dimers, trimers, tetramers, higher oligomeric species and ultimately fibrils. There is experimental evidence that submicellar concentration of surfactants, such as SDS, hastens the formation of soluble oligomers.[66, 67, 68] One isoform of the plasma protein ApoE4 also increases oligomer formation, while the other two isoforms (ApoE2 and ApoE3) do not have that effect. [69] The next two sections of the chapter briefly review the current state of knowledge about the structure and toxicity of both soluble and insoluble oligomers of β amyloid.

1.6 Structure and toxicity of β amyloid oligomers

Currently available evidence seems to suggest that there are two classes of soluble β amyloid oligomers.[70] These two classes are Low Molecular Weight (LMW) oligomers such as dimers, trimers, tetramers and High Molecular Weight (HMW) oligomers (multiples of dimers, trimers and tetramers). High quality structures of these oligomers are not available because they seem to lack a stable structure, which is a requisite for using methods such as X-ray crystallography or NMR. The majority of our limited information about the structures of these oligomers comes from CD, FTIR, Electron Microscopy (EM) and Atomic Force Microscopy (AFM). CD and FTIR studies seems to suggest that these oligomers do possess a larger amount of β sheet content than nascent monomers but less than fully formed fibrils.[71, 72] Electron microscopy shows the presence of two types of non-fibrillar aggregates of β amyloid.[73, 74] The smaller soluble oligomers are very

small and indistinct ‘blobs’ that barely stand out from background noise while larger spheroidal oligomers have a somewhat defined structure and size range.

Recently, Atomic Force Microscopy (AFM) and Scanning Tunnel Electron Microscopy (STEM) have been used to image soluble LMW oligomers. [70, 71] Data from AFM imaging suggests that LMW oligomers (see Figure 1.3 A and B) do possess a structure and size range compatible with multiple loose hairpin-like monomers stacked next to each other. The HMW oligomers, in contrast to LMW oligomers, show a definite circular cross section (see Figure 1.3 C), corroborating previous EM imaging data. AFM studies seem to indicate that circular HMW oligomers are discoidal, as opposed to spheroidal. It also appears that HMW oligomer disks stack on top of each other, and could explain the numerous reports of non-specific ion channel like activity ascribed to soluble oligomeric preparations of β amyloid.[75]

There is some ambiguity about the precise nature and contribution of each type of soluble oligomer to the toxicity of β amyloid. [76, 77, 78] However it is likely that the final toxicity observed in neurons of animal models or human AD patients is a combination of the net toxicity, and secondary effects, of various oligomers. Moreover HMW oligomers have been shown to bind to the acetylcholine receptor and negatively affect its normal function.[79] Regardless of the precise combination of oligomeric species responsible for the greatest damage in any given experimental system, it appears that oligomerization of β amyloid is the crucial step for expression of its latent toxicity. Therefore inhibition of the process of oligomerization is the most direct approach to blocking β amyloid toxicity and its subsequent effects such as increase in soluble *tau*, localized inflammation, and ultimately cell death.

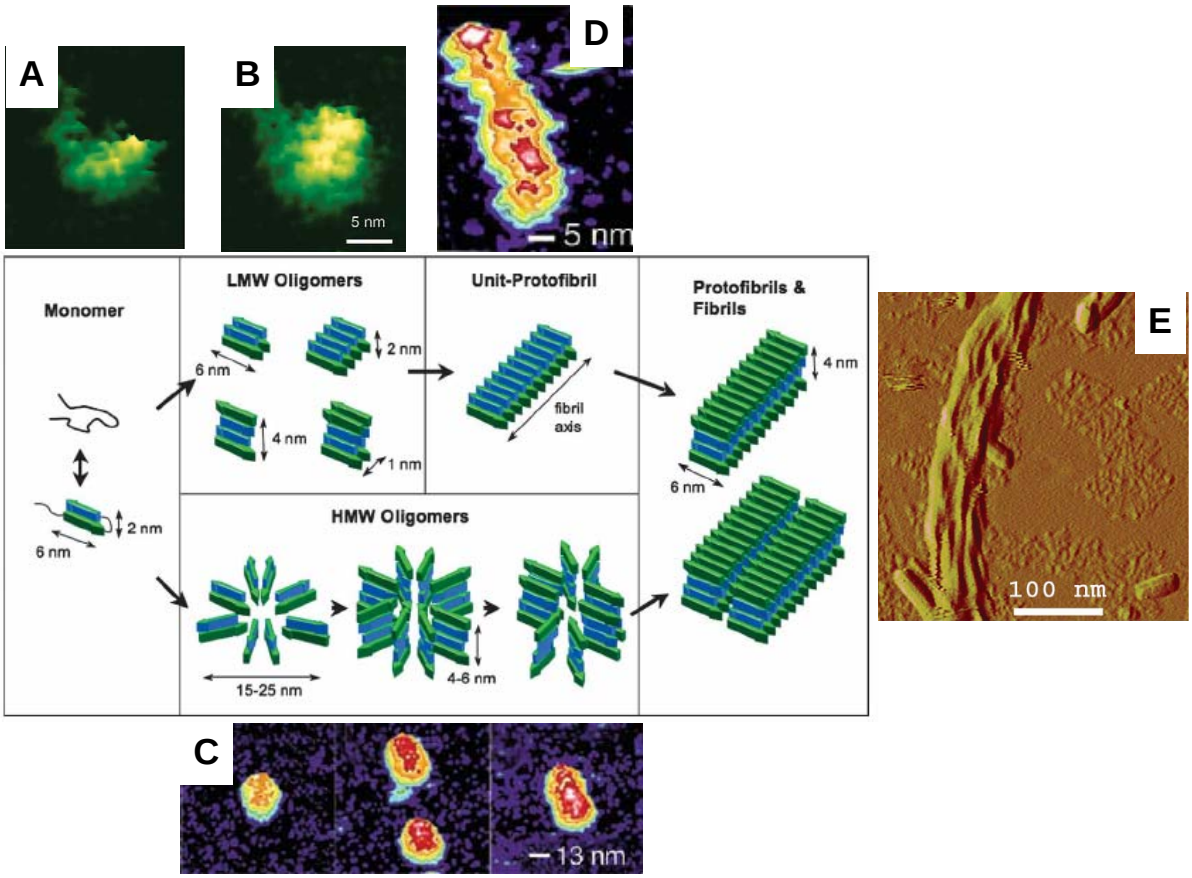

Figure 1.3 *A schematic illustration of the process of β amyloid oligomerization with representative AFM images of each major type of soluble and insoluble oligomers. A; monomer, B; tetramer, C; high molecular weight (HMW) soluble oligomer, D; protofibril, E; fibril. Reproduced from J Mol Biol. 2006, 358(1):106-19 with kind permission of Elsevier BV.*

Monomers and soluble oligomers of β amyloid are not the most stable form of β amyloid, and they are ultimately incorporated into β amyloid fibrils which are the major peptidic component of senile amyloid plaques. The next section of the chapter briefly reviews available data and proposed secondary, tertiary and quaternary structure of β amyloid fibrils.

1.7 Structure of β amyloid fibrils

Amyloid fibrils are the major component of amyloid plaques, and were for long considered to be the toxic form of β amyloid. We now know that they are, in fact, the non-toxic form of β amyloid.[80] A model of the secondary and tertiary structure of β amyloid fibrils is shown in Figure 1.4.

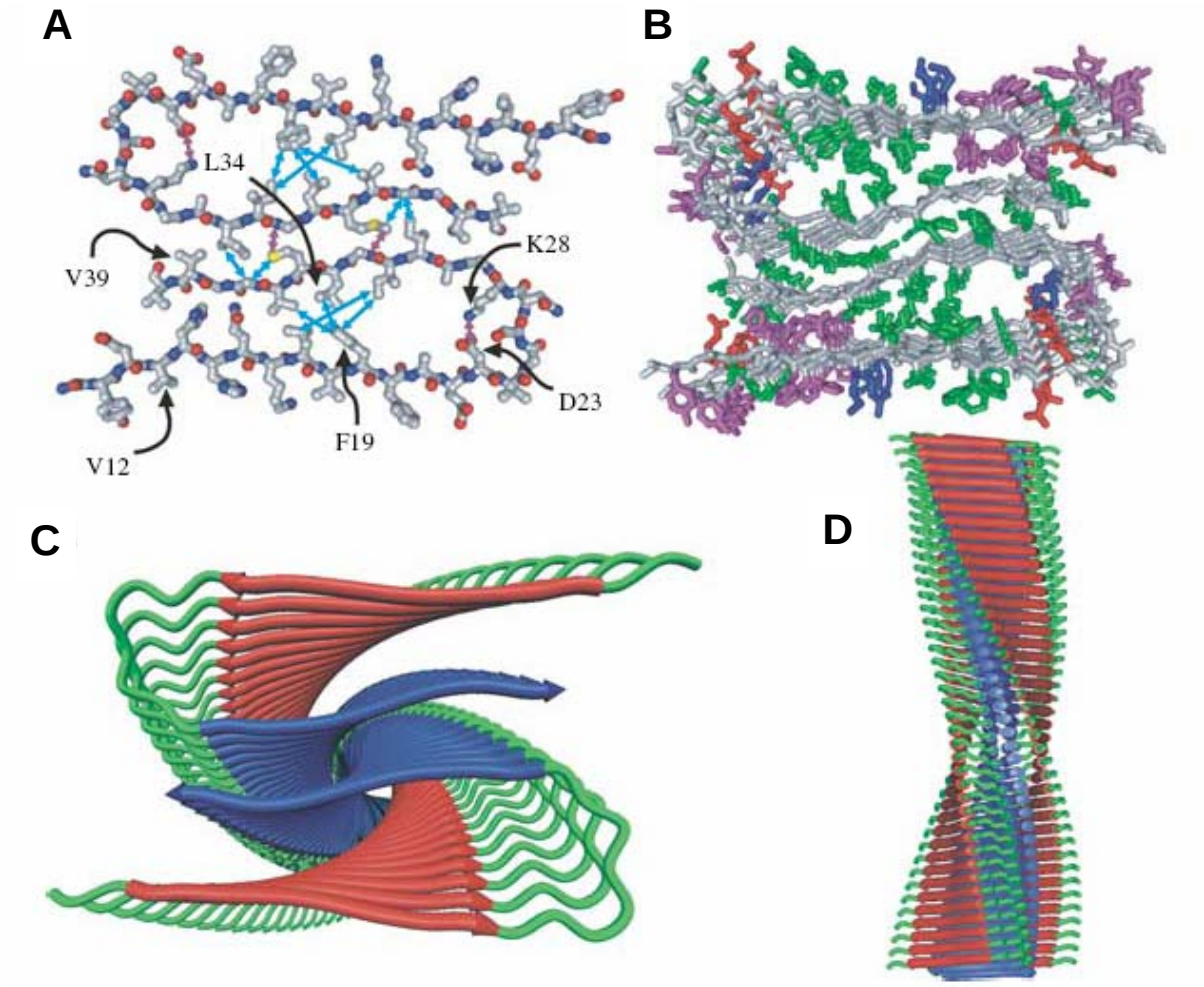

Figure 1.4 *Structural models for the protofilament in Aβ1–40 fibrils based on NMR data. Residues 1–8 are conformationally disordered and are therefore omitted. The long axis of the fibril is perpendicular to the page in panels* ***A*** *–* ***C****. The*

*long axis is vertical and parallel to the page in panel **D** . Reproduced from Q Rev Biophys. 2006, 39(1):1-55 with kind permission of Cambridge Journals.*

Freshly purified fibrils do not have any worthwhile cytotoxic effect within the first 48 hours; however prolonged incubation of purified fibril preparations does result in the release of a measurable amount of toxic soluble oligomers, which can be detected by cytotoxicity assays.[81] In contrast to the lack of detailed structural information about soluble oligomeric forms of β amyloid, a significant amount of structural information on the secondary & tertiary structure of β amyloid fibrils is available through solid state NMR studies done by Robert Tycko's group. [82] The proposed structures have been indirectly verified by data from other techniques such as hydrogen-deuterium exchange and proline mutagenesis.[83, 84 , 85, 86]

1.8 Cu(II) - β amyloid interaction and effects

The suggestion that Cu(II), or some other redox active metal, was involved in the pathology of AD has been around since the 1980s. While there have been many candidates for that position including zinc, aluminum and iron, redox chemistry considerations and experimental studies single out copper, in the Cu(II) form, as the redox active metal partially mediating the effects of β amyloid toxicity.[87, 88, 89] A considerable amount of experimental and computational chemistry has shown that Cu(II) has high affinity to β amyloid and is necessary for free radical generation, which is implicated in damage to cell membranes including those of neurons. [90] Computational studies have also helped us understand the chemical mechanism involved in free radical generation.[91, 92] A more thorough discussion of the role of Cu(II) in AD can be found in Chapter 2.

1.9 Peptidic inhibitors of β amyloid oligomerization.

Since β amyloid toxicity is linked to oligomer formation, potent inhibitors of β amyloid oligomerization could block both immediate toxicity, and the subsequent

destructive cascade, set up by β amyloid oligomers. A number of structurally diverse, peptidic and non-peptidic, compounds are known to block the process of β amyloid aggregation and subsequent neurotoxicity.[93]

Many currently known inhibitors were initially screened and optimized for their ability to block β amyloid fibril formation as they were, for a long time, considered to be the pathological species in AD. It is now clear that their therapeutic effects in animal models of AD were mediated through inhibition of soluble β amyloid oligomer formation. Concentrations of inhibitors that block amyloid fibril formation can also reduce or eliminate the toxicity of β amyloid solutions. [94, 95] and it is therefore likely that both fibrils and soluble oligomers are formed at different steps of the same process.

The binding sites for non-peptidic inhibitors are not well understood and most of them can also block aggregation of peptides like amylin and α synuclein, thus demonstrating their lack of specificity to β amyloid. Programs for the development of potent non-peptidic inhibitors have met with rather limited successes as they have a 'flat' Structure Activity Relationship (SAR), which is not conducive to medicinal chemistry based approaches for improving ligand potency.[96, 97]

In contrast, experimental data suggests that almost all peptidic inhibitors of beta-amyloid oligomerization bind to a region of β amyloid (16-22). [98] This region of β amyloid is widely recognized, based on experimental data, to be the 'self-recognition' region and is necessary for initiating oligomerization.

The history of peptidic inhibitors for β amyloid aggregation began with the work of Tjernberg *et al* and initially led to identification of the β amyloid self-recognition motif.[99] Previous to this publication there had been attempts at understanding the process of β amyloid self-recognition. [100, 101] However none of the previous attempts were systematic and often produced contradictory results.

Tjernberg *et al* synthesized 31 sequential and immobilized 10mers (based on the sequence of β amyloid) and measured the affinity of radiolabelled β amyloid (1-40) towards these sequential 10mers. They were thus able to identify 2 distinct regions (one major and one minor) of β amyloid that recognized complementary 10-mers (see Figure 1.5 A). The best self-recognition (major binding) occurred with 10-mers that spanned the region from residue 12-21 in β amyloid (1-40).[99] Synthesis and testing of fragments of that particular 10-mer identified KLVFF as the smallest fragment with reasonable binding to the self-recognition region of β amyloid (see Figure 1.5 B).[99] They also utilized an 'alanine walk' (see Figure 1.5 C) to obtain basic structure activity requirements for optimal binding of KLVFF to β amyloid (1-40). The hexapeptide Ac-QKLVFF-NH_2 was used to demonstrate inhibition of β amyloid fibrillization, as Ac-KLVFF-NH_2 has poor aqueous solubility.

An immobilized artificial receptor, derived from the core self-recognition sequence, was later used to measure the binding affinity of a wider number of ligands [102] including KLVFFAE and LVFFAE. Basic molecular modeling and potential energy measurements of the possible receptor-ligand complex were also made and initial data suggested that an anti-parallel arrangement of the ligand-receptor complex was favored over a parallel arrangement. Since then, the structure of the KLVFFAE region (the 'self recognition' site) has been explored with a variety of experimental and computational techniques.[103, 104, 105] Almost all of these studies suggest that the motif tends towards a beta-sheet conformation, especially when it is free and allowed to bind to itself. KLVFFAE is also the shortest region of β amyloid that can form oligomers and fibrils by itself.

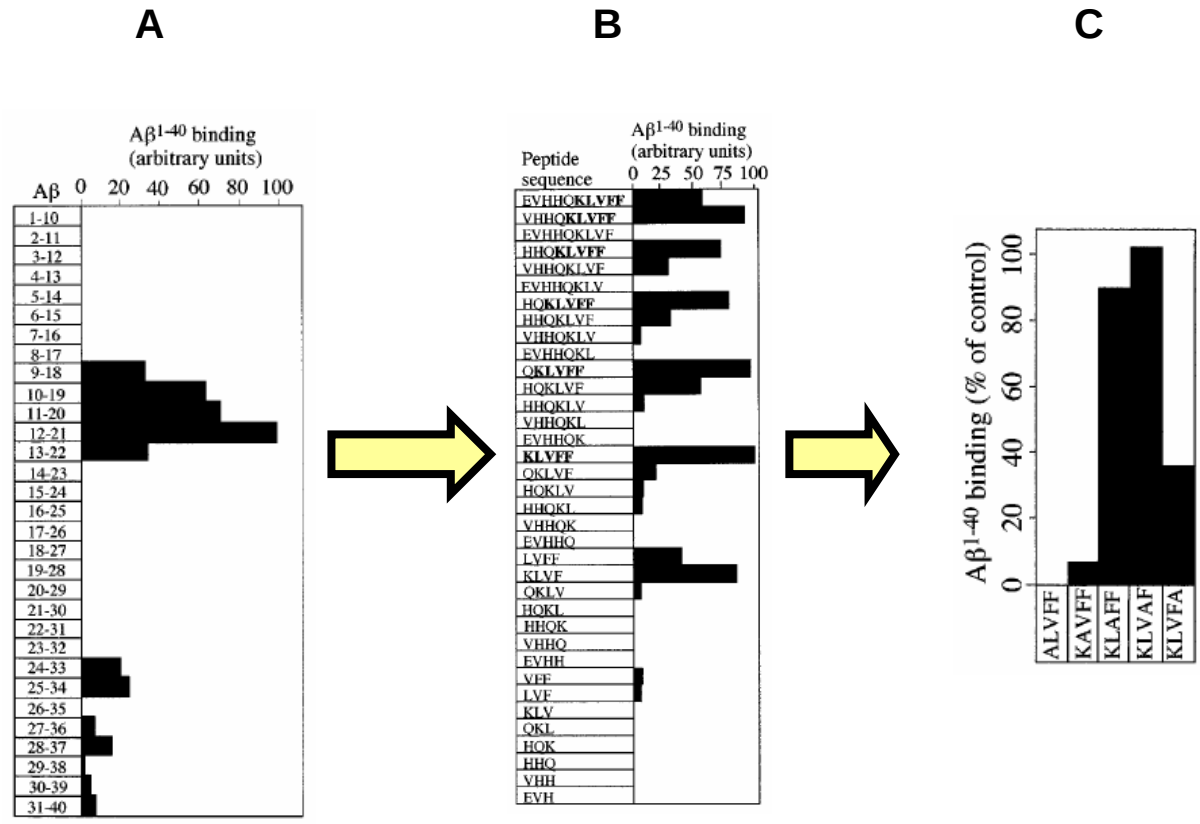

Figure 1.5 *A summary of experimental results that led to the discovery of the self-recognition site in β amyloid and its binding characteristics. A; identification of the β amyloid self-recognition site through the use of overlapping 10-mer sequences. B; discovery of the first useful pentapeptidic inhibitor of β amyloid aggregation. C; first Structure Activity Relationship (SAR) data for analogues of the pentapeptidic ligand Ac-KLVFF-NH_2. Reproduced from J Biol Chem. 1996, 271(15): 8545-8 with kind permission of JBC.*

Though most known peptidic inhibitors were based on the complementary KLVFF motif, Soto *et al.* tried another novel approach based on breaking β sheet conformation of the self-recognition site. This was achieved through designing peptides with structural homology to the self-recognition site, but with additional features for stabilizing a non- β strand conformation, and are known as β sheet breakers. They discovered two peptidic inhibitors, RDLPFFPVPID and LPFFD,

which were effective β strand breakers in their assay systems.[106] These peptides could inhibit fibrillogenesis as well as disassemble pre-formed fibrils. Soto *et al* subsequently showed that LPFFD could also block β amyloid induced cytotoxicity as well as block β amyloid deposition in a sub-acute animal model of AD. [107]

Soto *et al.* also tried to improve metabolic stability of the peptide by using D- amino acid residues as well as various N-methylations of the parent peptide.[108, 109] Serono Inc. was involved in developing the later class of compounds. Based on a brief medicinal chemistry program and pharmacokinetic data, Serono decided to use Ac-LP(me)FFD-NH_2 ‡ as their lead compound for future investigations in various animal models of AD. It had good stability in plasma (>24 hrs), CSF (>24hrs), good BBB penetration and a reasonable half-life (~2 hours) in the body. [109]

Another approach towards developing peptidic inhibitors of β amyloid aggregation was typified by the approach taken by Mark Findeis *et al.* at Praecis Inc. Information about that project is found, predominantly, in patent literature as opposed to peer-reviewed literature.[110] Their effort started with levorotary KLVFF based peptides, but eventually moved on to dextrorotary KLVFF based peptides. While N-terminus functionalizations for enhancing BBB penetration were tested, many pentapeptidic ligands had good BBB penetration without any extra functionalization. [94, 110] However the efficacy or potency of their ligands was not significantly superior to native KLVFF peptide. Their principal candidate drug (PP-1019), with the sequence Me-[(D-Leu)-(D-Val)-(D-Phe)-(D-Phe)-(D-Leu)]-NH_2, had favorable animal toxicity data and had good Blood Brain Barrier (BBB) penetration and is still used as a standard against which newer peptidic beta-amyloid aggregation inhibitors are tested.[111] Praecis Inc. discontinued development of this class of drugs in 2005 as it was bought by Glaxo Smith-Klein (GSK).[112] Mark

‡ In peptides such as Ac-LP(me)FFD-NH_2, the ‘(me)’ denotes the presence of an N-methylated amino acid residue (backbone not sidechain), e.g. (me)F = N-methyl phenylalanine.

Findeis has since started up his own biotech company called Satori Pharmaceuticals Inc.[113]

A modification of Tjernberg *et al.*'s approach for blocking β amyloid oligomerization with metabolically stable and membrane permeable peptidic drugs was put forth by David Gordon *et al.* [114, 115] They created versions of KLVFFAE and KLVFF with N-methylation on alternate amino acids. The purpose behind these modifications was to ensure that only one side of the inhibitor could bind to the receptor and that the other side could not, in any way, assist extension of the oligomer. [114, 115] KLVFFAE has not been previously developed as an inhibitor because though it had a better affinity than KLVFF to the receptor, its tendency to self-aggregate made it a poor oligomerization blocker. The N-methylated analog of KLVFFAE, Ac-K(me)LV(me)FF(me)AE-NH_2, was more potent than Ac-K(me)LV(me)FF-NH_2 and did not undergo self aggregation. They also found that N-methylated versions of KLVFF and KLVFFAE had better aqueous solubility and could cross cell membranes.

Another approach, somewhat similar to Findeis *et al*, to block β amyloid aggregation with dextrorotary residues containing peptides was proposed by a group from Neurochem Inc. [116, 117] Their work essentially confirmed that dextrorotary versions of KLVFF are more potent at inhibiting β amyloid (1-40) aggregation and β amyloid (1-42) induced cytotoxicity than KLVFF itself. They also demonstrated that only peptides containing residue number 15-20 and 16-22 of β amyloid had any anti-aggregation activity against β amyloid (1-40). Moreover their peptidic drugs candidates crossed the blood-brain barrier in concentration sufficient to have a therapeutic effect in animal models of AD.

Senexis Inc is the latest entry into the field of creating newer peptidic inhibitors. [98] They have utilized a medicinal chemistry based approach for optimizing the interactions of their ligands with the self-recognition site on β amyloid. The improvements in ligand potency, over earlier ligands, have however been minimal.

The company has raised some more venture capital funding for future development of these drugs.[118]

It should be clear from the information presented in this section that while peptidic inhibitors of β amyloid oligomerization do show promise for the treatment of AD type dementia, there is significant room for improvements in drug-like properties of these compounds.

1.10 Currently approved drugs for AD

Inhibition of central (brain) cholinesterase and modulation of the voltage gated N-Methyl D-Aspartate (NMDA) channel are the two currently available pharmacological approaches for the management of AD. There are currently three approved drugs for AD that target cholinesterase and one that acts as a NMDA channel modulator. The rest of this section provides a brief overview of these drugs, their pharmacology, development and their impact on the management of AD.

As discussed above, the first type of pharmacological approach possible in AD uses cholinesterase inhibitors for increasing the level of acetylcholine in the brain. The rationale behind this approach was based on the observation that AD seems to cause a somewhat preferential loss of cholinergic neurons and the first symptoms of AD (memory loss, problems with memory consolidation, disorientation, confusion) resemble the central effects of anticholinergic drugs.[119, 120] An increased level of acetylcholine in the patient's brain is supposed to enable the remaining functional synapses and neurons to function more efficiently. Cholinesterase therapy often allows the patient to retain a higher level of functioning for 6-18 months longer than would otherwise be possible, but it does not change the ultimate prognosis of AD. An important implication of the efficacy window for these drugs is that early stage AD probably does not involve neuronal loss sufficient to permanently affect cognition. Therefore an efficacious DMD could

halt or reverse the course of disease process even if it was used after the first symptoms of AD appeared.

An older compound, Tacrine, (see Figure 1.6) was the first cholinesterase inhibitor to demonstrate some therapeutic effects in AD and stimulated research into developing cholinesterase inhibitors for AD. It was first developed in the 1960s as a synthetic centrally acting parasympathetic drug [121, 122] and its main advantages over other existing parasympathomimetics, such as organophosphates and carbamates, was its relative specificity for brain cholinesterase and the ease of drug effect titration. It was also shown to have therapeutic effects in animal models of amnesia caused by brain lesions and anticholinergics.[123, 124] Starting in the early 80s, a few small clinical trials with Tacrine were performed in AD patients. [125, 126] It seemed to slow down the progression of the AD for about a year, before it lost its therapeutic effect. Tacrine was approved by the FDA for treating mild to moderate AD in 1993, in large part due to the lack of a similar but demonstrably less toxic drug being available at that time.[127] It was ultimately withdrawn from the market in 2006.[128]

In the early 90s, Esai Inc developed a benzylpiperidine derivative known as Donepezil (see Figure 1.6).[129] It is widely considered to be the first centrally acting cholinesterase inhibitor with good pharmacokinetic properties.[130] It was approved by the FDA for treating mild to moderate AD in 1996. Its long half-life (~ 70 hrs), good absorption (~100%) and lack of significant mechanism unrelated toxicity made it the first widely prescribed cholinesterase inhibitor for treating AD. While it is no more efficacious than any other cholinesterase inhibitor, it is widely considered to have the best side effect profile of any current cholinesterase inhibitor. This favorable side effect profile might be the result of it being specific for acetylcholinesterase, as opposed to also inhibiting butylcholinesterase. Donepezil also does not have a worthwhile affect on any other neurotransmitter system in the brain.

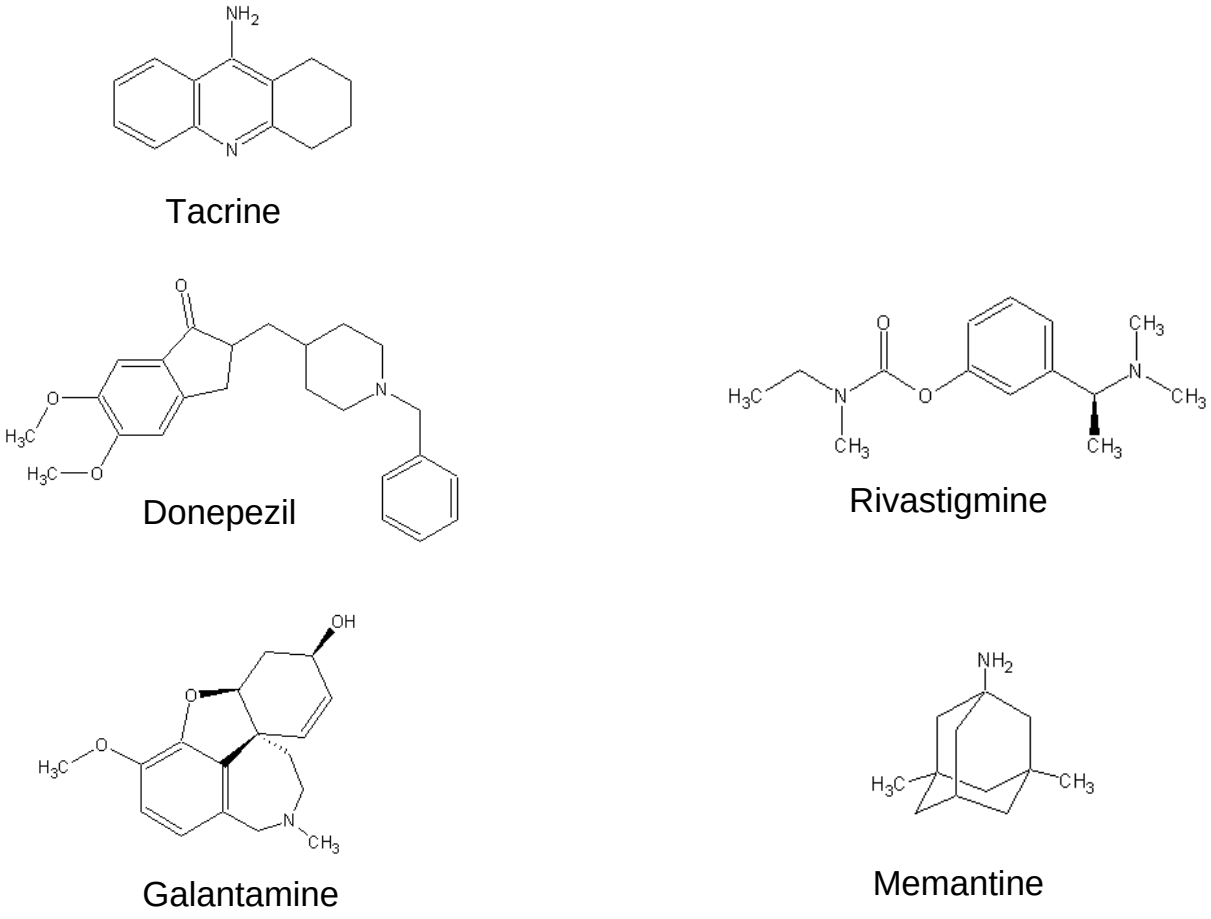

Figure 1.6 *A list of the structures of drugs approved for treating AD. Tacrine, Donepezil, Rivastigmine and Galantamine are reversible cholinesterase inhibitors and Memantine is a NMDA antagonist.*

The next cholinesterase inhibitor, approved by the FDA in 2000, for AD was a carbamate called Rivastigmine. [131] (see Figure 1.6). It has a short half-life (~ 2-3 hrs) but good absorption (~96%) and no significant mechanism independent toxicity. However it inhibits butylcholinesterase in addition to acetylcholinesterase. [132] The inhibition of butylcholinesterase is supposedly behind the higher incidence of nausea and vomiting encountered with this drug, an effect that can be reduced by giving the drug in divided doses with food. It is also now available in a transdermal patch formulation (approved in 2007) that produces a steady therapeutic plasma concentration without the serum concentration peaks that

cause the nausea and vomiting. Rivastigmine is supposedly a more efficacious drug for some AD patients with hallucinatory symptoms and dementia in patients with Parkinson's disease (PD). [133, 134]

The last cholinesterase inhibitor currently approved for AD is a phenanthrene alkaloid known as Galantamine.[135] (see Figure 1.6). The name galantamine is a simplified form of its earlier name – galanthamine. It was isolated from Caucasian snowdrop, *Galanthus woronowii*, by Bulgarian researchers in the 1950s. It was first isolated and occasionally used as a centrally acting parasympathomimetic in humans for treating post-operative paralytic ileus and post-poliomyleitis muscle weakness. [136, 137] In addition to its inhibition of cholinesterase, galantamine also modulates the nicotinic cholinergic receptors to increase acetylcholine release at nerve synapses. Whether this additional effect adds to the therapeutic effect of galantamine in AD is unclear. It has a reasonable half-life (~7 hrs), good absorption (80-100 %) and no significant mechanism independent toxicity.[138] In any case, all approved cholinesterase inhibitors have similar efficacy in slowing down the progress of AD by about a year, though some patients might experience better responses or fewer side effects with one particular drug.

Another approach to reducing the neuronal damage seen in AD involves reducing the activity of N-Methyl D-Aspartate (NMDA) receptors. NMDA receptor antagonists have been well investigated for their potential in reducing neuronal damage in many neurological conditions such as stroke and traumatic head injury. However the major approved use of NMDA antagonists is as general anesthetics (e.g. ketamine and phencyclidine).[139] Other lesser known NMDA antagonists include drugs such as dextromethorphan, riluzole, and the hallucinogenic drug ibogaine. All potent NMDA antagonists have a mechanism dependent risk of hallucinations and even careful dose titrations often cannot avoid this particular side effect. Therefore any NMDA antagonist for treating AD has to possess the peculiar attribute of not disrupting NMDA receptor function in the normal range of receptor activity.

The first drug that satisfied this requirement was an adamantane derivative known as Memantine.[140] (see Figure 1.6). It has a strong structural resemblance to the anti-viral adamantine derivatives- amantadine and rimantadine. It is a low-affinity voltage-dependent uncompetitive antagonist at glutamatergic NMDA receptors that competes with Mg^{2+} ions that normally regulate the influx of Ca^{2+} ions into neurons. An excessive Ca^{2+} ion influx into cells is supposed to contribute to some of the neurotoxicity and cellular dysfunction seen in AD. Curiously while memantine produces symptomatic improvement in moderate Alzheimer's disease, there is no evidence in humans that it protects neurons from any of the purported NMDA receptor-mediated excitotoxicity in AD. It also has some antagonistic activity at serotoninergic and nicotinic cholinergic receptors in the brain, but it is not clear if these effects contribute to its therapeutic activity in AD. It possesses a long half-life (60-100 hrs), has good absorption (~ 100 %) and no significant mechanism independent toxicity.

1.11 Experimental disease modifying drugs (DMDs) for AD

The current lack of drugs that can effectively stop or reverse the course of AD has stimulated a lot of research into development of disease modifying drugs (DMDs) for AD. One of the major problems in developing DMDs to treat AD is a lack of understanding about the precise sequence of events, and the role of various contributing factors, that lead to the eventual neuronal dysfunction/ death in AD. Soluble oligomers of β amyloid are the most likely initiators of neuronal damage and death seen in AD. The role and contribution of other contributing factors, such as impaired vascular perfusion and advanced glycosylation products, are poorly understood. Moreover secondary factors, downstream to the initial neuronal insult, such as localized inflammatory responses and increased soluble *tau* do play a significant role in the final demise of neurons in AD.

The lack of an easily identifiable and ‘traditional’ druggable target, such as a G-Protein Coupled Receptor (GPCR) or a unique enzyme, has also contributed to difficulties in developing DMDs for AD. Many older animal models of AD do not exhibit the characteristic extensive neuronal loss and attendant symptoms seen in humans with later stages of AD. Reasonably good animal AD models, such as 3xTgAD, have only recently been used to evaluate new DMDs. A list of important small molecule DMDs currently in human trials to treat AD is shown in Figure 1.7.

Tramiprosate (Neurochem Inc) was once the most advanced disease-modifying drug (DMD) candidate known to be in development (see Figure 1.7). It is a glycosaminoglycan mimetic designed to bind to Aβ peptides and stop the formation of amyloid plaques. The Phase II trial initially showed negligible therapeutic effect, however, an open-label extension of this trial supposedly showed some benefits on cognitive and global performance measures. [141] Tramiprosate was investigated in two larger 18-month Phase III clinical trials, but results from these studies failed to show any statistically significant changes in disease progression markers over and above the concurrently administered cholinesterase inhibitors. [142]

Scyllo-Inositol (Elan Inc.) is another small molecular inhibitor of β amyloid oligomerization (see Figure 1.7). [143] It stabilizes fibrillar forms of β amyloid while simultaneously reducing the formation of soluble oligomers. Initial results in animal models seem encouraging, but many other small molecule compounds with therapeutic activity in animal models of AD have failed in large human clinical trials.[144]

The inhibition of β or γ secretase is another possible avenue for lowering β amyloid levels, since enzymes are more familiar drug targets. However β and γ secretase have physiological functions other than splicing APP, and current drug candidates (especially γ secretase inhibitors) have been plagued by side effects such as intestinal ulceration and immune dysfunction. [145] While it is possible that not all

serious side effects are mechanism related, many side effects are common and dose dependent. [146]

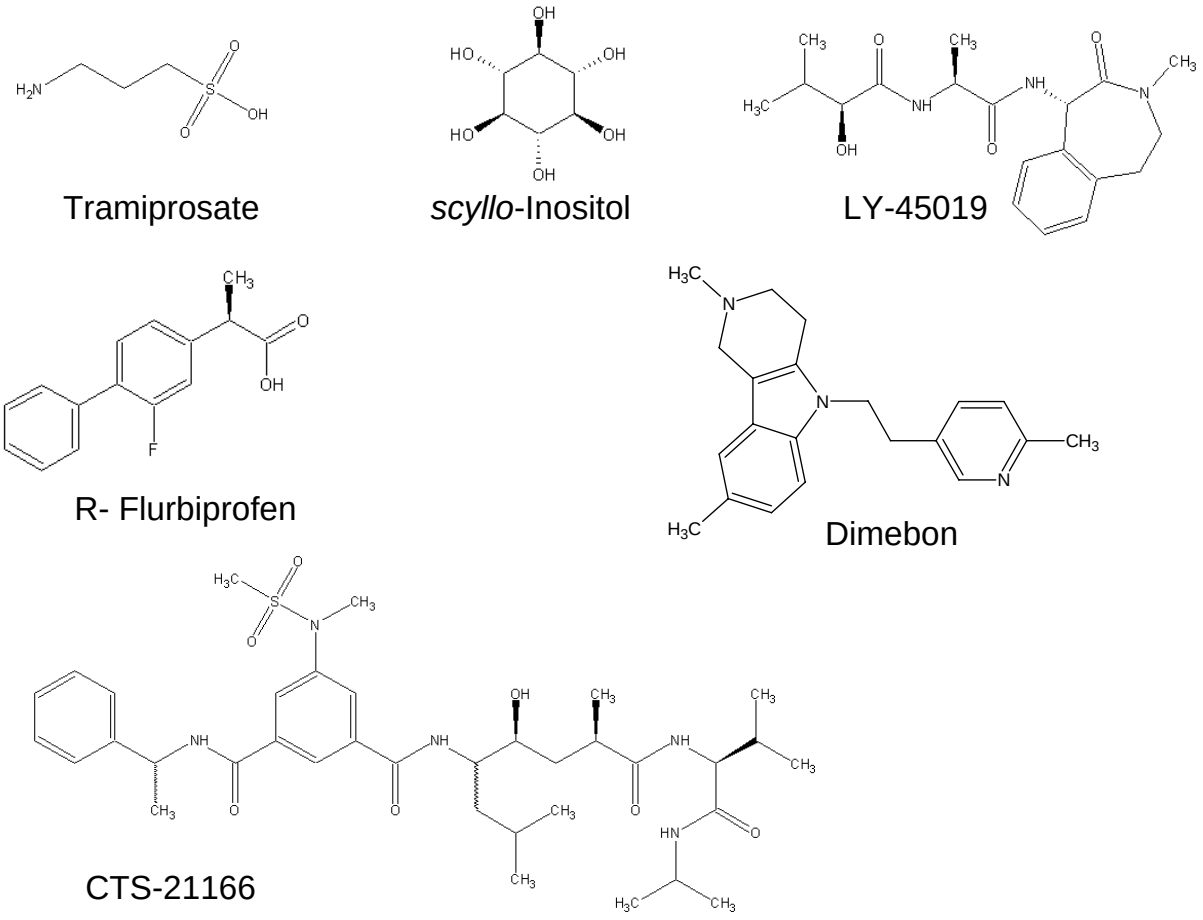

Figure 1.7 *A list of small molecule disease modifying drugs (DMDs) for AD that have entered human clinical trials. Tramiprosate and Scyllo-inositol are inhibitors/ modulators of β amyloid oligomerization. R-Flurbiprofen is a γ secretase modulator. LY-45019 is a γ secretase inhibitor and CTS-21166 is a β secretase inhibitor. Dimebon has multiple, and as yet not completely understood, modes of action.*

CTS-21166 (CoMentis Inc.) is the first β secretase inhibitor greenlighted for testing in human phase I trials, and results of initial tolerance and 'proof of concept' studies have been performed (see Figure 1.7*).* [147] Many other companies have similar drugs in their pipelines. [148] LY-45016 (Eli Lilly Inc.) is the first γ secretase

inhibitor to have undergone phase I and II clinical trials (see Fig 1.7). Initial short term dosing (6 weeks) does not seem to be associated with any significant side effects and a modest reduction in plasma β amyloid levels was achieved. However CSF levels of β amyloid seem to be unchanged by the dose used in Phase I trials. [149] There have been plans to combine β and γ secretase inhibitors such that their inhibition of β amyloid production is synergistic at doses associated with minimal toxicity. Whether such an approach can be translated into a therapeutic effect in humans without excessive side effects remains to be seen.

Another related therapeutic possibility is the modulation of β and γ secretase activity such that only the APP cleavage activity of these enzyme complexes is affected. It is hoped that cleavage of other substrates, responsible for their physiological roles, is unaffected. Tarenflurbil (Myriad Inc), a modulator of γ secretase activity, was one of the more advanced agents in clinical development for preventing Aβ formation by this mechanism.[150] Tarenflubril is the most recent name for the R- isomer (non anti-inflammatory isomer) of Flurbiprofen (see Fig 1.7). In a small Phase II trial in patients with mild-to-moderate AD, Tarenflurbil was found to be safe and well tolerated, and demonstrated a reduced rate of cognitive decline compared with a placebo, but it did not have measurable therapeutic effect in a pivotal Phase III study. [151]

Data from animal models of AD suggests that antibodies against Aβ, produced by the body after a vaccination (active immunization) or administered peripherally (passive immunization), can reduce amyloid deposition and produce functional improvements, thereby ameliorating cognitive deficits.[152] However, the most intractable problem with active immunization for an endogenously present peptide like β amyloid is that humans make antibodies of differing specificities due to their differing HLA subtypes and so autoimmune reactions are always a serious concern regardless of which part of the β amyloid peptide is used as the immunogen in the vaccine. The first-generation amyloid vaccine, AN-1792 (Elan/ Wyeth) did demonstrate a positive efficacy trend in that AD patients who developed a robust

antibody response to the vaccine did not deteriorate as fast as the poor antibody producers, over a 1-year period in a number of memory tests. [153] However, owing to the development of aseptic meningio-encephalitis in 6% of the patients, the AN-1792 program was discontinued. [154] A second-generation vaccine, ACC-001 (Elan/Wyeth), which has been engineered to have an improved safety profile, is now in a Phase I trial. [155]

Passive immunization is a more expensive and cumbersome approach, requiring frequent anti-Aβ monoclonal antibody (mAb) administration, but on the other hand, it does offer the promise of greater safety. Three mAbs against various domains of Aβ are currently in development: Bapineuzumab (Elan/Wyeth) and LY2062430 (Eli Lilly) in Phase II trials, and RN1219 (Pfizer) in Phase I. [156]

Finally there are atypical drugs such as Dimebon (see Figure 1.7). It was developed in Russia as a non-sedating anti-histamine drug. It was subsequently found to have broader neuroprotective effects in animal models of brain damage.[157] Results from small clinical trials seem to suggest that Dimebon has some therapeutic effect in AD. [158] However it is far from clear that its therapeutic efficacy is superior to cholinesterase inhibitors or it has any effect on the course of the disease. Longer and more thorough Phase II trials with a significantly larger patient population should answer these questions in the near future.

There is therefore currently no drug, either approved or experimental, that has been able to show disease modifying effects in AD. The evidence presented earlier in this chapter also suggests that β amyloid oligomers are the most likely initiators of the disease process. There is still an unfulfilled need for therapeutically effective disease modifying drugs to treat AD. The two most common paradigms in drug development, small molecules and engineered proteins, have been so far unsuccessful. Therefore pursuing the third option, peptidic drugs, seems reasonable even though that approach has its unique problems.

CHAPTER 2: THE 'ABSENT' HYPOTHESIS

2.1 Introduction

The current chapter is an updated version of material presented in a paper published in 2005 [159] which describes the formulation of a new hypothesis, known as the ABSENT hypothesis. ABSENT is an acronym for **A**myloid **B**eta **S**ynergistic **E**ndothelial and **N**euronal **T**oxicity. It was put forth to address the shortcomings of major popular hypotheses on the etiology of AD. They are especially apparent when these hypotheses are used to explain variable histopathological findings and known risk factors for late-onset idiopathic AD.

2.2 Current hypotheses on the etiology of AD

Current popular hypotheses for the etiology of AD can be divided into two broad classes- the 'Amyloid' hypothesis and the 'Vascular' hypothesis. The 'Amyloid Hypothesis' proposes that an increased concentrations of β amyloid in the brain of AD patients has a direct neurotoxic effect, and is the main cause of the extensive neuronal damage/ death seen in AD. The 'Vascular Hypothesis', on the other hand, proposes that vascular damage and hypoperfusion caused by chronic cerebrovascular diseases (in old age) is the main cause of the extensive neuronal damage/ death seen in AD. The evidence for, and problems with, each hypothesis are summarized in the next two sections of this chapter.

2.3 The amyloid hypothesis of AD

The most publicized and widely accepted hypothesis for the etiology of AD, outlined in Figure 2.1, revolves around the neurotoxicity of β amyloid oligomers. The presence of a large number of amyloid plaques (and neurofibrillary tangles) in *post mortem* brain tissue is still the 'golden standard' for confirming the diagnosis of AD since these features were first described by Alois Alzheimer in 1911. A

more detailed account of the first diagnostic and histopathological description of AD has been previously presented (see Chapter 1.3 and 1.4).

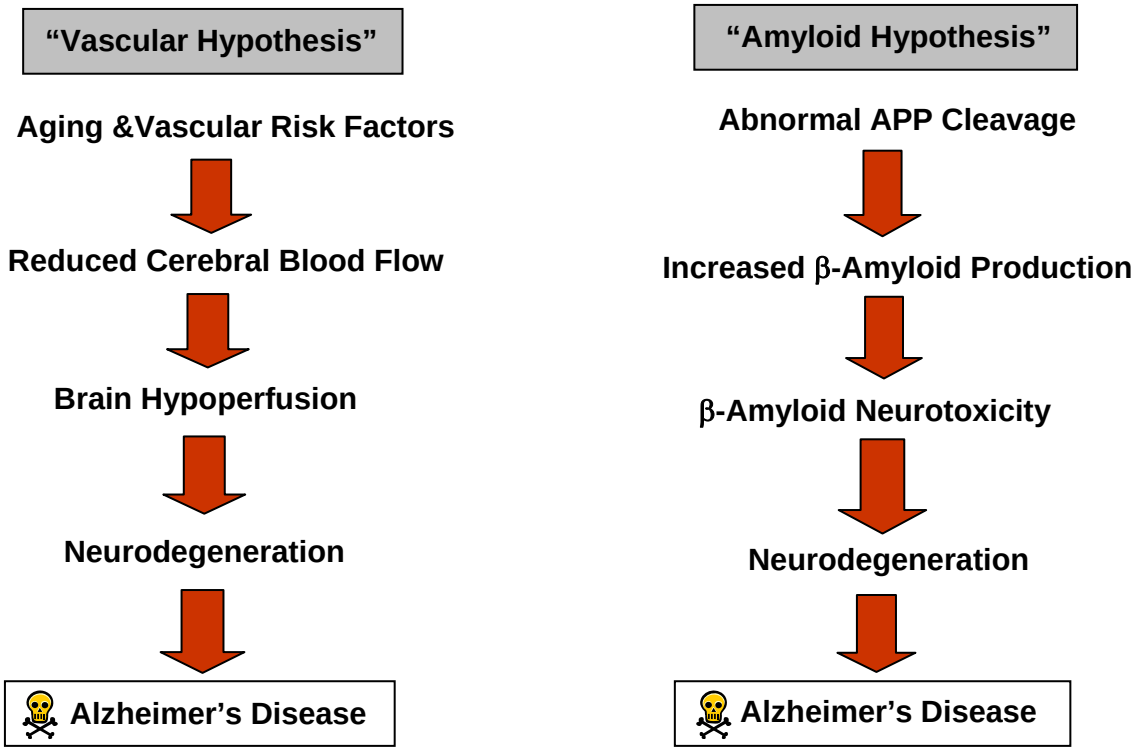

Figure 2.1 *The main steps of the two major hypotheses of AD etiology and their seemingly conflicting explanations of the pathological mechanisms behind the extensive neuron loss seen in AD. There are many sub-hypotheses in both groups, however sub-hypotheses tends to favor one school of thought over the other.*

However almost all known risk factors for idiopathic late-onset AD (stroke, high blood pressure, diabetes and other cardiovascular problems) are associated with vascular dysfunction.[160, 161, 162, 163] Postmortem studies have also shown that some subjects have significant amyloid plaque deposition without a concurrent diagnosable loss of mental function.[164, 165, 166] However many researchers still prefer to think of cerebrovascular dysfunction in AD patients as an etiologically separate coexisting disease condition.

2.4 The vascular hypothesis of AD

The vascular hypothesis for senile dementia (as outlined in Figure 2.1) has been around for a long time and before the amyloid hypothesis became popular, most cases of senile dementia were considered to have an underlying vascular pathology. There are very strong similarities between the symptoms of Vascular Dementia (VaD) and AD.[167, 168] It is often hard to draw a definite line between the symptoms and histopathology of VaD and AD.[169, 170, 171, 172]

AD is almost always associated with extensive cerebral capillary angiopathy and other cerebral macrovascular damage.[173, 174, 175, 176] As previously explained in section 1.4, *Ante mortem* tests are unreliable at distinguishing cases labeled as AD or VaD based on *post mortem* assignment.[162,177, 178] The *post mortem* assignments of a diagnosis of AD, mixed dementia and VaD are also more subjective than is widely understood.[179, 180]

As previously noted, cerebro- and cardiovascular diseases are known risk factors for developing AD. Patients with AD also exhibit a significantly higher risk of cerebrovascular incidents than an otherwise identical control population.[181, 182] Cholesterol lowering and vasculo-protective drugs like the 'Statins', ACE inhibitors and many anti-hypertensive drugs have been shown to decrease the incidence of AD and senile dementia. [183, 184, 185, 186] Experimental surgery to improve circulation to affected brain regions has been shown to improve the symptoms of AD. [187, 188]

The evidence of a vascular component in the etiology of AD does not invalidate the demonstrated role of β amyloid in early-onset familial AD and middle aged Down's syndrome patients. Nor is there any disagreement about the role of β amyloid oligomers in inducing oxidative stress and lipid peroxidation in the brain of early onset and late onset AD patients.[189, 190, 191, 192] Transgenic animal models of AD, though over-expressing mutant proteins, do demonstrate many histopathological

changes and symptoms similar to those seen in human AD. Some of the cellular and biochemical lesions seen in human AD are also similar to those seen in cell cultures treated with β amyloid.[193]

Moreover even though some people with significant β amyloid deposition often exhibit no symptoms, almost all people with heavy amyloid plaque load do have some symptoms of AD.[194, 195] Therefore a direct or indirect role for β amyloid induced neurotoxicity cannot be excluded from any comprehensive hypothesis for AD.

2.5 Comparison of the amyloid and vascular hypothesis

An overview of the 'amyloid' and 'vascular' hypotheses for AD demonstrates that neither type of hypothesis can, by itself, explain all of the known histopathological and biochemical lesions seen in AD. Neither hypothesis can account for the diversity of clinical symptoms, speed of disease onset and course of disease progression observed in patients diagnosed with AD. Each hypothesis, on its own, can only explain AD in patients without significant cerebrovascular damage, or VaD in patients without a significant amount of amyloid plaques. However *post mortem* and *ante mortem* studies show that the same histopathological, biochemical lesions and functional deficits are present in patients with diagnosed AD and VaD.[196, 197]

It was therefore necessary to create a new hypothesis for AD based on all known toxicities and effects of β amyloid. The ABSENT hypothesis was the result of an effort to collate and link the verifiable toxic effects (and underlying chemical mechanisms) of β amyloid into a coherent model that could explain the clinical entity known as late onset idiopathic AD.

2.6 Evidence for β amyloid mediated neurotoxicity

There is a very large body of published evidence for neuronal toxicity caused by β amyloid, previously mentioned in section 1.6 and 1.7. The most current understanding of β amyloid toxicity involves both direct (pore forming) and indirect (free radical based) damage to cell membranes, resulting in the secondary and tertiary effects such as *tau* hyperphosphorylation and inflammation.

2.7 Evidence for β amyloid mediated vascular dysfunction

The adverse effects of β amyloid on vascular function and endothelial cells *in vitro* and *in vivo* are less well known and therefore need to be discussed at some length. Cerebral capillary amyloid angiopathy (CCAP) is a hallmark of AD and is present in almost all patients with a definitive postmortem diagnosis of AD.[198, 199] Postmortem studies have shown a strong association between CCAP and both β amyloid plaque deposition and neuritic AD pathology.[200]

β amyloid has been shown to impair cerebrovascular blood flow, cause prolonged vasoconstriction and decrease endogenous endothelial NO production in tissues from normal animals.[201, 202, 203, 204, 205, 206, 207, 208] β Amyloid has also been shown to decrease transcapillary glucose transport and affect the integrity of the endothelial barrier.[209, 210]

Endothelial dysfunction is seen in blood vessels and cells in animals overexpressing β amyloid peptide/s. [201] Animals overexpressing human β amyloid also show a reduced CBF, less robust CBF autoregulation, reduced basal and peak cerebral glucose utilization and a reduced cortical functional hyperemia in response to stimulation.[211, 212] The 'reverse β amyloid peptide' (40-1), and a $Methionine_{35} \rightarrow Norleucine_{35}$ mutant, which has a significantly reduced ability to generate superoxide and H_2O_2, does not have any adverse/ toxic effects on the

vascular endothelium or vascular function. The ‘reverse sequence’ peptide also does not have any direct neurotoxic effects. [213]

All negative effects of the β amyloid peptide on the normal function of the vasculature can be prevented/ reversed by Superoxide Dismutase (SOD), SOD mimetics and other free radical scavengers capable of quenching superoxide. [211, 214] Moreover, SOD3 (extracellular isoform) knockout mice display cognitive and other neurological deficits that include impaired learning and long-term memory. [215] The oligomeric forms responsible for the vascular effects of β amyloid are poorly characterized, but soluble low molecular weight oligomers are the most likely culprits.

To better appreciate the effects of chronic hypoperfusion to the brain, it is necessary to understand the peculiarities of Cerebral Blood Flow (CBF) and CBF changes in aging and vascular disease.

2.8 Cerebral blood flow and metabolism

The human brain weighs about 2% of body weight but uses about 20% of the available blood and oxygen. It has an almost exclusively aerobic metabolism but has virtually no reserves of oxygen or glucose. Moreover, the brain has almost no capacity for emergency anaerobic respiration in the event of ischemia. Therefore it must have a constant blood supply and interruption of blood supply for as little as 4 minutes can result in irreversible damage to the brain. In contrast, most other organs can be revived after up to 8 hours of ischemia. The brain has therefore evolved a remarkably robust and effective system of ensuring constant perfusion and regulating blood flow to its various parts. Cerebral Blood Flow [CBF] in healthy humans is regulated primarily by two mechanisms – Autoregulation and Metabolic Control. [216]

Autoregulatory mechanisms consisting of a balance of myogenic tone regulation, secondary metabolite receptors and endothelium-derived factors like nitric oxide [NO] that sense the arterial pressure and adjust vascular resistance to keep CBF relatively constant. Autoregulation in healthy humans works best over the normal range of blood pressure [60–160 mm Hg], and abrupt changes in incoming arterial pressures are compensated for within a few seconds. [217]

Metabolic Control uses CO_2 levels [among other metabolic indicators] to provide extra blood [or divert blood] to active parts of the brain. Since not all parts of the brain can be constantly perfused at maximum capacity, metabolic control mechanisms make sure that currently active parts of the brain receive the maximum possible blood supply on an 'as needed' basis.

Normal aging causes autoregulatory mechanisms to become less effective in maintaining a constant CBF thereby decreasing the 'safe' range of incoming arterial pressure for maintaining a constant CBF. [218] The adverse changes caused by normal aging in the cerebral vasculature are both histological and functional. Adverse histological changes are seen both in the vasculature and the innervations to the major blood vessels. Metabolic control of the blood flow to more active areas of the brain can also be affected by aging. Co-existing vascular diseases exacerbate all age-related changes in the status of the autoregulatory and metabolic controls mechanism for maintaining a 'normal' CBF. [219, 220]

2.9 Synergy of β amyloid mediated neurotoxicity and vascular dysfunction

Neurons require constant oxygenation and glucose because the brain has a very limited capacity for anaerobic metabolism. Neurons are therefore particularly sensitive to a combination of hypoxic/ hypoglycemic/inflammatory insults. The β amyloid- induced neuronal damage and vascular dysfunction could therefore have a synergistic negative effect on neuronal function and viability by creating a hostile neuronal environment through a combination of impaired functional

hyperemia, hypoxia, hypoglycemia and inflammation in addition to direct neuronal damage.

AD should therefore be seen as a condition in which β amyloid, in concert with coexisting circulatory and age related problems, launches an assault on the neurons and cerebral vasculature that perfuse them. β amyloid damages the neurons (directly and indirectly) causing progressive dysfunction leading to neuronal death. The relative contribution of the vascular and neuronal damage from β amyloid towards this end might vary in each case, but β amyloid is the critical factor/ingredient in all patients with AD and almost all patients with vascular dementia.

2.10 The ABSENT hypothesis

Hypotheses for the etiology of AD that involve a combination of the vascular and neuronal toxicity of β amyloid have been previously proposed. [221, 222, 223, 224] However, the ABSENT hypothesis, depicted in Fig. 2.2, differs from such previous hypotheses in that it proposes a unified and feasible chemical mechanism to explain the observed β amyloid-mediated vascular dysfunction and neuronal damage. The chemical mechanism is explained in more detail in subsequent sections of the current chapter and Figures 2.3 & 2.4.

In the ABSENT hypothesis, β amyloid itself generates all of the free radicals (superoxide, lipid based free radicals) that cause both vascular dysfunction and the initial neuronal damage seen in AD. All further reference to β amyloid in this chapter should be understood as referring to LMW β amyloid oligomers unless otherwise stated.

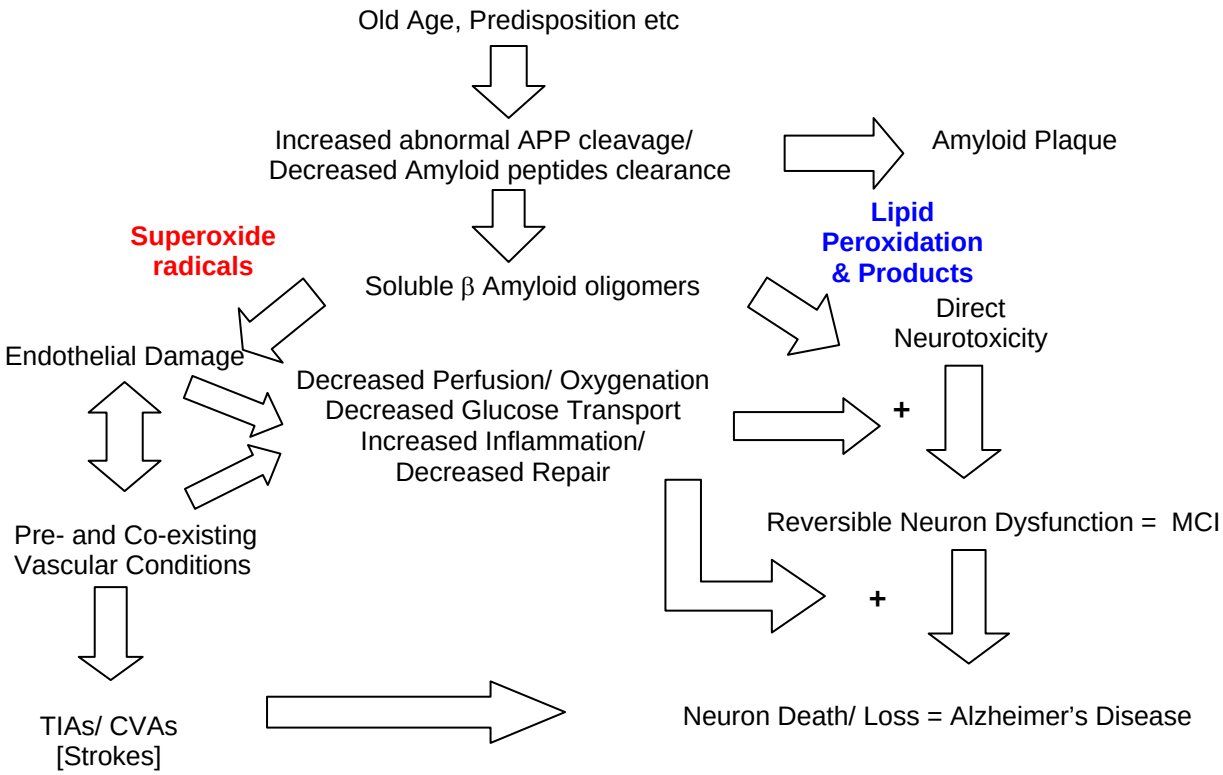

Figure 2.2 *An overview of the ABSENT hypothesis depicting various important steps in the pathogenesis of AD and their interconnections (shown with arrows). These steps and their synergistic interactions ultimately lead to the extensive neuron damage and death seen in areas of the brain afflicted by AD. A combination of primary and secondary insults is most likely the cause of neuronal death observed in AD.*

The ABSENT hypothesis also proposes that different stages of AD involve a different and changing balance of vascular dysfunction and neuronal damage caused by β amyloid. Thus, vascular dysfunction caused by low concentrations of β amyloid could account for a greater part of the neuronal dysfunction seen in pre-AD MCI (Mild Cognitive Impairment). Vascular dysfunction caused by β amyloid is known to occur at much lower concentrations than those required for the known direct neurotoxic effects. [225, 226, 227, 228, 229, 230] The extensive neuronal dysfunction/ death observed in mid- or end-stage AD is most likely due to direct primary and

indirect secondary neurotoxic effects of β amyloid on neurons. The direct primary and secondary neurotoxic effects start occurring at much higher concentrations of β amyloid than the vascular effects, and probably require significant local deposits of β amyloid, such as those seen in patients with mid- stage AD. Moreover, neurons in the mid- and end-stages of AD afflicted brains have also experienced prolonged hypo-perfusion, which magnify the direct β amyloid-mediated neuronal damage.

It is therefore likely that a combination of direct (neuronal) and indirect (vascular) neurotoxic effects of β amyloid cause a series of events that start with neuronal damage and end in neuronal death. The secondary effects of β amyloid induced neuronal damage such as localized inflammation and excessive soluble *tau* protein formation also likely contribute towards the ultimate fate of the affected neurons. The ABSENT hypothesis proposes that the extent of each factor's (direct and indirect) contribution towards the damage, dysfunction and death of affected neurons varies in each AD patient and is thus responsible for the *range* of histopathology and disease progression seen in AD.

The ABSENT hypothesis further states that the impact of each type of β amyloid toxicity is both negatively and positively modified by factors like genetic predisposition (excess/mutant β amyloid production), head injury (increased APP), "lifestyle", local inflammation, "good genes", vascular status, presence or absence of co-existing vascular diseases, current drug therapy for cardiovascular diseases etc.

According to the ABSENT hypothesis, co-existing cardiovascular conditions like hypertension, atherosclerosis potentiate the cerebrovascular dysfunction caused by β amyloid and increase the extent of hypoperfusion induced neuronal damage. The potentiation between cerebrovascular disease and AD is thus the result of structural vascular damage potentiating vascular dysfunction caused by β amyloid

as well as a more direct additive effect though excess superoxide generation by elevated levels of glycosylated proteins and homocysteine.

Type 2 Diabetes Mellitus (Type II DM) might also directly contribute to an increased AD risk through generation of excess superoxide via advanced glycation end products (AGE) thereby cause an increase in the cerebrovascular damage and accelerate the rate and percentage of patients with pre-AD MCI developing clinical AD.

According to the ABSENT hypothesis, VaD patients are especially sensitive to β amyloid-induced cerebrovascular dysfunction due to co-existing vascular diseases. Thus even moderately increased β amyloid levels can cause significant neuronal damage (and clinical symptoms) in VaD patients. On the other hand, some elderly people with moderate plaque buildup might not suffer from clinical AD because their robust vascular function reduces the impact of increased β amyloid levels. Moreover, evidence suggesting that cerebral hypo-perfusion causes an increase in β amyloid production in the brain exists. [231, 232, 233] Therefore maintaining a robust cerebral perfusion, inspite of moderate β amyloid levels, might slow down the progress towards clinical AD in the elderly with moderate amyloid deposition but no signs of clinical AD

One major difference between ABSENT hypothesis and similar 'mixed' hypotheses is that the ABSENT hypothesis suggests a plausible chemical mechanism for the neurotoxic and vascular effects of β amyloid, and is explained in the next few sections of this chapter.

2.11 The β amyloid redox cycle

The β amyloid peptides have a high affinity for copper [Cu] ions and Cu–β amyloid complexes cycle between various redox states.[90, 234, 235, 236] The Cu^{2+} ion forms a

complex with β amyloid and an electron is transferred from an antioxidant, like ascorbate, to the copper ion to form the Cu^{+} – β amyloid complex.

The Cu^{+} – β amyloid then adds oxygen [O_2] to form the Cu^{2+}– β amyloid- $O_2^{-\cdot}$ complex. The reactions either (a) release the superoxide radical [$O_2^{-\cdot}$] or (b) result in further reduction to release hydrogen peroxide (H_2O_2). The H_2O_2 is normally further detoxified by enzymes like catalases. Under conditions such as those found in brain tissue, $O_2^{-\cdot}$ produced by one molecule of the Cu^{+}– β amyloid complex is further converted to H_2O_2 by the same molecule as it is energetically more favorable than $O_2^{-\cdot}$ leaving the complex. However in the absence of reducing agents and high O_2 levels, such as those found in bloodstream, $O_2^{-\cdot}$ release is preferred over further conversion to H_2O_2.

The healthy human brain has a very low level of β amyloid.[237] The low levels of β amyloid in a healthy brain do not overwhelm the detoxification system for β amyloid generated free radicals and therefore no tissue damage results from these low β amyloid levels.

2.12 The β amyloid redox cycle in the brain

AD results in an increase in the brain concentrations of β amyloid thereby placing an increased amount of Cu–β amyloid in the redox cycle. The redox cycle of the Cu–β amyloid complex in the brain is summarized in Figure 2.3. The normal detoxification mechanisms (antioxidants like glutathione/ascorbate) are no longer sufficient to take away the charge from all Cu–β amyloid complexes. The lack of insufficient anti-oxidant mechanisms thus allows aberrant reactions like peptide backbone based radical formation. According to the ABSENT hypothesis, the lipid peroxidation seen in AD and β amyloid treated neurons is caused by peptide backbone radicals. [238, 239, 240] In the neuronal environment, no excess superoxide

is released and only H_2O_2 is ultimately released as a side product of conversion of Cu^{+}–β amyloid to Cu^{2+}–β amyloid.

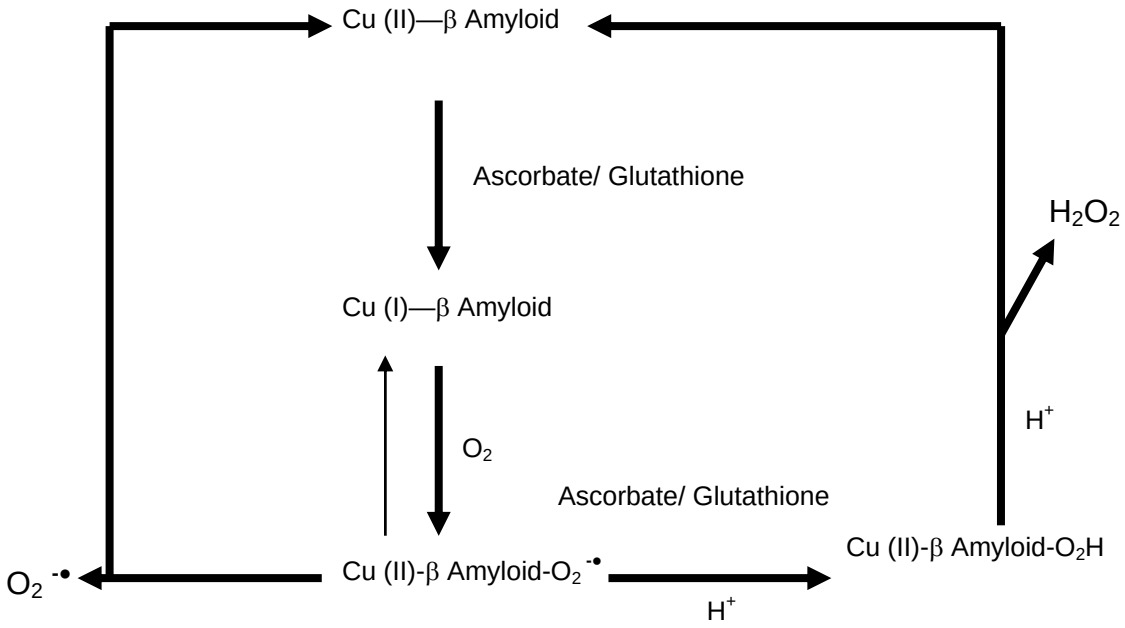

Figure 2.3 *Redox chemistry of the Cu(II)-β Amyloid complex in the body. Two possible pathways for directly generating radicals exist. The pathway resulting in the production of hydrogen peroxide (H_2O_2) is important in environments resembling those in the brain (low oxygen tension and excessive reducing agents). The other pathway produces superoxide ($O_2^{-\bullet}$) and is more common in high oxygen tension such as those encountered in the vascular system.*

The direct evidence for increased lipid peroxidation in the brain of AD patients comes from chemical analysis of lipids extracted from brain tissue that show elevated levels of peroxidated cell membrane lipids. There is evidence for increased membrane damage (cellular and mitochondrial) in histopathological studies of neurons from AD afflicted brains. The levels of lipid peroxidation by products and markers in brain tissue, CSF and blood of AD patients are also elevated.[193] The lipid peroxidation byproducts and markers are also known to be toxic to neurons. These changes are also seen in β amyloid treated cell cultures and transgenic animals overexpressing human β amyloid.

The precise mechanism of lipid peroxidation in the brain is still controversial. One of the popular hypothesis is that hydrogen peroxide (H_2O_2) causes peroxidation of the lipids, through formation of the $OH^{\cdot}$ radical, in the cell membranes of neurons. Indeed, experiments have consistently shown that catalase prevents β amyloid-induced neurotoxicity in cell-based assays. [241, 242, 243, 244] However, there is evidence that catalase amelioriates β amyloid induced neurotoxicity by complexing with soluble β amyloid. Catalase has a very high affinity [Kd ~ 3 nm] for β amyloid. [245] Furthermore, there is no difference in the protective ability of inactivated catalase and catalase as far as prevention of β amyloid toxicity is concerned. The characteristic biochemical lesions caused by addition of hydrogen peroxide are also not seen when β amyloid is added in cell based assays, nor is the toxicity of β amyloid reversed by compounds that do so for cells exposed to H_2O_2. [246]

The above factors and the short half-life of the hydroxyl radical make hydrogen peroxide and the $OH^{\cdot}$ radicals unlikely candidates for the majority of the lipid peroxidation and neurotoxicity seen in the AD afflicted brain. A relatively long lived and 'lipid soluble' radical like a peptide backbone- based radical or its peroxy derivative, is the most likely candidate for causing the increased lipid peroxidation seen in brains of AD patients. The toxicity caused by lipid peroxidation is probably both direct (structural) and indirect (signal transduction dysfunction, toxicity of lipid peroxidation products).

2.13 The β Amyloid Redox Cycle in the Vasculature

AD also results in a net increase in β amyloid concentrations in the blood and vascular tissues. The proposed redox cycle of the Cu–β amyloid complex in the vasculature is also depicted in Figure 2.3. According to the ABSENT hypothesis, both peptide backbone free radicals and superoxide are generated by the Cu–β amyloid complex in vascular tissues, though superoxide generation predominates over the other pathway. Moreover, the lipid peroxidation caused by peptide

backbone-based free radicals predominantly targets the membranes of passerby red blood cells [RBCs] and other cells in the circulation which are constantly recycled.

The principal vascular toxicity of β amyloid in the vasculature is therefore caused by superoxide radicals attacking endothelial-derived relaxing factors like NO and thereby adversely affecting the normal functioning of underlying vascular smooth muscle. Superoxide generation, by β amyloid, also causes stress, dysfunction and altered signal transduction in the endothelial cells lining blood vessels.

However, most physico-chemical experiments with Cu–β amyloid complexes have shown hydrogen peroxide generation (SOD like activity) but failed to show generation of the superoxide radicals.[234, 247, 248, 249, 250] Many of these reactions are supposed to initially generate superoxide as an intermediate step. It is likely that these experiments do not recreate conditions in the vasculature (lack of reducing agent combined with high oxygen tension) which favor superoxide release.

Literature referenced earlier in this chapter on the other hand suggests that superoxide radicals generated by β amyloid seem to be responsible for almost all of the β amyloid-induced vascular dysfunction since the *in vitro* and *in vivo* toxic effects of β amyloid on the endothelium and vascular function can be reversed by SOD and SOD mimetics.

The mechanism proposed to explain the phenomenon is biphasic. In the first phase, high O_2 tensions such as those seen in the bloodstream favor generation of superoxide by the Cu^{+}–β amyloid complex over further conversion of the nascent superoxide to hydrogen peroxide (see Figure 2.3). The rapid generation of superoxide by the Cu^{+}–β amyloid complex depletes the available 'pool' of Cu^{+}–β amyloid complexes that could transform superoxide to hydrogen peroxide, therefore the amount of hydrogen peroxide generated is substantially

reduced. Thus the Cu–β amyloid complex tends to produce superoxide over hydrogen peroxide under conditions encountered in the vascular system.

The hypothesis also considers the possibility that additional factors (and as yet undefined factors) like other metal ions and naturally occurring compounds present in the vasculature interact with the Cu^{+}–β amyloid complex and further make it harder for the complex to convert superoxide to hydrogen peroxide.

2.14 Aging, diabetes, homocysteine induced vascular dysfunction and AD

The mechanisms behind the increased incidence of AD in old age, diabetes, hypertension and other cardiovascular diseases have been conventionally attributed to indirect potentiation of β amyloid neurotoxicity by the structural vascular damage caused by these comorbidities. The ABSENT hypothesis proposes an additional and more direct mechanism, depicted in Figure 2.4, to explain the increased incidence of AD seen in patients with these comorbidities.

The mechanism proposed involves production of additional superoxide by transition metal complexes of glycosylated proteins, glycosylated hemoglobin, and homocysteine resulting in increased cerebrovascular dysfunction beyond that caused by the superoxide generated by β amyloid (a list of references is found in the next paragraph). The increased cerebrovasculardysfunction speeds up the course of AD and causes an increased incidence of clinical AD in these patients. The evidence used in developing this sub-hypothesis is presented below.

Diabetes and advanced age both increase the risk of acquiring AD. Aging and diabetes both cause endothelial dysfunction and vascular hypercontractibility. [251, 252] Aging and diabetes induced endothelial dysfunction can be partially reversed by treatment of tissues with SOD or SOD mimetics. [253, 254, 255] Glycosylated proteins generate superoxide at oxygen tensions present in the vasculature, especially in the presence of metal ions.[256, 257, 258, 259] Glycosylated proteins (especially blood

proteins) are increased in aging and diabetes. [260] Glycosylated hemoglobin is known to cause endothelial dysfunction in tissues from young animals, and the dysfunction is reversible by SOD and SOD mimetics. [261, 262,]

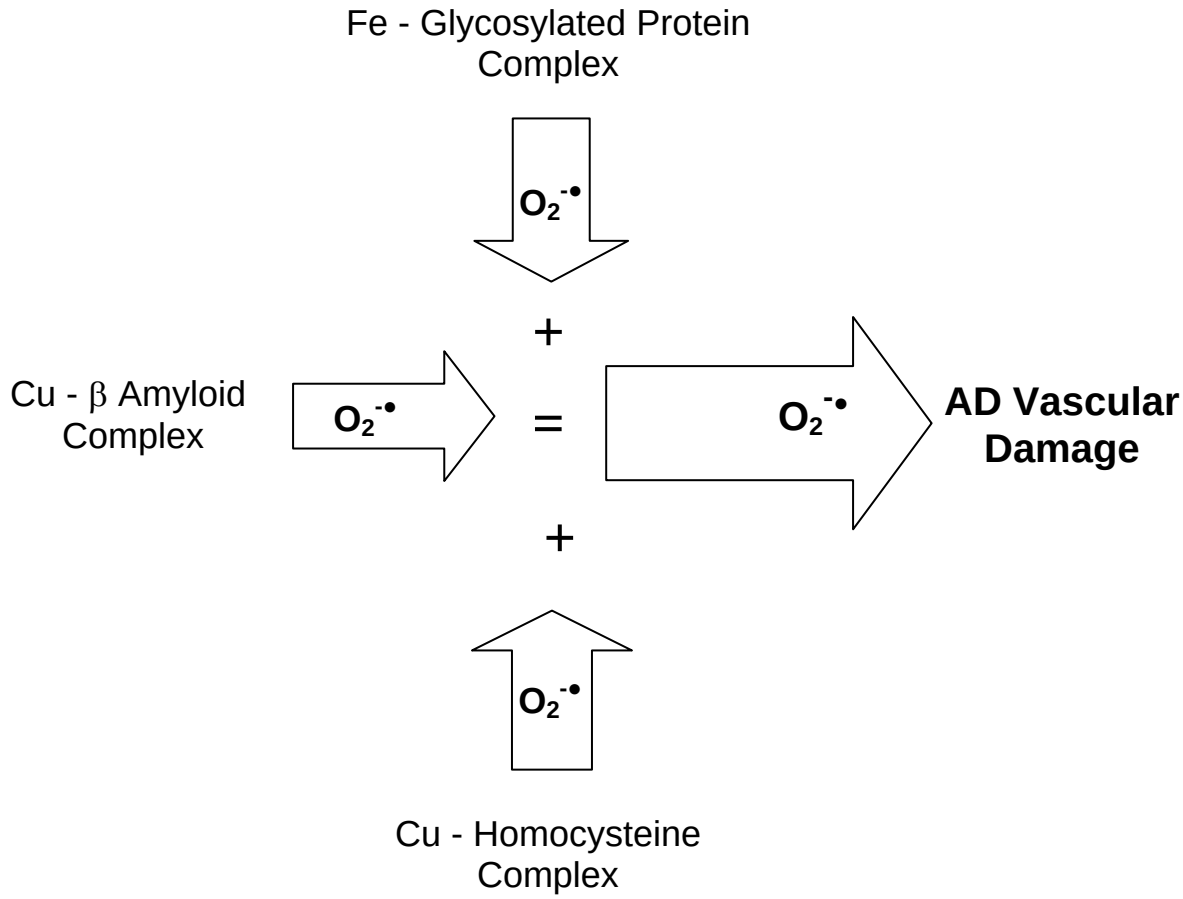

Figure 2.4 *Production of superoxide [$O_2^{-\cdot}$] radicals by various metal–protein complexes in the blood stream result in an increase in blood superoxide levels. These constantly increased levels of superoxide in the blood create more vascular dysfunction than β amyloid could by itself. Hence age, vascular diseases and diabetes all increase the risk of developing AD.*

Homocysteine plasma levels are increased in vascular disease conditions like hypertension and atherosclerosis and elevated blood homocysteine levels are an independent risk factor for morbidity and mortality. [263] Homocysteine causes

vascular dysfunction through superoxide production. [264, 265, 266, 267] Superoxide production by homocysteine (like β amyloid and glycosylated proteins) is dependant on copper being present as a cofactor for completing the redox cycle. [268, 269]

It is therefore likely that the increased incidence of AD in patients who are old and have diabetes or vascular diseases, is partially due to a direct additive vascular toxicity of superoxide radicals produced by β amyloid along with superoxide radicals produced by glycosylated proteins and homocysteine.

2.15 Salient features of the 'ABSENT' hypothesis

1. It can explain the variety of presentations, progress and clinical symptoms seen in AD, especially the late onset idiopathic form.

2. It can give a more integrated explanation for the apparent increased incidence and severity of late onset AD in patients with preexisting vascular conditions.

3. It can explain the reasons behind and role of almost all the histopathological and functional changes seen in AD.

4. It provides an understanding of the chemical mechanisms behind the toxic effects of β amyloid on both the neurons and their supporting vasculature.

5. An understanding of the mechanisms of the damage caused by β amyloid allows us to justify the use of newer assays (vascular) to assist in the discovery of disease modifying drugs to treat AD.

CHAPTER 3: DESIGN AND VALIDATION OF PEPTIDIC DOCKING TECHNIQUES

3.1 Introduction

The current chapter deals with design and validation of a new method for docking and scoring the interaction of peptidic inhibitors of β amyloid oligomerization to the 'self recognition' motif in β amyloid. The methods and algorithms developed in this chapter were later used to develop novel β amyloid oligomerization inhibitors.

The development of Disease Modifying Drugs (DMDs) for Alzheimer's Disease (AD) has been an unsuccessful endeavor and many small-molecule DMDs based on the amyloid hypothesis of AD have failed in clinical trials.[270] Peptidic inhibitors of β amyloid oligomerization are both specific and fairly non-toxic, however their potency and pharmacokinetic characteristics ("druggability") need significant improvement. The use of peptidic compounds as drugs is still widely seen as less than desirable, for reasons that were true a couple of decades ago. These reasons include susceptibility to enzymatic hydrolysis, the need for administration by injection and the potential to elicit immune responses. Therefore, peptidic drugs were often seen as niche products that addressed small therapeutic areas, such as Vancomycin for treating multi-drug resistant bacterial infections and Cyclosporine for immune suppression after organ transplant.

However, advancements such as an expanded repertoire of unnatural amino acid residues, newer methods for derivatizing peptidic drugs and the need to target receptors other than G-Protein Coupled Receptors have made peptidic drugs a competitive option. A number of very profitable and widely used drugs such as various haemopoietic factors, Pramlintide, Exenatide and a host of monoclonal antibodies to treat conditions ranging from auto-immune diseases to cancers have been approved in the past 15 years. Many of these peptidic/ protein drugs are

used for chronic conditions in preference to or in combination with small molecule drugs.

Such drugs range from cytotoxic anti-cancer drugs (dactinomycins, bleomycins), haemopoietic drugs (erythropoetin, sagramostim,fiilgastrim), immunosuppressive drugs (cyclosporin A and G, daclizumab, basiliximab, infliximab, etanerecep), immunomodulatory drugs (interferon beta and analogues, copaxone), hormonal drugs (insulin, growth hormone, IGF-1, desmopressin, octreotide, leuprolide, buserelin, ganirelix), cardiovascular drugs (nesiritide), anti-viral drugs (saquinavir, ritonavir, nelfinavir, lopinavir , enfuvirtide, interferon alpha and analogues), antibacterial drugs (vancomycin, teicoplanin, qinupristin/dalfopristin, polymyxins, bacitracins, colistins, capreomycin).

Computer Assisted Drug Design (CADD) is one of the possible approaches for speeding up the development of newer, and hopefully better, peptidic inhibitors of β amyloid aggregation. Recent advances in the field of Computer Assisted Drug Design (CADD) have made it a competitive and viable method for identifying and developing small-molecule ligands to many, large and semi-rigid, conventional receptor systems such as enzymes and G-Protein Coupled Receptors (GPCRs).[271, 272] CADD is primarily used to speed up the process, and reduce the cost, of developing pre-clinical drug candidates, though it can also be used to assist in the optimization of druggable ligands that are already in preclinical studies.

Established CADD methodologies are, however, not directly applicable to the development of peptidic ligands targeted towards unconventional receptors such β amyloid. Unlike ‘conventional’ receptors, such as GPCRs and enzymes, β amyloid is a flexible peptide without a well defined ligand-binding pocket. While there has been some progress in modeling protein-protein interaction with CADD, these techniques have not yet been successfully used to design peptidic ligands for modulating such interactions.[273, 274, 275, 276] Moreover, there have been very few

serious efforts at using computational chemistry based methods to study the interaction of peptidic ligands with amyloid -type receptors.[277, 278]

3.2 Computer assisted drug design

Rational drug discovery is an alternative to the use of High Throughput Screening (HTS) -type approaches for developing new drugs. Rational drug discovery techniques, such as computer assisted drug design, have been successfully used to help develop drugs including Angiotensin Converting Enzyme (ACE) inhibitors, Angiotensin II antagonists, HIV protease inhibitors and various anti-cancer kinase inhibitors.[279, 280] A number of books on CADD, such as 'Molecular Modeling: Principles and Applications' by Dr. Andrew Leach, are available and should be used to better understand the concepts and techniques underlying CADD.[281]

CADD methodologies fall into two categories, namely 'ligand-based' techniques and 'receptor-based' techniques. Ligand-based CADD have been successfully used to assist in the discovery and development of new druggable ligands for a variety of receptors.[282 , 283] The majority of ligand-based CADD techniques fall under the rubric of 'cheminformatics' and these two terms are often used in an interchangeable manner.[281]

Cheminformatics involves analyzing structural features of ligands, known to bind to the receptor of interest, with various data-processing algorithms to create structural 'fingerprints' associated with receptor affinity or activity. These structural 'fingerprints' can then be used to search for similar ligands in chemical databases and develop structure-activity relationship (SAR) models for prioritizing the next round of ligand synthesis. Ligand-based techniques do not require much information about the target receptor's structure and might therefore appear to be ideally suited for elucidating the SAR of peptidic ligands to β amyloid. However, ligand-based techniques are also exquisitely sensitive to the 3D spatial placement

of ligand pharmacophores and are therefore unsuitable for semi-flexible peptidic ligands.

Receptor-based techniques, in contrast to ligand-based techniques, are typically used only if a good quality model of the receptor's structure is available. In some cases, high-quality homology-based models of the receptor are an acceptable substitute and have produced good results.[284] As previously stated, the current chapter describes development and use of receptor-based techniques (such as receptor-ligand docking) to reproduce experimentally known structure-activity relationships of peptidic ligands to the 'self recognition' site in β amyloid. The methods developed and assumptions made, while based on experimental evidence, were unconventional and therefore necessary to first understand the conventional receptor-ligand docking/ scoring paradigm.

Software suites that can reliably replicate (or approximate) the X-ray crystal structures of ligand-receptor complexes are readily available.[285, 286, 287] The majority of receptor-ligand docking software suites and modules do however use a fairly similar approach to the receptor-ligand docking problem, namely a predominantly rigid model of the receptor. Some now implement varying degrees of flexibility for residue side chains lining the ligand-binding pocket, and have sub-modules/ scripts to help the user with basic chores such as checking the completeness of the receptor model and identifying ligand-binding cavities. The docking software then places a ligand (usually from a ligand database) in a random position, with pseudo-random perturbations of bond angles, inside the pre-defined ligand-binding cavity.

The next step involves a quick energy minimization of each starting conformation inside the receptor pocket to generate a docked pose. Each ligand undergoes this sequence of events for a few hundred to a few thousand times to ensure that it has thoroughly sampled the energy surface (and conformational space) inside the receptor cavity. All docked poses for a given ligand are scored with a scoring

algorithm and only the top 10-100 ligand poses are saved (and written) in an output database. Popular scoring algorithms are based on a direct or indirect measure of calculated binding energy. The procedure is repeated with each subsequent ligand in a given database until all ligands in the input database have been docked.

While finding the best conformation for a ligand in a receptor cavity is fairly easy, comparing the best docked poses of two or more ligands is harder and more subjective. Consensus scoring, which utilizes a number of popular scoring algorithms, is the most widely accepted method of identifying high affinity ligands. [288] Scoring algorithms like ChemScore, DrugScore, PMF, Score, and Ludi are implemented in many docking software suites. [289, 290 ,291, 292, 293] Recently, knowledge based and customizable scoring functions have been implemented in some docking software suites such as GOLD. [294] Computer Aided Drug Design (CADD) techniques have been most successful when high quality structures of the target receptor and a few ligands are available.[295, 296]

3.3 Challenges to *in silico* screening of β amyloid ligands

Successful application of receptor-based CADD techniques for *in silico* screening of peptidic ligands to β amyloid required the development of workable solutions for some systemic problems, which are listed below.

1. Since a high quality structural model of the ‘oligomerization ready’ receptor was unavailable, it was necessary to create a reasonable and evidence-based, receptor model for use in the docking/scoring studies.

2. The majority of current docking protocols were not designed for handling large and partially flexible ligands, nor were they designed to utilize receptors that lacked a typical ‘active site’ pocket. It was therefore necessary to modify existing generic docking protocols for use with the β amyloid receptor model.

3. Popular ligand-scoring algorithms were not designed or optimized for ranking peptidic ligands bound to 'open' ligand binding sites. Therefore, a modified version of an existing generic scoring algorithm (BHB) was developed for scoring β amyloid receptor-ligand complexes.[297]

3.4 Insights into the structure of β amyloid monomers

The process by which a nascent random coil monomer becomes a highly structured unit in a fibril is poorly understood.[298] Since high quality experimentally derived structures of 'oligomerization ready' β amyloid monomers were not available, it was necessary to perform a meta-analysis of all available structural data to obtain an insight into the putative structure of these monomers.[299] Our current understanding of the process of β amyloid oligomerization suggests that nascent cleaved β amyloid has no defined secondary structure (see Figure 3.1 A). Incubation of the nascent peptide causes progressive increase in the β sheet content of its secondary structure (see Figure 3.1 B, C, D) until it is incorporated in fibrils with very high β sheet content (see Figure 3.1 E).[300] The structures shown in Figure 3.1 are based on the results of MD simulations (nascent monomer),[301] best case fits for indirect experimental evidence (hairpin monomer and dimer)[302], protein-protein docking servers (soluble oligomer)[303] and direct experimental data (fibrils).[82]

Experiments measuring rates of β amyloid oligomerization have consistently shown the presence of a 'lag phase' during which oligomer formation is almost absent. It is likely that nascent β amyloid monomers exist as ensembles of random coils that might have some temporary secondary structure, but rapidly shift from one low energy form to another. An example of such a semi-stable coiled structure can be seen in Figure 3.1 - A. CD studies of the nascent 11mer and 7mer are also compatible with a random coil-type structure. [304]

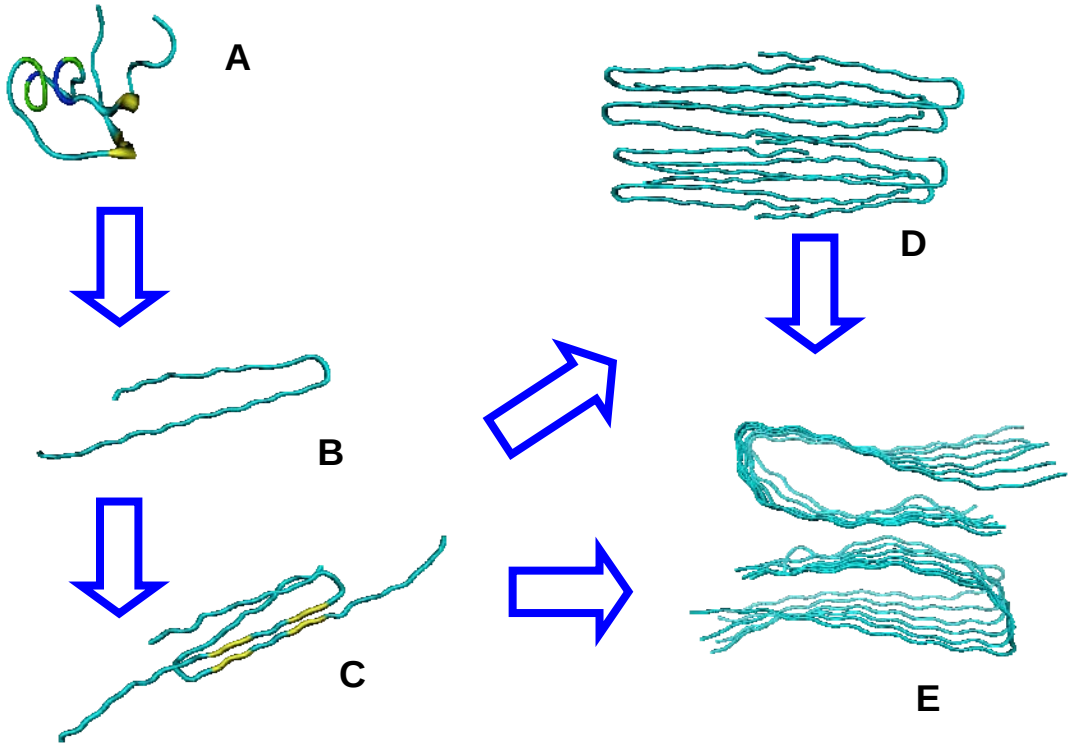

Figure 3.1 *A simplified version of the chain of events leading from nascent β amyloid monomers to their insoluble fibrillar form. The naming scheme- A;nascent monomer, B; monomer with loose hairpin, C; dimer, D; soluble oligomers, E; fibrils.*

The first stage of oligomerization (A→B in Figure 3.1) likely involves the formation of an intra-molecular salt bridge between the residues D_{23} and K_{28}. Modified β amyloid peptides with a preformed D_{23}-K_{28} linkage start oligomerizing almost immediately, thereby suggesting that the interaction is important for initiating the process of β amyloid oligomerization. [305, 306] It is therefore likely that a loose hairpin like structure (Figure 3.1 - B) formed subsequent to this interaction is necessary for the next step in β amyloid oligomerization.

The process of β amyloid oligomerization (B→C and C→D in Figure 3.1) has been studied with techniques such as Circular Dichroism (CD), Fourier Transform Infrared Spectroscopy (FTIR) and Atomic Force Microscopy (AFM). Data obtained from CD and FTIR seem to suggest that oligomerization is accompanied by an increase in β strand content of secondary structure. [307] . The catalytic effect of sub-micellar concentrations of surfactants such as Sodium Dodecyl Sulfate (SDS) on oligomerization is another recently uncovered and potentially important area of research.[67, 308]

While neither CD nor FTIR can identify individual amino acid residues involved in the initiation and propagation of observed secondary structure changes, AFM seems to show folded hairpin like structures binding each other to form dimers and higher oligomers. [302, 309] Experimental evidence, discussed in Chapter 1, suggests that β amyloid oligomerization occurs via self recognition through a 7-mer motif, $K_{16}LVFFAE_{22}$, in β amyloid. [310] Recent experimental evidence also suggests that soluble oligomers have anti-parallel β strands as opposed to the parallel β strands seen in β amyloid fibrils.[302, 311] The β amyloid dimer model in Figure 3.1 - C is based on an extrapolation of such experimental data.

The basic 7-mer 'self recognition' motif, $K_{16}LVFFAE_{22}$, can form β sheet rich fibrils. [103] Larger peptides that incorporate the 'self recognition' motif such as β amyloid (13-23), β amyloid (14-23) also form β sheet rich fibrils that are morphologically very similar to β amyloid.[310, 312]. Solid-state NMR experiments on fibrils formed by even larger pieces of β amyloid exhibit substantial β strand-type secondary structure. CD/ FTIR studies of peptides containing the self recognition region as an induced dimer also suggest that their secondary structure has significant β strand content. [313, 314] The observation of ordered and regular fibrils by Electron Microscopy (EM) backs up the conclusions of solid-state NMR experiments.

Based on this evidence, it is likely that the sequence containing the ‘self-recognition’ site and its immediate vicinity have a tendency to adopt a β strand-type secondary structure. It is also likely that two molecules of β amyloid bind to each other when their ‘self recognition’ motifs have β strand-type secondary structure. Moreover MD simulations on the 11mer done in our research group suggest that the 11mer has a predominantly extended β strand-type secondary structure.

A majority of the current (and next chapter) concern the use of computational chemistry to model the interaction of β amyloid with peptidic ligands, and therefore it is worthwhile to understand the concepts underlying these computational treatments and algorithms.

3.5 Basics of molecular mechanics

All theoretical chemistry techniques that were developed and used in this thesis are based on the treatment of molecules by Molecular Mechanics. A brief summary of the basics of Molecular Mechanics (MM) and other techniques used in this thesis is given below.
Molecular Mechanics (MM) uses concepts derived from Newtonian mechanics to model and simulate molecular systems. The potential energy of all systems in molecular mechanics is calculated using empirical potential functions. Molecular mechanics is especially suited to study a wide size range of molecules as well as the interactions of diverse types of molecules, such as ligand-receptor interactions

The molecular system's total potential energy (E) in a given conformation is expressed as a sum of the covalent and non-covalent energy terms.

$$E_{total} = \sum_{bonds} \frac{k_i}{2} \Delta r_{ij}^2 + \sum_{angles} \frac{k_i}{2} \Delta \theta_{ijk}^2 + \sum_{torsions} \frac{V_n}{2} (1 + \cos(n\omega - \gamma)$$
$$+ \sum_{i=1}^{N} \sum_{j=i+1}^{N} \left(4\varepsilon_{ij} \left[\left(\frac{\sigma_{ij}}{r_{ij}} \right)^{12} - \left(\frac{\sigma_{ij}}{r_{ij}} \right)^{6} \right] + \frac{q_i q_j}{4\pi\varepsilon_0 r_{ij}} \right) \quad (3.1)$$

The first term in the equation models the interaction between a pair of bonded atoms (*i* and *j*), where $\Delta r_{ij} = r_{ij} - r_{ij}^0$ is the difference between the actual and reference bond lengths for that particular atom pair. The second term applies a similar treatment to the valence angles of connected atom triplets in the molecular system such that $\Delta\theta_{ijk} = \theta_{ijk} - \theta_{ijk}^0$ is the difference between actual and reference bond angles for any connected atom triplet (*i-j-k*). The third term models torsion induced energy changes in the bond (j-k) between a connected atom quadruplet (i-j-k-l). The fourth terms models non-bonded interactions between all pairs of atoms in the system, that are either separated by at least three bonds or are not connected. Van der Waals interactions are typically modeled with a 6-12 Lennard-Jones potential and electrostatic interactions are modeled through a Coulomb potential term.

The values and parameters for each atom type and interaction are defined by the force field used for that molecular mechanics calculation. Force field functions and parameter sets are derived from both experimental work and high-level quantum mechanical calculations. "All-atom" force fields provide parameters for every atom in a system, including hydrogen. Well known “all atoms” molecular mechanics force fields such as AMBER, OPLS, MMFF94 are implemented in many molecular modeling suites. [315, 316, 317] "United-atom" force fields such as GROMACS, which are used in simulations of very large (>20k atoms) molecular systems, treat the hydrogen and carbon atoms in methyl and methylene groups as a single interaction center to simplify calculations. [318]

The Merck Molecular Force Field 94 (MMFF94) used for all computational work described in this thesis, is a highly regarded and well-implemented Class 3 force field, which can account for effects such as electronegativity and hyperconjugation.

3.6 Basics of the MMFF94 force field family

The general form of MMFF94 energy expression can be written as:

$$E_{MMFF} = \sum EB_{ij} + \sum EA_{ijk} + \sum EBA_{ijk} + \sum EOOP_{ijk;l} + \sum ET_{ijkl} + \sum EvdW_{ij} + \sum EQ_{ij} \quad (3.2)$$

where E_{MMFF} and all it's constituent terms are expressed in kilocalories per mole when distances and degrees are measured in angstroms and degrees respectively. Each term is further explained below:

Bond Stretching

MMFF94 models bond stretching through a modified quartic function:

$$EB_{ij} = 143.9325\frac{kb_{ij}}{2}\Delta r_{ij}^2 \times \left(1 + cs\Delta r_{ij} + \frac{7}{12}cs^2\Delta r_{ij}^2\right) \quad (3.3)$$

where kb_{ij} is the force constant (md/Å), $\Delta r_{ij} = r_{ij} - r_{ij}^0$ is the difference between actual and reference bond lengths, and cs= (*-2 Å*$^{-1}$).

Angle Bending

Angle bending in MMFF94 is modeled with a cubic expansion, however it uses a much more extensive set of parameters, as compared to other common force fields (e.g. AMBER), for modeling delocalized single bonds and small or unusual ring systems. The form is:

$$EA_{ijk} = 0.048844\frac{ka_{ijk}}{2}\Delta\theta_{ijk}^2\left(1 + cb\Delta\theta_{ijk}\right) \quad (3.4\ a)$$

where ka_{ijk} is the force constant (md Å/rad^2), $\Delta\theta_{ijk} = \theta_{ijk} - \theta^0_{ijk}$ is the difference between actual and reference bond angles (degrees) and cb = -0.007 deg^{-1} (or -0.4rad^{-1}) is the "cubic bend" constant. For linear or near-linear bond angles, MMFF94 employs:

$$EA_{ijk} = 143.9325\, ka_{ijk}\left(1+\cos\theta_{ijk}\right) \qquad \text{(3.4 b)}$$

Stretch Bend Interaction

Older MM force fields (MM2, AMBER) do not model stretch-bend interactions for the sake of simplicity, however modeling this interaction is crucial for coupling the *i-j* and *k-j* stretches to the *i-j-k* bend. MMFF94 uses the form:

$$EBA_{ijk} = 2.51210\left(kba_{ijk}\Delta r_{ij} + kba_{kji}\Delta r_{kj}\right)\Delta\theta_{ijk} \qquad \text{(3.5)}$$

where kba_{ijk} and kba_{kji} are force constants (md/ rad) that couple the i-j and k-j stretches to the i-j-k bend.

Out of Plane Bending at Tricoordinate Centers

Out of Plane Bending is another interaction that is not independently modeled by older MM force fields (MM2, AMBER). They often try to indirectly model this effect through the creation of special atom classes to deal with the most common examples of such effects (e.g. chiral amines). However modeling this as an independent entity allows MMFF94 to apply this effect to every atom system. The functional form is:

$$EOOP_{ijk;l} = 0.043844\ \frac{kcoop_{ijk;l}}{2}\chi^2_{ijk;l} \qquad \text{(3.6)}$$

where $kcoop_{ijk;l}$ is the force constant (md Å/rad^2) and $\chi_{ijk;l}$ is the angle between the bond j-l and plane i-j-k.

Torsion Interactions

MMFF94 uses a fairly conventional model of torsional interactions with the form:

$$ET_{ijkl} = 0.5\ ((V_1(1+\cos\phi) + V_2(1-\cos 2\phi) + V_3(1+\cos 3\phi)) \qquad (3.7)$$

where V_1, V_2 and V_3 depend on the atom types for atoms *i,j,k* and *l*, where *i-j*, *j-k* and *k-l* are bonded pairs and ϕ is the *i-j-k-l* torsion angle.

Van der Waals Interactions

MMFF94 uses a "buffered 7-14" version of Lennard-Jones potential instead of the more classical 6-12 version used in equation 3.1

$$EvdW_{ij} = \varepsilon_{IJ}\left(\frac{1.07R_{ij}^{*}}{R_{ij}+0.07R_{ij}^{*}}\right)^{7}\left(\frac{1.12R_{ij}^{*7}}{R_{ij}^{7}+0.12R_{ij}^{*7}}-2\right) \qquad (3.8)$$

where R_{IJ}^{*} is the buffering constant and is linked to the atomic polarizability. A more detailed version of this equation can be found in the original MMFF94 paper.

Electrostatic Interactions

MMFF94 models electrostatic interaction through a buffered coulombic term:

$$EQ_{ij} = 332.0716 \times q_i q_j / D\left(R_{ij}+\delta\right)^{n} \qquad (3.9)$$

where q_i and q_j are partial atomic charges, R_{ij} is the internuclear separation in Å, δ = 0.05 Å is the "electrostatic buffering" constant and D is the dielectric constant. The exponent *n* usually taken as 1, though one can also use *n*=2 to simulate a simple distance-dependent dielectric constant. In MMFF94, 1-4 electrostatic interactions are scaled by a factor of 0.75.

3.7 Energy minimization in molecular mechanics

In computational chemistry, energy minimization methods are used to compute the equilibrium configuration of molecules under the given force field parameter regimen. Molecules, especially those that are complex and flexible, often have both local and global energy minima.

Energy minimization algorithms employ various mathematical procedures to move atoms and reduce the net forces (the gradients of potential energy) on the atoms until they become insignificant. A well established algorithm of energy minimization can be an efficient tool for molecular structure optimization and can often match the bond lengths and angles obtained with *ab initio* methods. The same cannot be said about relative energy differences and changes, where *ab initio* methods are significantly superior to molecular mechanics. The implementation of energy minimization in MOE modeling suite is explained in its help files ("Energy Minimization"), and is summarized below. MOE uses a succession of three methods to effect an energy minimization, namely Steepest Descent (SD), Conjugate Gradient (CG) and Truncated Newton (TN). Switching from one method to another occurs at preset levels of gradient convergence.

Under SD optimization, the search proceeds along the direction of the forces. SD is intuitive but extremely inefficient after a few iterations and it is only used when the gradient is extremely high. When the gradient is sufficiently small (but still quite high) the CG method is used. The Conjugate Gradients (CG) method improves upon SD by choosing the next search direction in a way so as to not undo the progress accomplished by the previous step. CG performs well in strained conditions; however, it exhibits poor convergence properties. Once the gradient is reasonable, the TN method is used.

The Truncated Newton (TN) method is the most efficient large-scale nonlinear optimization method known, but it is also very resource intensive to implement

when the input structure is of poor quality. TN is based on the idea that an exact solution of the Newton equation is unnecessary at every step and is indeed computationally wasteful in the framework of a basic descent method. Any direction of descent will suffice if the objective function is not well approximated by a convex quadratic and, as a solution to the minimization problem is approaching, more effort in solution of the Newton equation may be warranted. The appeal of TN to energy optimizations in molecular mechanics lies in their ability to exploit function structure to accelerate convergence.

3.8 Solvation in molecular mechanics

The vast majority of chemical systems are solvated, but the basic molecular mechanics equation treats space between two unconnected atoms as a vacuum. Under such conditions, surface charges that would ordinarily interact with solvent molecules can interact with each other, producing molecular conformations that are unlikely to be present in any physiological environment. It is almost always necessary to model the effects of solvation in a molecular mechanics calculation.

The use of explicit water molecule models in the simulation box with the molecules of interest is the ideal, but computationally expensive, solution to this problem. The use of distance dependent dielectric constant and various implicit solvation methods are computationally inexpensive alternatives to the use of explicit water molecule models. These approximations try to model the average behavior of water and do reproduce the effects of solvation with varying degrees of accuracy,

A variety of solvent dielectric models are implemented in MOE. They range from simple Coulomb models to Generalized Born solvation models. All the molecular modeling, docking and simulations described in this thesis were performed using either Distance Dependent Dielectric (DDD) or Generalized Born/ Solvent Approximation (GB/SA).

A distance dependent dielectric tries to mimic the electrostatic shielding effect of water by reducing the strength of charged atoms in a distance dependant manner.

While it is a poor substitute for explicit water or even GB/SA in molecular dynamic simulations, it is perfectly adequate for energy minimization routines.

The implementation of Distance Dependent Dielectric (DDD) in MOE is explained in the help contents section - “Potential Energy Selection and Configuration”. The equation for implementing DDD in MOE has been reproduced below.

$$E_{ele} = \frac{W_{ele} e^2}{4\pi\varepsilon_0 d} \sum_{i<j} q_i q_j \left[\frac{1}{\left(r_{ij} + b_{ele}\right)^2} \right] s\left(r_{ij}\right) T_{ij} I_{ij}^{ele} \qquad (3.10)$$

where E_{ele} is the electrostatics energy, W_{ele} is a weight, d is the dielectric constant in the interior of the solute, s is a vdW smoothing (cutoff) function and T_{ij} is an interaction scale factor used to scale particular non-bonded interactions, q_i is the partial charge on atom i, b_{ele} is a buffering constant to prevent zero denominators. I^{ele}, similarly to I^{vdw}, is an interaction scale factor defined to be 0 for 1-2 and 1-3 interactions, a parameter set-dependent scale value for 1-4 interactions, and 1 for other interactions.

The Generalized Born model of solvent approximation is more suitable for molecular dynamic-type simulations where the increased electrostatic shielding is useful to better sample the conformational space. It is based on modeling the protein as a sphere whose internal dielectric constant differs from the external solvent. GB/SA is simply a Generalized Born (GB) model augmented with the hydrophobic solvent accessible Surface Area (SA) term. GB/SA can however exaggerate or reduce the shielding effect of water, depending on the interaction. [319] The implementation of GB/SA in MOE can also be found in the help file for “Potential Energy Selection and Configuration” and is reproduced below.

$$E_{sol} = -w_{sol} W \left(d^{-1} - d_x^{-1}\right) \frac{e^2}{4\pi\varepsilon_0} \frac{1}{2} \sum_{i=1}^{n} \sum_{j=1}^{n} \frac{q_i q_j \sqrt{G_i G_j}}{\sqrt{y_{ij} + \exp\left(-y_{ij}\right)/4}} s\left(r_{ij}\right) T_{ij} \qquad (3.11)$$

E_{sol} is the implicit solvation energy calculated using the Generalized Born model (GB/VI), w_{sol} and W are weights, d is the dielectric constant in the interior of the

solute, d_x is the dielectric constant of the solvent and *s* is the smoothing (cutoff) function and T_{ij} is an interaction scale factor used to scale particular non-bonded interactions. G_i is the self energy of the atom and $y_{ij} = r_{ij}^2 G_i G_j$

3.9 Generating the β amyloid receptor model.

The majority of the molecular modeling tasks in this thesis were performed with the Molecular Operating Environment (MOE) modeling suite version 2004.03 to 2008.10. [320] The 'protein builder' module was used to create a β strand 11mer with the following sequence – H_{13}HQKLVFFAED$_{23}$. The final form of the model can be seen in Figure 3.3.

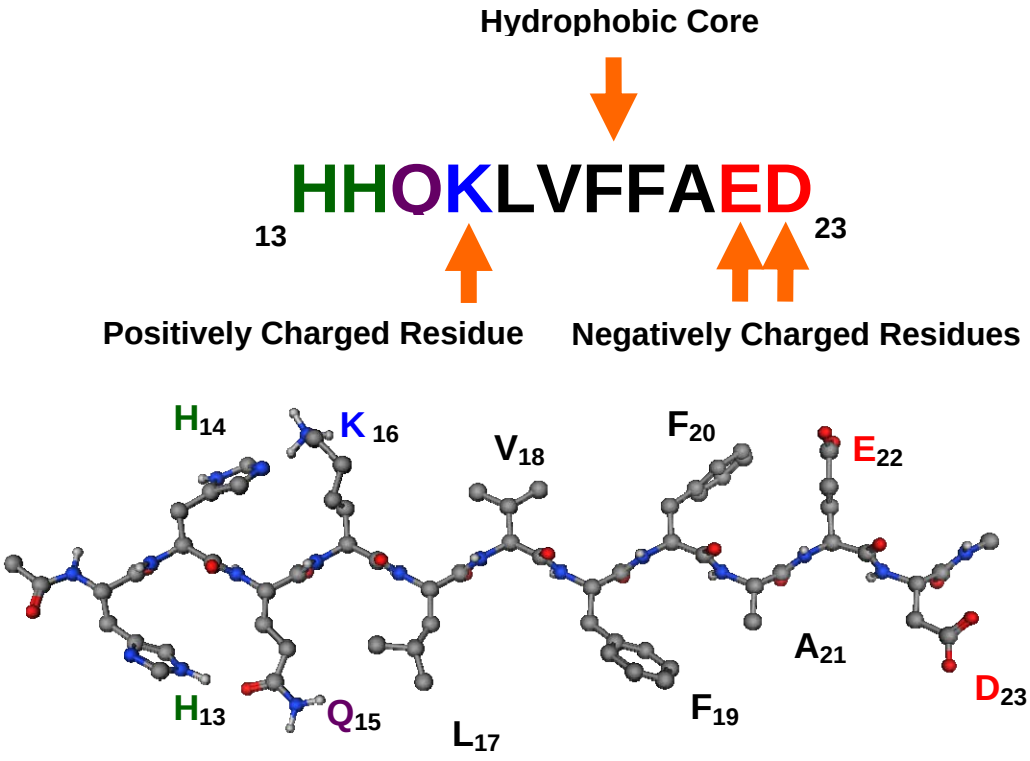

Figure 3.2 *A molecular model of the receptor (rendered without non-polar hydrogen atoms) used in docking simulations. The backbone of the receptor is a β strand to approximate it's conformation in an 'oligomerization ready' monomer.*

The 11mer was chosen as it had both the self-recognition motif and the major part of the Cu (II) binding site. The 11mer model used unprotonated histidine residues at both H_{13} and H_{14}. Histidine residues have a pKa of approximately 7.The N-terminus was acetylated and C-terminus amidated to better reproduce the characteristics of the 11 mer motif in a β amyloid monomer. The structure was optimized using the MMFF94x force field under GB/SA solvation. [321, 322]

The placements and conformations of AA residue side-chains were optimized by performing a conformational search after the backbone atoms of the model receptor were fixed. Default settings for stochastic conformational search in MOE were used with two important exceptions (chiral inversion = off and conformation limit = 500). The lowest energy conformation was used as the 11mer receptor model.

A similar protocol was used for creating and optimizing the structures of test ligands. The creation of a receptor and ligands without significant conformational strain but still possessing an intact β strand backbone was the main reason for the above mentioned protocol.

3.10 The receptor-ligand docking protocol

Conventional docking protocols utilize cavity detection algorithms and random starting conformations for each docking run and thus work well for docking rigid small molecule ligands inside well defined receptor cavities. However these features make them virtually useless for docking two peptide strands to each other. In such cases, there is no well defined cavity and random starting conformations make it hard and very time consuming for the peptidic ligand to find an acceptable conformation that binds to the receptor peptide strand. Therefore it was necessary to use a simpler docking protocol, which would still allow the ligand to thoroughly sample the conformational space around the receptor.

It should be noted that a single type of docking protocol was inadequate to allow anything close to modeling a flexible interaction of the receptor and ligand, which was essential for replicating a peptide strand to strand interaction. The docking protocol used therefore had 3 consecutive docking routines that tried to replicate the interactions as they would occur *in vitro* (or *in vivo*). Only the first step was a classical receptor-ligand docking and was performed with ‘dock.svl’. The subsequent two steps, performed with ‘analysis_dock.svl’, were essentially energy minimization steps that allowed for graduated receptor and ligand flexibility. The three steps are summarized below and are shown in Figure 3.3.

1. Simulated annealing of a fixed receptor and a flexible ligand in Generalized-Born (GB) salvation was performed with the dock.svl script (see Figure 3.3).
2. Energy minimization with a fixed receptor and a flexible ligand in a distance dependent dielectric was performed with analysis_dock.svl (see Figure 3.3).
3. Energy minimization with a flexible receptor and ligand in a distance dependent dielectric was once again performed with analysis_dock.svl, but with a different set of settings (see Figure 3.3).

The scripts ‘dock.svl’ and ‘analysis_dock.svl’ are reproduced in the data CD accompanying this thesis, along with a commentary on the procedure to use them in Appendix A. The *.svl extension of these scripts indicates that they are written in Scientific Vector Language (SVL), which is the native scripting language implemented in all versions of the MOE software suite.

The docking box was adjusted such that it contained the receptor-ligand complex in a tight space that was nonetheless sufficient for the AA side-chains and backbone amides to sample a variety of conformations and viable interactions. Simulated annealing (montecarlo based) was used for docking as it is somewhat more thorough at sampling conformational space.

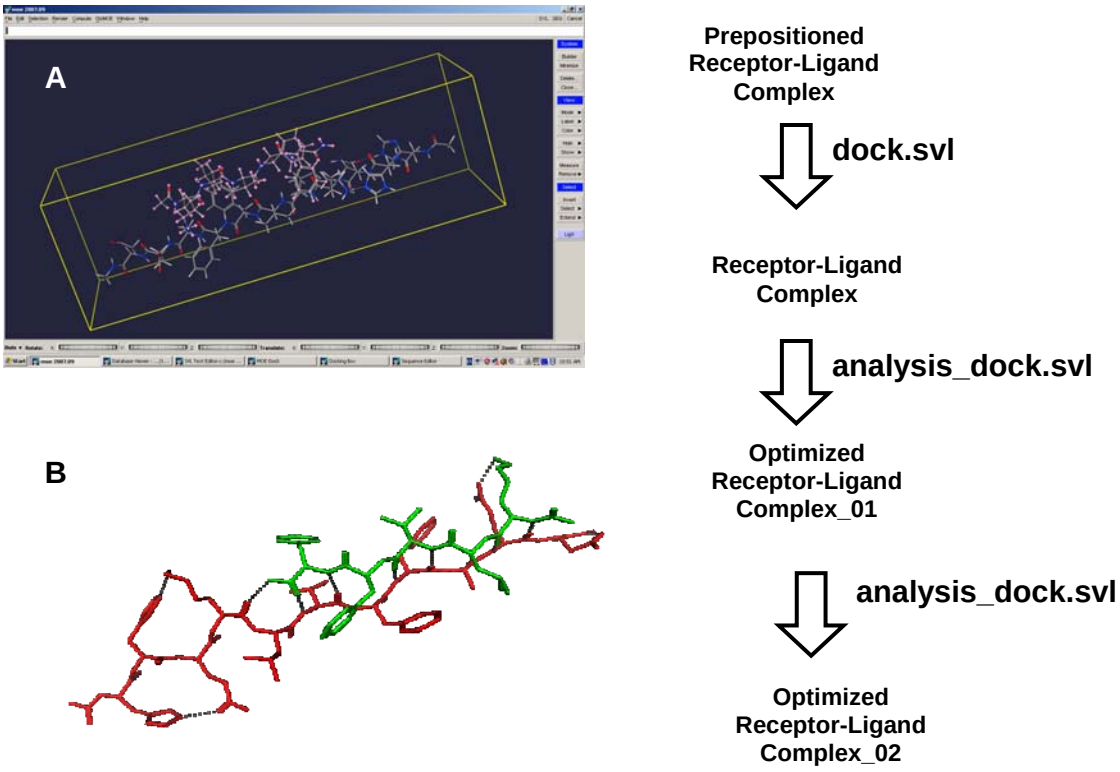

Figure 3.3 *Overview of the ligand docking procedure. A; screen capture of the beginning of a docking run, B; one representative docked and minimized optimized receptor-ligand complex (red= receptor, green= ligand). The flowchart to the right of A & B summarizes the overall workflow of ligand docking procedure.*

Simulated annealing explores various states of a configuration space by generating small random changes in the current state and then accepting or rejecting each new state according to the Metropolis criterion.[323] According to this criterion, moves that decrease the energy of the system are always accepted, while moves that increase the energy of the system are accepted according to probability *p*.

$$\rho = \exp\left(\frac{-\Delta u}{kT} \right) \qquad (3.12)$$

where $\Delta u = u_1 - u_0$ and u_0 is the energy of the current state, u_1 is the energy of the new state, T is the temperature of the simulation, and *k* is Boltzmann's constant.

A simulated annealing *run* consists of a sequence of Monte Carlo *cycles*, each cycle consisting of a number of *moves*, or steps. The temperature is held constant during each cycle, and is systematically reduced from one cycle to the next. The second and third steps of the docking process were performed with a script known as 'analysis_dock.svl'. The script, and settings used for the second and third step of the docking process, can be found in Appendix B. The rationale and implementation of energy minimization in that script has also been explained in other publications.[324]

3.11 Scoring the receptor-ligand complex

Assessing the fit and strength of ligand-receptor interactions is an essential component of modern drug discovery. While the most accurate measurements of ligand-receptor affinity still require a receptor-binding assay, current CADD methodologies can now achieve a fair degree of discrimination between, and gradation of, ligands based on their calculated affinities. Methods used to compare the top docked structures of two or more ligands to the same receptor are known as docked 'ligand scoring' functions.

The use of scoring functions to compare the 'best' docked structures of different ligands is a much harder problem than comparing various docked 'poses' of the same ligand. Established scoring functions, such as ChemScore, DrugScore, PMF, Score and Ludi attempt to assess ligand-receptor interactions by estimating the free energy of their interaction. While the best docked pose of a ligand to a receptor can be easily identified by calculating the approximate binding energy of each of the docked poses to the receptor, comparing two ligands by comparing calculated binding energies alone is less than satisfactory and was the reason behind the development of the BHB ligand scoring system.

The acronym of BHB is based on the descriptors it utilizes: **B**inding energy, **H**ydrogen bonding, and receptor **B**uriedness. The BHB scoring function is knowledge-based in the sense that some information about receptor-binding in the specific receptor system is incorporated into it. The major factors in our scoring function are two important properties of the ligand-receptor system: the full spatial complementarity of the ligand and the receptor (described as “buriedness”) and the occurrence of hydrogen bonding with a list of specific residues. BHB utilizes environment-dependent surface functions implemented in SVL. These functions are used to calculate receptor buriedness and hydrogen bonding.

Receptor buriedness is a measure of how well the docked ligand occupies it’s binding site in comparison to known high-affinity ligands or, alternatively, whether they have contact with identified residues in the pocket. The possibility of hydrogen bond formation is checked for selected residues that are recognized as being important in the binding of known ligands. The approximate binding energy is calculated from optimized bound and free conformations of the ligand-receptor system. A visual description of these three functions can be seen in Figure 3.6.

A simplified form of the generic BHB equation can be written as:

$$BHB_{score} = [-0.05E\_bind] + [20(RB + RB^3)] + [\#HB * 5] \qquad (3.13)$$

where E_bind = approximate binding energy (in kcal/mol), RB = receptor buriedness (ratio less than 1.0) and # *HB* = number of hydrogen bonds to which additional weight is assigned. In the context of this receptor system, all important HBs are salt bridges formed between complementary charged residue sidechains.

As an approximate binding energy (E_bind) can be calculated, the question may be asked why additional descriptors are necessary. Unfortunately, there are a few conceptual and practical problems with excessive reliance on an approximate measurement of binding energy. [325] Large errors in the binding energy can arise

due to several different factors (e.g., full or partial rigidity of the receptor, the neglect of entropic terms, errors in the molecular mechanics energy expressions, unknown position of water molecules etc).

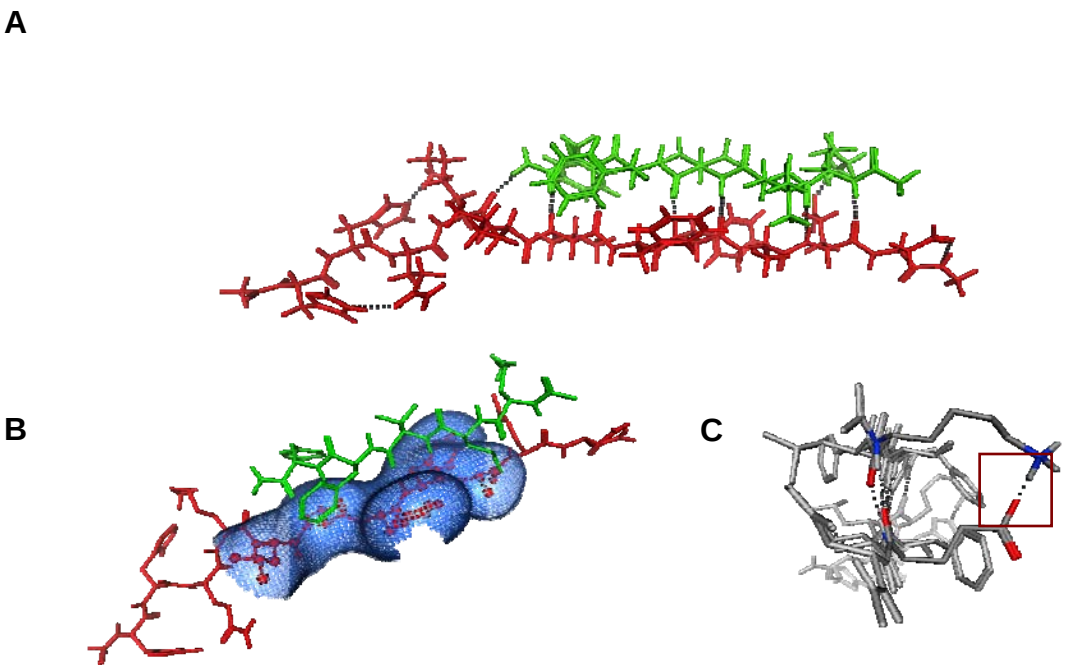

Figure 3.4 *The BHB Ligand Scoring System. A; approximate ''binding energy' is calculated by subtracting the sum of localized potential energy minima for ligand (green) and receptor (red) by themselves from the potential energy of the complex. B; the 'buried' part of receptor's vdw surface is rendered with the mesh. C; one of the salt bridges ('hydrogen bonds') between side chains of the ligand and receptor is highlighted.*

The calculated binding energy does however correctly predicts reduced activity for those molecules that have internal strain, mismatches of pharmacophoric points or hydrophobic surfaces, and those that make bad van der Waals contact with the receptor. For this reason, the binding energy was found most useful in combination with the other descriptors such as Hydrogen Bonds (HB) and Receptor Buriedness

(RB). A more complete account of the settings, methodology and script for performing the binding energy calculations used in this thesis can be found in Appendix B.

The Hydrogen Bond (HB) function in BHB does not measure all HBs between the ligand and the receptor. It only enumerates HBs that have a measurable and pivotal role in ligand affinity, as it appears that not all HBs between ligand and receptor carry the same “weight” as far as ligand affinity is concerned. A significant part of a ligand’s affinity can often be attributed to 2-3 HB interactions and salt bridge HBs between charged side-chains on the receptor and ligand to be especially important for β amyloid peptidic ligand binding. Experimental structure-activity relationship seems to suggest that a ligand that can make such an interaction (eg Ac-KLVFF-NH_2) has a much higher affinity than one that cannot (eg Ac-ALVFF-NH_2), inspite of an identical number of other HBs arising from the interactions of their amide backbones.[99] Specified HB interactions were identified by functions built in MOE and its implementation is briefly explained in Appendix B. In the basic BHB equation all such ‘important’ hydrogen bonds were normalized to a weight of 10. Given that the smallest self-recognition domain in β amyloid is the KLVFFAE motif which has the potential for 2 side-chain salt-bridge interactions, we used a weight of 5 for each instance of salt-bridge formation.

Receptor buriedness (RB) is a proxy measurement for hydrophobic interactions between the receptor and ligand. It is calculated by a series of steps that begin with measuring the surface area of the hydrophobic part of the receptor, the LVFFA motif in this case, by generating closely packed spheres of 0.3 Å radius on the vdW surface of the selected residues. The script calculates the total exposed area of this beaded surface and it is considered to be approximate surface area of the receptor. The script then identified the fraction of this surface area within 4.5 Å of any ligand atom. This is considered to be the buried surface area and receptor buriedness is the ratio of buried receptor surface area to total receptor surface

area. Receptor buriedness (RB) was also calculated by using ‘analysis_dock.svl’ in MOE and relevant info on this script can once again be found in Appendix B.

3.12 Selection of the test ligand set

While a fair amount of data on the experimental structure-activity relationship (SAR) of peptidic inhibitors of β amyloid aggregation is available, there are two major problems with using most of the available SAR data for modeling the docking of peptidic inhibitors to β amyloid.

1. Most available SAR data concerns the ability of these inhibitors to block β amyloid fibril formation and cytotoxicity. While both assays are relevant to drug development, they are at best proxy measurements for the real (or even relative) binding affinity of these compounds to β amyloid. Since our virtual screening methodology tries to quantify the binding of these ligands to β amyloid, proxy measurements of such activity are best used in a supporting role.

2. Various proxy assays for β amyloid aggregation (fibrilization, cytotoxicity) are often not standardized either in their experimental conditions or by the presence of a few well known ‘standard’ ligands.

There are very few publications that have reported any SAR data on the affinity of their ligands to β amyloid. Fortunately, one of the earliest publications by Tjernberg et al on the SAR of peptidic inhibitors contains a very extensive series of relative affinity measurements.

3.13 Possibilities for ligand-receptor interactions

It is not widely appreciated that two peptidic β strands can bind to each other in 8 different modes. Most are aware of two basic modes (parallel and anti-parallel), but

since each β strand peptide has 2 binding edges perpendicular to the axis of amide backbone, it creates 4 different possibilities for both parallel and anti-parallel modes. For small fragments of β amyloid, parallel modes are not favored in computational analysis or experimental NMR data. The energetic difference between anti-parallel and parallel binding modes is however quite small, and the dominance of one mode over the other is driven by favorable sidechain interactions. In the case of β amyloid fragments, salt-bridge formation between charged residues (K and E, D) is the dominant sidechain interactions and strongly favors the anti-parallel binding mode. All four anti-parallel binding modes for the 11-mer receptor are shown in Figure 3.5.

The charge complementarities are based on a feature of the 11mer and indeed any β amyloid peptide fragment that contains the sequence QKLVFFAED. In one mode both K_{16}-E_{22} and E_{22}-K_{16} will interact, while in another mode, K_{16}-D_{23} and D_{23}-K_{16} interact, as seen in Figure 3.5.

The first mode is similar to that observed in solid state NMR of fibrils formed by small peptides containing the self recognition site and is referred to henceforth as the ‘A’ Mode, while the second mode is called as the ‘B’ mode. Sidechain stacking is another variable with 2 possibilities. The ‘ligand’ can interact with one edge of the β strand or it can interact with the other edge. These edges are defined by the direction of backbone –NH moieties, and we chose to name backbone -NH moieties of all even numbered (based on position in β amyloid 40 and 42) residues as ‘Up’ and odd numbered ones as ‘Down’.

The 4 possible anti-parallel binding combinations summarized in Figure 3.5 and it transpires that ‘Up-A’ is the favored binding mode. Both E_bind (binding energy) and BHB scores identify the same mode, UpA, as the favored mode of binding. It seemed that both electrostatic contact patterns and packing of hydrophobic sidechains were important for ensuring the best ligand-receptor fit.

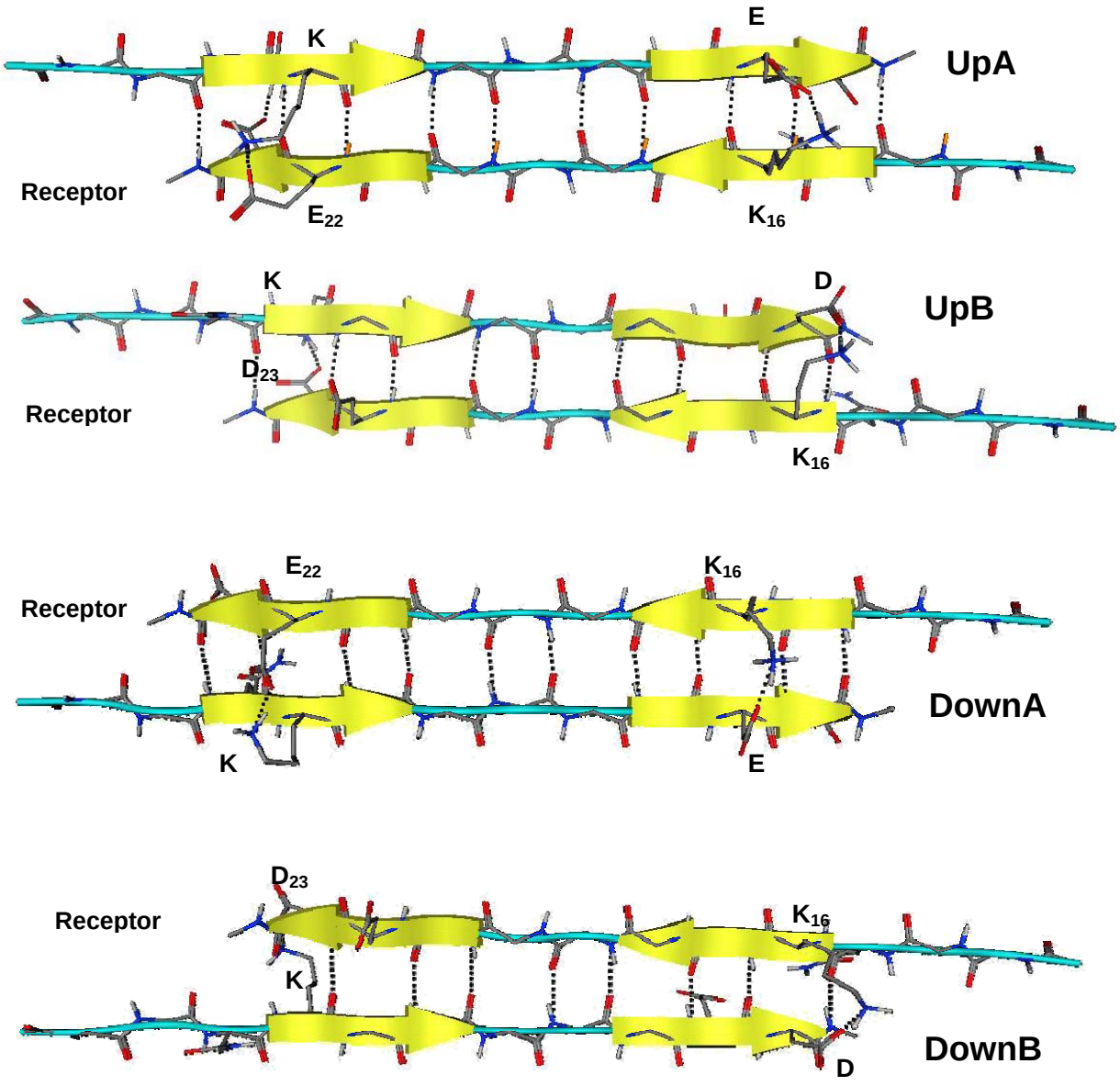

Figure 3.5 *A depiction of all four versions of the 'anti-parallel' binding mode. The "up" edge of the receptor is defined by the direction of the backbone -NH moieties of all even numbered (based on position in β amyloid 40 and β amyloid 42) amino acid residues. The receptor strand has numbered residues, while the ligand strand uses unnumbered residues.*

The binding energies and BHB scores are:

UpA = - 289.7 kcal/mol and 51.2
UpB = - 271.6 kcal/mol and 39.7
DownA = - 258.4 kcal/mol and 39.8
DownB = - 218.0 kcal/mol and 40.2

Therefore the UpA orientation was chosen for the rest of the docking/ scoring simulations.

3.14 Results

Ligand docking/ scoring simulations to the receptor model were performed with each ligand in the UpA binding mode. The protocol, methods and scripts used for these simulations have been previously described. Docking runs with 100 runs per ligand and 25 runs per ligand were performed to ascertain the minimum number to runs that would allow ligands to sample available conformational space. The results for the 100 runs per ligand simulations are summarized in Table 3.1, and the results for the 25 runs per ligand simulations are summarized in Table 3.2.

It appears that 25 docking runs per ligand are adequate to reproduce the quality of ligand docking and scoring obtained with 100 runs per ligand. Both lengths of docking runs found similar low energy conformations, hydrophobic interactions and hydrogen bonds for any given ligand. In cases where the top final conformations had energies within 1 kcal/mol, the docked pose with the highest receptor buriedness was chosen as the top conformation.

Table 3.1 Results from 100 runs per ligand docking-scoring simulations.

Name	E_bind[1] (kcal/mol)	RB[2]	# HB[3]	BHB Score[4]	Experimental affinity[5]	Normalized BHB Score[6]
Ac-ALVFF-NH_2	-80.5	0.654	0	22.7	0	16
Ac-KAVFF-NH_2	-134.1	0.623	0	24.0	10	29
Ac-KLAFF-NH_2	-135.4	0.649	1	30.2	90	88
Ac-KLVAF-NH_2	-155.0	0.558	1	27.4	100	61
Ac-KLVFA-NH_2	-135.8	0.639	0	24.8	40	36
Ac-KLVFF-NH_2	-131.9	0.681	1	31.5	100	100
Ac-LVFFA-NH^2	-74.9	0.749	0	27.1	50	58
Ac-LVFFAE-NH_2	-146.4	0.706	1	33.5	90	118
Ac-QKLV-NH_2	-134.7	0.422	1	21.7	5	7
Ac-QKLVF-NH_2	-146.7	0.410	1	21.9	20	9
Ac-QKLVFF-NH_2	-170.3	0.684	1	33.6	90	119
Ac-LVFF-NH_2	-66.3	0.701	0	24.3	30	31
Ac-VFF-NH_2	-56.9	0.685	0	23.0	5	19
Ac-KLV-NH_2	-105.7	0.359	1	18.4	0	-25

*[1] E_bind = ligand binding energy, [2] RB = receptor buriedness, [3] #HB = number of salt bridges. [4] BHB Score was obtained by using equation 3.15, [5] experimental affinity was derived from literature, [6] Normalized BHB Score = BHB-21*10.9, so that KLVFF (standard ligand) would have a normalized score of 100, in comparison to inactive ligands.*

A graphical representation of the data as seen in Figures 3.6 demonstrates that 'normalized' BHB scores fit experimental ligand activity quite well. The 25 docking runs per ligand protocol gives a slightly better fit (R^2 = 0.93) with the experimental data that the 100 docking runs per ligand protocol (R^2 = 0.82). The results might seem somewhat counterintuitive, in that docking with lower number of runs gave a slightly better correlation than a higher number of runs.

Table 3.2 Results from 25 runs per ligand docking-scoring simulations.

Name	E_bind[1] (kcal/mol)	RB[2]	HB[3]	BHB score[4]	Experimental Affinity[5]	Normalized BHB Score[6]
Ac-ALVFF-NH_2	-72.7	0.635	0	21.5	0	5
Ac-KAVFF-NH_2	-128.3	0.580	0	21.9	10	10
Ac-KLAFF-NH_2	-123.1	0.649	1	29.6	90	94
Ac-KLVAF-NH_2	-120.0	0.648	1	29.4	100	92
Ac-KLVFA-NH_2	-135.5	0.624	0	24.1	40	34
Ac-KLVFF-NH_2	-132.5	0.651	1	30.2	100	100
Ac-LVFFA-NH_2	-78.8	0.752	0	27.5	50	71
Ac-LVFFAE-NH_2	-136.4	0.644	1	30.0	90	99
Ac-QKLV-NH_2	-132.9	0.446	1	22.4	5	15
Ac-QKLVF-NH_2	-143.5	0.460	1	23.4	20	26
Ac-QKLVFF-NH_2	-153.5	0.665	1	31.9	90	118
Ac-LVFF-NH_2	-66.6	0.673	0	22.9	30	21
Ac-LVF-NH_2	-56.9	0.685	0	22.9	5	27
Ac-KLV-NH_2	-104.4	0.440	1	20.7	0	-3

*[1] E_bind = ligand binding energy, [2] RB = receptor buriedness, [3] #HB = number of salt bridges. [4] BHB Score was obtained by using equation 3.15, [5] experimental affinity was derived from literature, [6] Normalized BHB Score = BHB-21*10.9, so that KLVFF (standard ligand) would have a normalized score of 100, in comparison to inactive ligands.*

However the difference in correlations between the two sets of docking runs is within the limits of variation seen in many docking algorithms where repeated dockings of the same ligand produce results that are similar but never identical. The variation in BHB score between multiple independent (5-6) docking runs is usually less than 5% and always less than 10% of the average score value (not shown). The Receptor Buriedness (RB) and Hydrogen Bonds (HB) values of

optimized ligand-receptor complexes are remarkably constant (<5%) across independent docking runs for the same ligand.

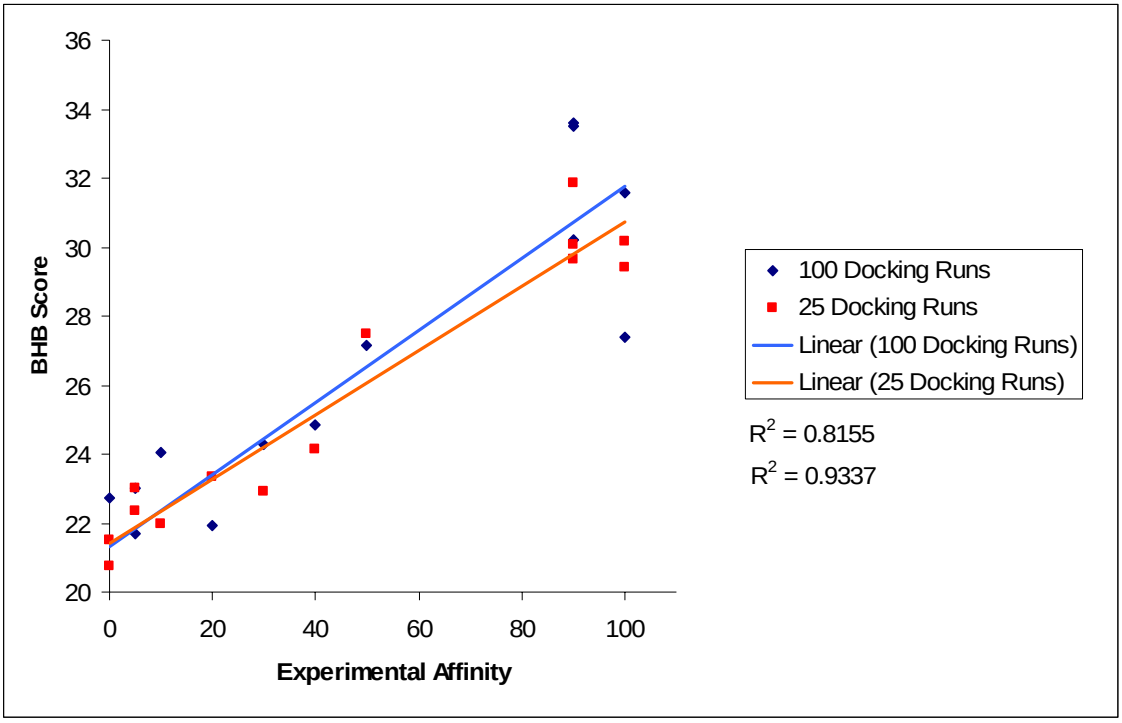

Figure 3.6 *BHB scores have a high correlation with experimental affinity. The correlation for both types of docking runs is not identical, but within the margins of variations seen in multiple docking runs of the same ligand.*

Calculated binding energy values are the biggest source of variation between independent docking runs on the same ligand. The effects of this phenomenon on the conformation of optimized docked complex, and interactions, is minimal. However these numerical variations are unavoidable because of the very nature of energy minimization (pseudo-random integers and convergence cutoffs) as implemented in molecular mechanics. It is worthwhile to note that neither type of docking run identified a poor ligand as a good ligand or vice versa.

3.15 Conclusion and discussion

The research work described in this chapter was performed to develop a new docking/ scoring system for reproducing the experimental affinity of peptidic ligands that bind to the self recognition motif of β amyloid. The results demonstrate both the feasibility and capability of our new docking/ scoring system for reproducing the experimental affinity of peptidic ligands to the self recognition motif of β amyloid.

It appears that our model of the 'oligomerization ready' 11mer self-recognition site of β amyloid (as part of a β amyloid (1-40/42) molecule is a reasonably realistic and usable representation of the 'in vitro' version of the same. Our assumptions, and methodology, for docking and scoring peptidic ligands to the receptor model seem to be realistic and reasonably precise. It was remarkable that a generic ligand scoring function (BHB) validated on many classical receptor-ligand systems [297] performed well on an unconventional receptor- ligand system.

Given the lack of literature about successful *in silico* modeling of experimental SAR on a series of peptidic β amyloid ligands, our research work in this area is novel. It also appears that docking ligands with 25 independent runs is adequate for further work with this, or a similar, receptor-ligand system. While the high quality of results is still not definitive proof that our assumptions and protocols are a good replica of the molecular interactions in biochemical assays, it creates enough confidence to use these protocols to develop new β amyloid aggregation inhibitors. The application of these protocols to discover new ligands is discussed in the next chapter.

The use of such receptor-ligand docking/scoring techniques could potentially reduce the time and cost of designing more ligands to the self-recognition site of β amyloid. The same techniques could also be used to develop inhibitors of amylin (Type II Diabetes Mellitus) and α synuclein oligomerization (Lewy Body Dementia and Parkinson's Disease).

CHAPTER 4: DESIGNING PEPTIDIC INHIBITORS OF β AMYLOID AGGREGATION

4.1 Introduction

The current chapter describes the process of design and *in silico* optimization of four novel classes of peptidic inhibitors of β amyloid oligomerization using the ligand docking/scoring methods described in the previous chapter. Non-computational considerations influencing ligand design are also described in this chapter.

4.2 Defining high affinity β amyloid ligands

Ligand docking simulations, described previously in Chapter 3, showed that well characterized peptidic ligands to the β amyloid self recognition site had 'normalized' BHB ligand binding scores in the range of 60-120. These ligands have to be present at a molar excess, ranging from 1:10 to 1:2 (β amyloid: ligand), to exert optimal anti-oligomerization activity in assays.[115, 109, 110]

The 11-mer receptor, with the sequence Ac-HHQKLVFFAE-NH_2, was used as a surrogate for the self-recognition site in β amyloid as it is known to exhibit measurable self-recognition.[310] Docking simulations of one 11-mer receptor strand to another in an 'UpA' anti-parallel binding mode (as seen in the previous chapter) gave a normalized BHB score of ~ 320. The experimental and calculated affinity of peptidic ligands, from literature, to the receptor (and hence β amyloid) is hence significantly less than for receptor self-recognition. Effective competition with the receptor's self-affinity thus required development of ligands with a normalized BHB receptor binding score that was equal to or exceeded 320.

A careful examination of docked structures of known ligands, like Ac-KLVFF-NH_2, revealed possibilities for improvement of the binding affinity of future ligands

through design optimizations and addition of new pharmacophores. These improvements were vetted through the filter of potential pharmacokinetic characteristics and synthetic accessibility. Considerations behind new ligand designs, and filters for these designs, are described in the next three sections of this chapter.

4.3 Structural improvements to known β amyloid ligands

An analysis of ligand-receptor interactions in the docked structure of Ac-KLVFF-NH_2, revealed potential for improvement in ligand affinity, with minimal increases in its molecular weight. Proposed improvements are illustrated in Figure 4.1 and Figure 4.2.

Two charged residues on the receptor (K_{16} and D_{23}), see in Figure 4.1, cannot interact with any pharmacophore on the standard ligand. Additional ligand pharmacophores could bind to these receptor sidechains and improve ligand affinity. Experimental data with known peptidic ligands suggest that this course of action is viable. Ligands with the sequence LVFFAE and LPFFD bind to the self-recognition site, presumably through an interaction between acidic ligands residues (E or D) and K_{16}.[102, 109]

Ligands based on LVFFAE and KLVFF are equivalent in affinity, suggesting that salt-bridge formation between a negatively charged ligand sidechain and K_{16} (receptor) is equivalent to one between a positively charged ligand sidechain and E_{22} (receptor). Furthermore ligands with the sequence KLVFFAE are more potent that either KLVFF or LVFFAE, suggesting that such interactions are additive in nature.[326]

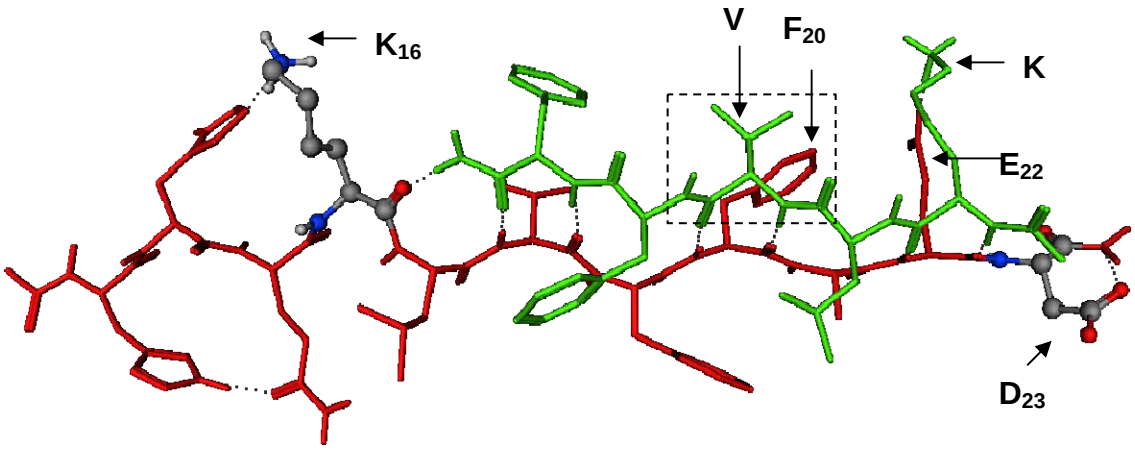

Figure 4.1 *Docked complex of the standard ligand, Ac-KLVFF-NH_2 (green) to the receptor (red). The unnumbered charged sidechain of K (ligand) interacts with the numbered charged sidechain of E_{22} (receptor). Hydrophobic residue sidechain contacts (LVFFA ←→ AFFVL) are seen in the center of the complex. One hydrophobic interaction (V-F_{20}) is shown with a dashed box.*

The addition of another positively charged residue to the ligand N-terminus could result in formation of an extra ligand-receptor salt-bridge between itself and D_{23} (receptor). Such an interaction would be competitive to the D_{23}-K_{28} interaction necessary for initiation of oligomerization in β amyloid (see section 1.6 and 1.7) Addition of charged residues to existing β amyloid ligand designs could increase receptor binding affinity by improving the enthalpic component of ligand-receptor interaction.

The entropic favorability of the ligand-receptor interaction could also be improved by judicious replacement and selection of ligand residues. Replacement of lysine (K) with ornithine (O) could improve entropic favorability of an electrostatic

sidechain interaction (to E_{22}) through the use of a shorter and more rigid side-chain. The selection of a γ-diaminobutyric acid (dab) residue as the additional N-terminal residue (for interacting with D_{23}) in ligand designs was influenced by this consideration.

Interactions between core lipophilic residues could be optimized through the use of lipophilic residue sequences other than LVFFA in the ligand. Optimization of hydrophobic interactions could increase both enthalpic and entropic favorability of the ligand-receptor interaction. Optimizing interactions between lipophilic aromatic side-chain residues (F) was another possibility, since such interactions are important in peptidic recognition and binding for many proteins (and peptides) including amyloidogenic peptides. [327, 328] The use of dextrorotary amino acids has been shown to improve hydrophilic interactions for β amyloid ligands.

4.4 Pharmacokinetic considerations in ligand design

The vast majority of promising compounds in pre-clinical and clinical testing fail to advance because of unacceptable pharmacokinetics and toxicity. [329, 330] While it is not possible to predict all aspects of the pharmacokinetic and toxicity profile for a given compound, it is possible to minimize the worst case scenarios by considering previously known information on (the consequences of using) various pharmacophores and their combinations.

Optimizing pharmacokinetic profiles is especially important for peptidic drugs as they present some peculiar and unique problems, including susceptibility to proteolytic degradation and an ability to stimulate a direct immune response. The proteolytic susceptibility of peptidic drugs can be reduced by using unnatural amino acid residues [331, 332] such as N-methylated residues, substituted alanines, and dextrorotary residues. All of the above three approaches were used, often in combination. The replacement of K by O, for example, was intended to increase resistance to trypsin-like enzymes, in addition to improving the entropy of the

interaction. [333, 334] Similarly the use of properly placed alternate N-methylated residues, as shown in Figure 4.2, and utilized in our designs, was meant to increase resistance to enzymatic degradation. Moreover N-methylated residues also prevent ligands from self-aggregating and improve aqueous solubility and dextrorotary residue containing β amyloid ligands are very resistant to enzymatic degradation.

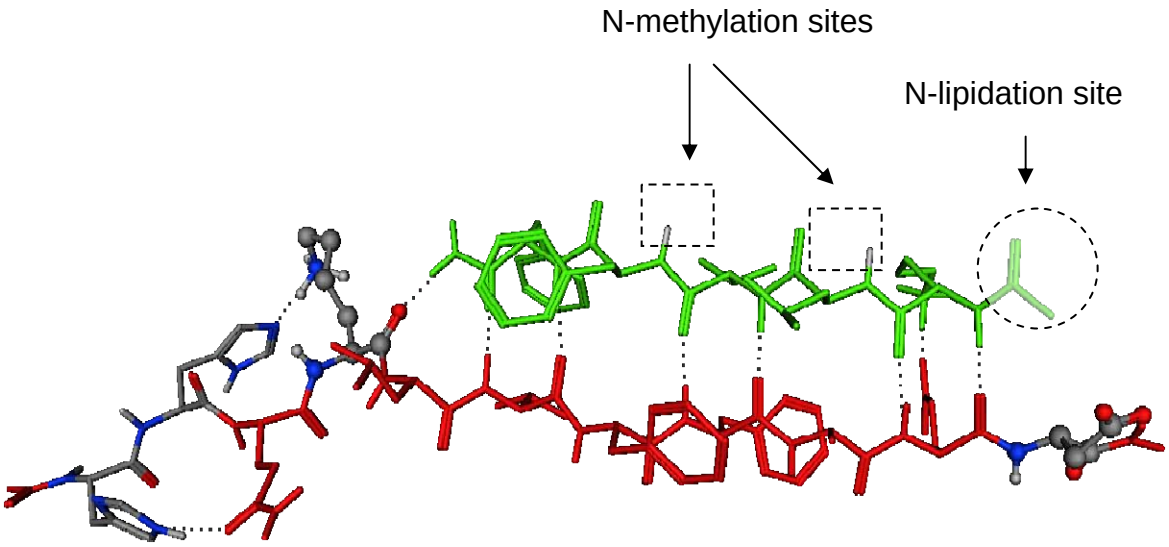

Figure 4.2 *Another view of docked complex of Ac-KLVFF-NH_2 (green) to the receptor (red). Positions for N-methylation of residues is shown with dashed boxes. The acetylated N-terminus of the ligand (dashed circle) should be suitable for coupling to carrier molecules such as lipid.*

The ability of a peptide to generate an immune response is a consideration specific to peptidic drugs. While immune responses such as antibody formation have not been a therapeutic hurdle to peptidic and protein drugs such as non-human insulin analogs, amylin analogs and various humanized monoclonal antibodies, it is prudent to use peptidic sequences smaller than 9-mer fragments used by the

immune systems antigen processing mechanisms. [335] The *judicious* use of unnatural and dextrorotary amino acids can also reduce visibility of peptidic drugs to the immune system.[336]

The interaction of β amyloid with cell membranes of neurons and endothelial cells, increases oligomer formation and results in generation of free radicals.[89,337] Therefore it is worthwhile to conjugate peptidic drugs (for AD) to moieties that would assist in targeting neuronal and endothelial cell membranes, where β amyloid oligomerizes.[338, 339]

Membrane targeting can be achieved by coupling the ligand to a lipid, such that the lipid moiety would help the ligand bind to cell membranes without affecting its pharmacophore presentation. Synthetic considerations make it easier to couple the N-terminus of the ligand, so that the N-acetyl group on a peptide could be replaced with an N-fatty acid. The choice of fatty acids was dictated by synthetic considerations and previous studies of N-lipidated peptides. [340, 341, 342, 343, 344] The ability of a lipid to be transported across the blood brain barrier was a major factor [345, 346, 347] Myristic acid and docosahexaenoic acid emerged as the best choices for N-lipidation of our ligands.

Myristic acid was used for creating the lipidated versions of some ligand designs as it has both a fully saturated and more universal lipid chain. While N-myristylated ligands are suitable for testing in cell cultures and animal models of AD, coupling to docosahexaenoic acid is more suitable for targeting ligands to the human brain. The use of another popular technique for improving the pharmacokinetic profile of proteins, PolyEthylene Glycosylation (PEGylation), was considered and dismissed because it would interfere with pharmacophore presentation for smaller peptidic ligands (as opposed to large proteins and antibodies).

4.5 Ligand types and binding modes

Initial inputs for the ligand designs were derived from patent literature and publications on peptidic ligands to β amyloid.[99, 110, 115] Factors such as capacity for further development, synthetic accessibility, potential metabolic stability and potential toxicity of component unnatural residues also guided ligand design. Ligand docking techniques, previously described in chapter 3, were utilized to explore various ligand design concepts. Data from each round of ligand dockings was used to optimize the next round of ligand design. Ligands were docked in the 'UpA' orientation (previously shown in Figure 3.6).

Four broad classes of ligands, based upon chirality of residues used and complementarity to the receptor, were designed and developed. The binding modes for these four ligand classes are shown in Figure 4.3 and Fig 4.4.

Levorotary and dextrorotary complementary ligands seen in Fig 4.3 (A and B respectively) bind the receptor in an anti-parallel β sheet mode, such as that seen in fibrils of 7-,10- and 14-mer β amyloid fragments containing the self-recognition motif.[103, 312, 348] While individual strands of β amyloid in insoluble fibrils are arranged in a parallel β sheet mode, there is some evidence for an anti-parallel binding mode in soluble oligomers, especially dimers. [349] In any case, based on solid state NMR data for 7, 10- and 15-mers, binding modes for the 11-mer receptor and our designed ligands would almost certainly be anti-parallel. Type A ligands are levorotary residue based ligands that are designed to bind to β amyloid in an anti-parallel manner. Dextrorotary residue containing (Type B) ligands were designed because of evidence suggesting better sidechain interaction with the receptor. [110, 117] Docking studies on Type A and B ligands (as seen in Figure 4.4) confirmed that dextrorotary ligands did exhibit better sidechain interactions, especially for hydrophobic residues, between ligands and receptor. Sidechain interaction for different classes of ligands are shown and compared in Figure 4.4. Moreover dextrorotary ligands are far more resistant to proteolytic degradation.[95]

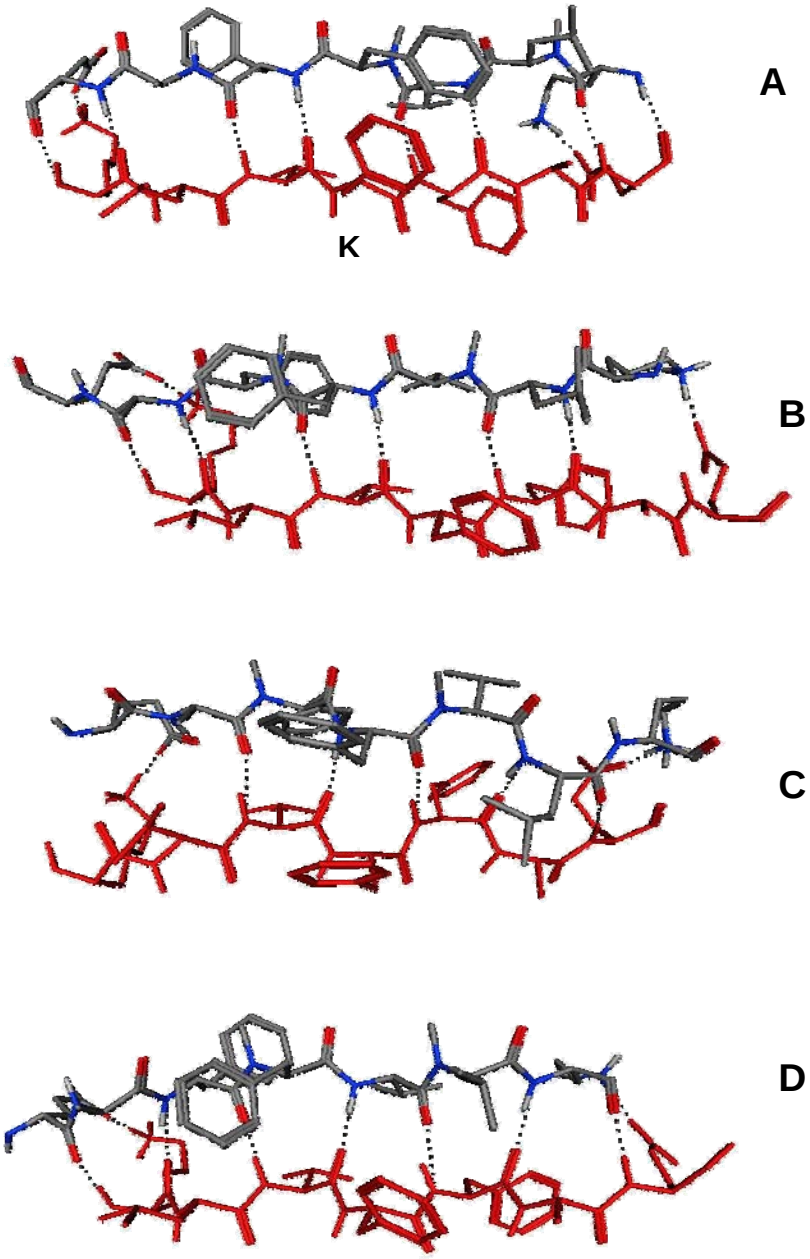

Figure 4.3 *Peptidic backbone interaction modes for all four categories of ligands with the receptor (red). A; Levorotary complementary ligands, B; Dextrorotary complementary ligands, C; Levorotary 'inverso' ligands, D; Dextrorotary 'inverso' ligands. In each case, only the KLVFFAE motifs of the receptor (red) and OLVFFAE motif of the ligand are shown for clarity.*

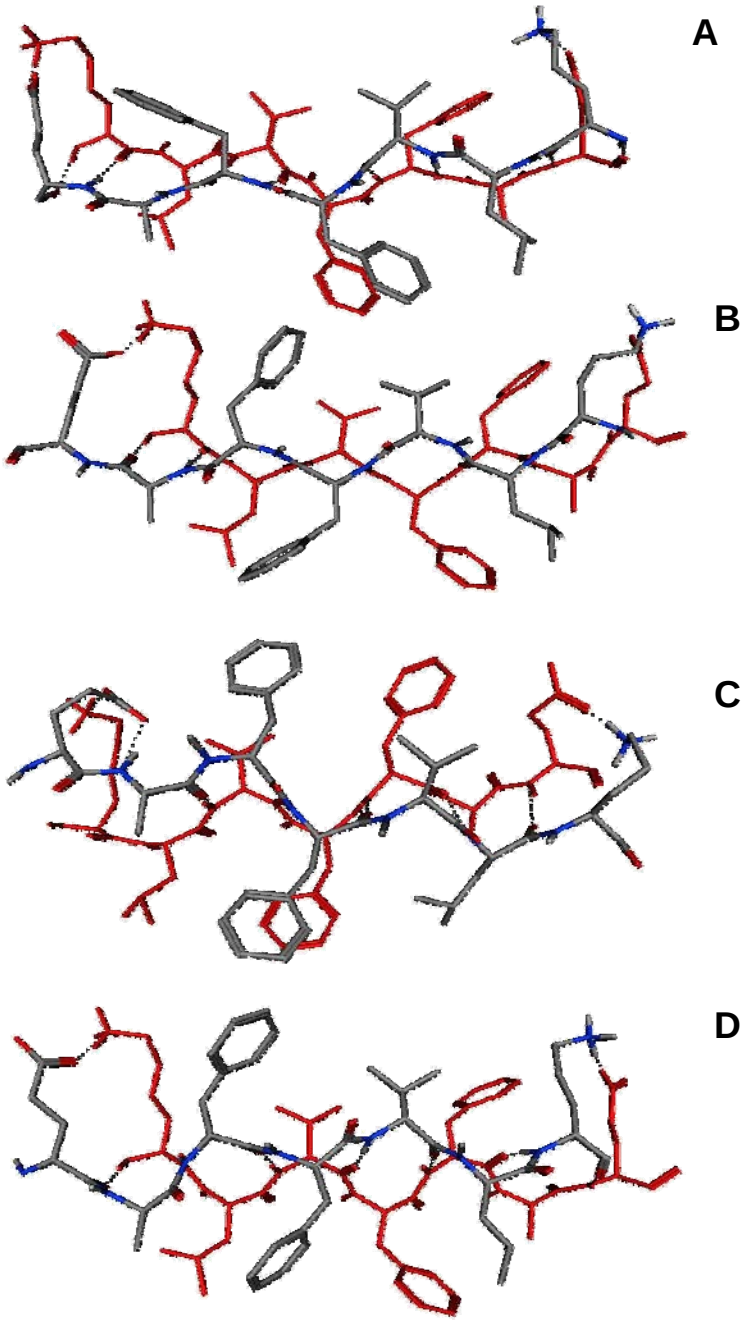

Figure 4.4 *Sidechain stacking for all four categories of ligands with the receptor (red). A; Levorotary complementary ligands, B; Dextrorotary complementary ligands, C; Levorotary 'inverso' ligands, D; Dextrorotary 'inverso' ligands. In each case, only the KLVFFAE motifs of the receptor (red) and OLVFFAE motif of the*

ligand are shown for clarity. The differences in sidechain interactions between the 4 classes of ligands, for the same ligand sequence, are clearly visible.

Ligands with an 'inversed' residue sequence (e.g EAFFVLO instead of OLVFFAE) were also designed and their binding mode is seen in Figure 4.3 and Figure 4.4 (C and D). The idea behind designing such ligands arose because β amyloid fibrils have a parallel β strand structure[350], unlike the anti-parallel mode seen in fragments of β amyloid (and between β amyloid and small peptidic ligands). The easiest solution for recreating that binding mode between the peptidic backbones of receptor and ligand, while maintaining optimal interaction between charged sidechains is inversion of the ligand residue sequence such that E is at the N-terminus instead of the C-terminus, and K is the C-terminus instead of the N-terminus.[351], Both levorotary and dextrorotary 'inversed' ligand designs were created and tested. Docking studies on Type C and D ligands suggested a different sidechain interaction than that seen in Type A and B ligands. Calculations suggest that the UpA binding mode is also the favored mode for parallel binding ligands (Type C and D). These interactions are shown and compared in Figure 4.4

4.6 Type A ligands

Ligands in this category are based on the backbone interaction seen in Figure 4.3 A, and replicate the most familiar binding for complementary peptide fragments binding to the self recognition site of β amyloid.

The first ligand in the current series (Type A - I) was a conservative design based on previous research studies which had shown that KLVFF, LVFFAE and KLVFFAE bound to the 'self-recognition' motif in β amyloid.[99, 110, 115] The relative positions of N-methyl amino acids were based on research by other groups. [114, 115] The core hydrophobic sequence, LVFFA, was based on β amyloid (17-21). Changes previously known ligands were substitution of Lysine (K) by Ornithine (O) and addition of a γ diaminobutyric acid (dab) residue as the new N-terminus. The

sequence of this first ligand design was Ac-dab-O-(me)L-V-(me)F-F-A-E-NH_2 (also known as SG2). It was synthesized and the results of experimental studies are found in Chapter 5. A docked complex of SG2 with the receptor can be seen in Figure 4.5

The next steps in the ligand design process involved systematic sequential replacements of various amino acid residues with isosteres of varying sizes, rigidity and similarity to the residues they replaced. The effects of these replacements on predicted ligand binding scores are shown in Table 4.1.

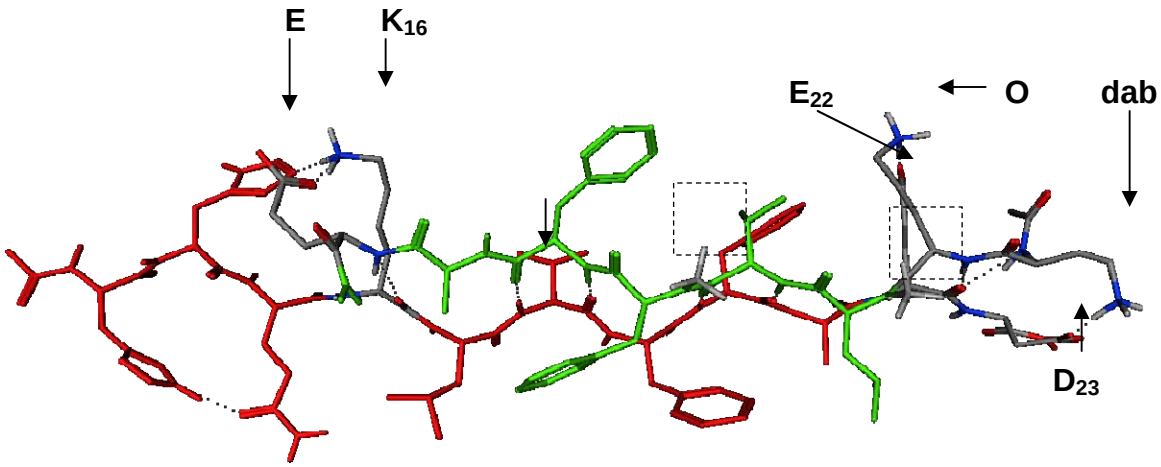

Figure 4.5 *Docked complex of the first designed ligand SG2, Ac-dab-O-(me)L-V-(me)F-F-A-E-NH_2 (green) and receptor (red). The important interactions (E-K_{16}, O-E_{22}, dab-D_{23}) are highlighted. N-methylations at F and L are shown with dashed boxes.*

A variety of natural and unnatural isosteres were used for aliphatic residues. These included residues such as A (alanine), V (valine), L (leucine), tbA (tertiary butyl - alanine), cpA (cyclopropyl-alanine) and chA (cyclohexyl-alanine). Aromatic

hydrophobic residues like F (phenylalanine) , 1-npA (1-napthyl-alanine) and 2-npA (2-napthyl-alanine) were occasionally used as isosteres for aliphatic residues. Many unnatural isosteres were rejected on concerns about potential toxicity. [352] Even otherwise non-toxic isosteres found in approved peptidic drugs, such as tbA and chA, were used in a judicious manner, as peptides with more than a large number of unnatural residues can be very potent ligands but poor drugs, because they are often significantly more lipophilic or hydrophilic (as the case may be) than natural residues.

Since commercially available N-methylated residue precursors are largely limited to natural amino acids, those residue positions (K**L**V**F**F) ligands were not substituted. In any case, previous structure activity studies had suggested that both N-methylated residue positions (L and 1st F) were hard to substitute without a large reduction in binding affinity. [99]

The substitution process started with substitutions at position 7. Bulkier replacements did not increase lipophilic interactions or BHB scores (see Table 4.1), and it seems that a small aliphatic residue (like A) was optimal for this position.

The next amino acid to undergo substitution, V at position 4, required a bulky and rigid replacement (chA) for a worthwhile increase in predicted ligand affinity. Substitution of the non N-methylated phenylalanine (F) with residues such as L, tbA, cpA and chA (data shown) and 1-npA, 2-npA (data not shown) failed to increase activity. However another doubly substituted ligand with the sequence, Ac-dab-O-(me)L-**F**-(me)F-**L**-A-E-$NH_{2,}$ (seen in Table 4.1) did have a high predicted affinity. It is worthwhile to note that neither single substitution (V→F or F→L) increased predicted affinity, but the combination did increase affinity. This particular design was based on trial dockings of smaller pentapeptidic ligands with alternate hydrophobic cores (not shown).

Table 4.1 BHB Scores for Type A-I Ligand-Receptor Complexes.

Name [a]	Normalized BHB Score	Comments [b]
Ac-dab-O-(me)L-V-(me)F-F-A-E-NH_2	322 (214) [c]	1st Ligand (SG2)
Ac-dab-O-(me)L-V-(me)F-F-**V**-E-NH_2	301	A→V
Ac-dab-O-(me)L-V-(me)F-F-**L**-E-NH_2	298	A→L
Ac-dab-O-(me)L-V-(me)F-F-**tbA**-E-NH_2	295	A→tbA
Ac-dab-O-(me)L-V-(me)F-F-**cpA**-E-NH_2	295	A→cpA
Ac-dab-O-(me)L-V-(me)F-F-**chA**-E-NH_2	302	A→chA
Ac-dab-O-(me)L-V-(me)F-F-**F**-E-NH_2	320(235)[c]	A→F
Ac-dab-O-(me)L-**A**-(me)F-F-A-E-NH_2	253	V→A
Ac-dab-O-(me)L-**L**-(me)F-F-A-E-NH_2	311	V→L
Ac-dab-O-(me)L-**tbA**-(me)F-F-A-E-NH_2	301	V→tbA
Ac-dab-O-(me)L-**cpA**-(me)F-F-A-E-NH_2	329 (252) [c]	V→cpA
Ac-dab-O-(me)L-**chA**-(me)F-F-A-E-NH_2	382 (242)[c]	V→ChA
Ac-dab-O-(me)L-**F**-(me)F-F-A-E-NH_2	311	V→F
Ac-dab-O-(me)L-V-(me)F-**L**-A-E-NH_2	306	F→L
Ac-dab-O-(me)L-V-(me)F-**tbA**-A-E-NH_2	281	F→tbA
Ac-dab-O-(me)L-V-(me)F-**cpA**-A-E-NH_2	310	F→cpA
Ac-dab-O-(me)L-V-(me)F-**chA**-A-E-NH_2	302	F→chA
Ac-dab-O-(me)L-**F-**(me)F-**L**-A-E-NH_2	409 (238)[c]	V→F and F→L

a Unnatural amino acid glossary: O= ornithine, dab= γ diamino-butyric acid, (me)L = N-methyl Leucine, Me(F) = N-methyl-Phenylalanine, tbA= tertiary butyl Alanine, cpA= cyclopropyl Alanine, chA = cycloyhexyl Alanine.
b If the original residue in 1st ligand = X and substituted residue = Y, then substitution is shown as X→Y
c The self-affinity normalized BHB score for potent ligands in shown in parentheses.

Aliphatic and aromatic residue replacements other than those shown in Table 4.1 (e.g isoleucine, allyl-alanine, norvaline, aminocaproic acid, terbutyl-glycine, homophenylalanine, 3-/ 4- methyl phenylalanine) were tried and found to be unsatisfactory. It should be noted that the range of variation in BHB scores for the same ligand is about 10%, so it cannot predict the precise order of potency for ligands with close BHB scores. It can however reproducibly separate higher affinity

ligands from those with measurably lower affinity. Therefore a 15% increase in the normalized score is not remarkable, especially if the residue replacement is known to cause significant changes in ligand solubility.

Four ligands in this particular series (A-I) had predicted BHB scores above 320, and were considered for synthesis. They underwent further computational analysis including potential self-binding affinity. While smaller ligands (e.g. KLVFF and LVFFAE) cannot bind to themselves with any worthwhile affinity, non N-methylated KLVFFAE can bind to itself. Since a ligand must have a higher affinity to the receptor than to itself to be active, it was necessary to calculate self-affinity for every ligand that was considered for synthesis and testing. The selection of SG2 (Ac-dab-O-(me)L-V-(me)F-F-A-E-NH_2) as the first synthesized ligand (from this group) was based on it's conservative structure, low self-affinity and ease of synthesis.

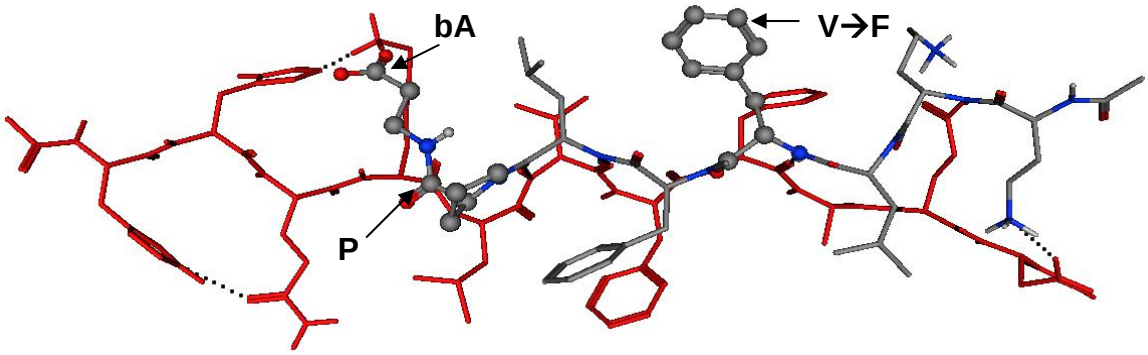

Figure 4.6 *The docked complex of SG1, Ac-dab-O-(me)L-F-(me)F-L-P-bA-COOH, (green) and the receptor (red). Important features of the ligand (P-bA-COOH, V→F) are highlighted. Two N-methylations on the ligand are present but not highlighted.*

The other subfamily of ligands in this group were based on a novel concept, namely that use of a rigidified C-terminal end to further decrease the entropic penalty for ligand would increase ligand potency. Similar N-terminal modifications were considered but ultimately dismissed due to the lack of availability of appropriate unnatural residues.

Attempts to find a suitable replacement for the AE portion of KLVFFAE motif identified a proline-β amino acid (with a charged C-terminal end) as the most appropriate and synthetically accessible replacement. While more rigid replacements (e.g various trans-cyclohexane acids) were available, it was decided that they would be developed only after the design concept was validated in experimental assays. A novel high affinity hydrophobic core LFFL was used as a replacement for LVFF, because it had been validated in our previous docking studies (see Table 4.1) The first designed ligand of this sub-series (A-II) had the sequence Ac- dab-O-meL-F-meF-LP-bA-COOH and it's docked structure is shown in Figure 4.6.

The next steps in the ligand design process involved systematic replacement of various amino acid residues in SG1 with isosteres of varying sizes, rigidity and similarity to the residues they replaced. The effects of important replacements on predicted ligand binding scores are shown in Table 4.2.

The first designed ligand of this subtype, SG1, had an excellent predicted BHB score. However subsequent substitutions did not improve activity and therefore SG1 was the only member of this group considered for synthesis. SG1 has a predicted self-binding optimized BHB score of 218 which was much lower than its receptor binding optimized BHB score of 369.

Table 4.2 BHB Scores for Type A-II Ligand-Receptor Complexes.

Name [a]	Normalized BHB Score	Comments [b]
Ac-dab-O-(me)L-F-(me)F-L-P-bA-COOH	369 (218)[c]	SG1
Ac-dab-O-(me)L-F-(me)F-L-P-**abu-**COOH	327	bA→abu
Ac-dab-O-(me)L-F-(me)F-L-**2aza**-bA**-**COOH	286	P→2aza
Ac-dab-O-(me)L-F-(me)F-L-**2pip**-bA-COOH	290	P→2pip
Ac-dab-O-(me)L-F-(me)-**1npA**-L-P-bA-COOH	361	F→1npA
Ac-dab-O-(me)L-F-(me)-**2npA**-L-P-bA-COOH	305	F→2nPA
Ac-dab-O-(me)L-F-(me)F-**F**-P-bA-COOH	325	L→F
Ac-dab-O-(me)L-**1nPA**-(me)F-L-P-bA-COOH	313	F→1npA
Ac-dab-O-(me)L-**2nPA**-(me)F-L-P-bA-COOH	331	F→2npA

[a]Unnatural amino acid glossary: O= ornithine, dab= γ diamino-butyric acid, (me)L = N-methyl Leucine, Me(F) = N-methyl-Phenylalanine, bA= beta Alanine, abu= Amino butyric acid, 2aza = *S*-azetidine 2-carboxylic acid, 2pip= *S*- piperidine 2-carboxylic acid, 1npA= 1 napthy alanine, 2-npA= 2-napthyl alanine.
[b] If the original residue in 1st ligand = X and substituted residue = Y, then substitution is shown as X→Y
[c] The self-affinity normalized BHB score for potent ligands in shown in parentheses.

4.7 Type B ligands

The second types of ligands, namely Type B, utilized dextrorotary residues but bound to the receptor in a mode similar to Type A ligands (see Figure 4.3 B and Figure 4.4 B). However the use of dextrorotatory residues meant that structural aspects of the ligand, such as sidechain interactions and the placement of N-methylated residues would be different from Type A ligands. Dextrorotary versions of SG2 and SG1 were starting points for the Type B series of ligands.

A dextrorotary (D-) version of SG2 was the starting point for the first series (Type B-I) because it possessed a conserved hydrophobic core (LVFFA) and experimental data suggested that D- version of the hydrophobic core LVFFA, and LVFFL, possessed good activity as β amyloid oligomerization inhibitors.[110]

SG1 was chosen as the starting point for other subtype (Type B -II) because it was likely to exhibit favorable aromatic sidechain interactions with the receptor in spite of its unorthodox hydrophobic core (LFFLP instead of LVFFA). It quickly became obvious that the positions of the two N-methylations used in levorotary versions of SG1 and SG2 were inappropriate for D-versions of these ligands. The effects of changes in residue chirality on both ligand-receptor sidechain stacking and interstrand hydrogen bonds (see Figure 4.3 and 4.4 B) meant that N-methylation positions based on the levorotary versions faced the receptor's 'UpA' binding surface. A change in the position of N-methylation by one residue rectified this problem.

Therefore the sequence of the D-version of SG2, D-SG2 is:
Ac-dab-O-L-(me)V-F-(me)F-A-E-NH_2.

Similarly, the sequence of the D-version of SG1, D-SG-1 is:
Ac-dab-O-L-(me)F-F-(me)L-P-bA-COOH.

Sidechains of dextrorotary residue ligands bound a levorotary receptor seem to interdigitate as opposed to stack on top of one another (compare Figure 4.4 A and B). The effects of subsequent substitutions on predicted ligand binding scores are shown in Table 4.4. None of the used aliphatic substitutions increased affinity significantly beyond that seen for D[Ac-dab-O-L-(me)V-F-(me)F-L-E-NH_2]. However some ligands in which aromatic residues substituted aliphatic residues did exhibit a significant increase (see Table 4.3) in predicted binding affinity, unlike Type A ligands (see Table 4.1 and Table 4.2).

Table 4.3 BHB Scores for Type B –I Ligand-Receptor Complexes.

Name[a]	Normalized BHB Score	Comments[b]
D[Ac-dab-O-L-(me)V-F-(me)F-A-E-NH_2]	339	D-SG2
D[Ac-dab-O-L-(me)V-F-(me)F-**L**-E-NH_2]	390 (246)**c**	A→L
D[Ac-dab-O-L-(me)V-F-(me)F-**tbA**-E-NH_2]	371	A→tbA
D[Ac-dab-O-L-(me)V-F-(me)F-**chA**-E-NH_2]	391	A→chA
D[Ac-dab-O-L-(me)**L**-F-(me)F-**L**-E-NH_2]	358	V→L, A→L
D[Ac-dab-O-**F**-(me)V-F-(me)F-**L**-E-NH_2]	313	L→F, A→L
D[Ac-dab-O-L-(me)**F**-F-(me)F-**L**-E-NH_2]	440 (227)[c]	V→F, A→L
D[Ac-dab-O-**F**-(me)**F**-F-(me)F-**L**-E-NH_2]	402 (245)[c]	L→F,V→F,A→L
D[Ac-dab-O-**F**-(me)**F**-F-(me)F-F-E-NH_2]	357	L→F,V→F,A→F

[a]Unnatural amino acid glossary: O= ornithine, dab= γ diamino-butyric acid, (me)L = N-methyl Leucine, Me(F) = N-methyl-Phenylalanine, tbA= tertiary butyl Alanine, cpA= cyclopropyl Alanine, chA = cycloyhexyl Alanine.bA= beta Alanine.

[b] If the original residue in 1st ligand = X and substituted residue = Y, then substitution is shown as X→Y

[c] The self-affinity normalized BHB score for potent ligands in shown in parentheses.

Three ligands with receptor binding BHB scores close to or past 400 were considered for potential synthesis (compared to 4 ligands passing the 320 score mark for Type A ligands). Self-affinity scores for all three ligands were acceptable and the most potent ligand, D[Ac-dab-O-L-(me)F-F-(me)F-L-E-NH_2], also had the lowest predicted self-affinity score in this group. The docked complex of this ligand, to the receptor, can be seen in Figure 4.7.

The other subtypes in the Type B ligand series were based on a dextrorotary version of SG1. D-SG1, D [Ac-dab-O-L-(me)F-F-(me)L-P-bA-COOH], had a predicted affinity of over 400. However subsequent substitutions only gave a marginal improvement in ligand affinity. The effects of important substitutions on predicted ligand binding scores are shown in Table 4.4.

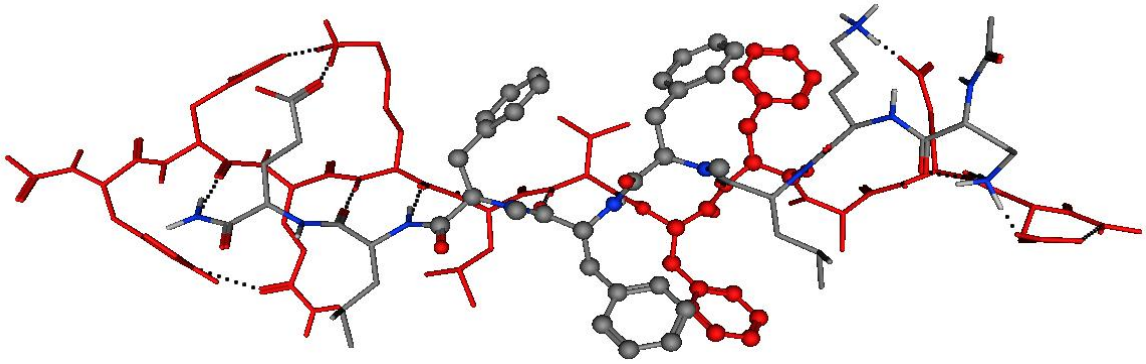

Figure 4.7 *Docked complex of the first designed ligand,* D[Ac-dab-O-L-(me)F-F-(me)F-L-E-NH_2], *and receptor (red). Note the close packing and interactions of highlighted phenylalanine sidechains on both ligand and receptor.*

The self-affinity score of the two best, and synthetically most accessible ligands, turned out to be fairly low, and therefore it appears that they would be suitable for future synthesis and testing in various assays.

Table 4.4 BHB Scores for Type B -II Ligand-Receptor Complexes.

Name[a]	Normalized BHB Score	Comments[b]
D [Ac-dab-O-L-(me)F-F-(me)L-P-bA-COOH]	415 (190)[c]	D-SG1
D [Ac-dab-O-**tbA**-(me)F-F-(me)L-P-bA-COOH]	427 (197)[c]	L→tbA
D [Ac-dab-O-**F**-(me)F-F-(me)L-P-bA-COOH]	399	L→F
D [Ac-dab-O-**F**-(me)F-F-(me)**F**-P-bA-COOH]	357	L→F, L→F
D [Ac-**O**-**dab**-L-(me)F-F-(me)L-P-bA-COOH]	359	dab-O→O-dab

[a]Unnatural amino acid glossary: O= ornithine, dab= γ diamino-butyric acid, (me)L = N-methyl Leucine, Me(F) = N-methyl-Phenylalanine, tbA= tertiary butyl Alanine, cpA= cyclopropyl Alanine, chA = cycloyhexyl Alanine.bA= beta Alanine.

[b] If the original residue in 1st ligand = X and substituted residue = Y, then substitution is shown as X→Y

[c] The self-affinity normalized BHB score for potent ligands in shown in parentheses.

4.8 Type C ligands

The third types of ligands, Type C, utilized an inversed sequence of levorotary residues to force a parallel β strand interaction between the ligand and receptor (see Figure 4.4 C and Figure 4.4 C). They have no real similarity, in either sidechain or backbone interactions to either Type A or B. Ligands designed to date have reasonable activity (see Table 4.6) but a structure activity relationship unlike that seen for either Type A or B.

Table 4.5 BHB Scores for Type C Ligand-Receptor Complexes.

Name[a]	Normalized BHB Score	Comments[b]
Ac-E-A-(me)F-F-(me)V-L-O-dab-NH_2	334	1st Ligand – Type C
Ac-E-**V**-(me)F-F-(me)V-L-O-dab-NH_2	346	A→V
Ac-E-**L**-(me)F-F-(me)V-L-O-dab-NH_2	335	A→L
Ac-E-**tbA**-(me)F-F-(me)V-L-O-dab-NH_2	237	A→tbA
Ac-E-**cpA**-(me)F-F-(me)V-L-O-dab-NH_2	311	A→cpA
Ac-E-**chA**-(me)F-F-(me)V-L-O-dab-NH_2	334	A→chA
Ac-E-A-(me)F-F-(me)V-**tbA**-O-dab-NH_2	351 (209)[c]	L→tbA
Ac-E-A-(me)F-F-(me)V-**cpA**-O-dab-NH_2	321	L→cpA
Ac-E-A-(me)F-F-(me)V-**chA**-O-dab-NH_2	323	L→chA
Ac-E-A-(me)F-F-(me)**L**-L-O-dab-NH_2	336	V→L
Ac-E-A-(me)F-F-(me)**cpA**-L-O-dab-NH_2	309	V→cpA
Ac-E-A-(me)F-F-(me)**chA**-L-O-dab-NH_2	337	V→chA
Ac-E-A-(me)F-F-(me)**F**-L-O-dab-NH_2	361 (238)[c]	V→F
Ac-E-A-(me)**L**-F-(me)**F**-L-O-dab-NH_2	358	F→L, V→F

[a] Unnatural amino acid glossary: O= ornithine, dab= γ diamino-butyric acid, (me)L = N-methyl Leucine, Me(F) = N-methyl-Phenylalanine, tbA= tertiary butyl Alanine, cpA= cyclopropyl Alanine, chA = cycloyhexyl Alanine.

[b] If the original residue in 1st ligand = X and substituted residue = Y, then substitution is shown as X→Y

[c] The self-affinity normalized BHB score for potent ligands in shown in parentheses.

Levorotary versions of SG2 were starting points for the Type C series of ligands, as versions based on SG1 cannot be created without serious alterations and redesign

to find an appropriate N-terminal version of SG1s constrained C-terminal (P-bA-COOH). A dextrorotary (D-) version of SG2 was the therefore the only starting point for the Type C series. It is also much harder to get the high calculated hydrophobic sidechain contacts ratios (receptor buriedness) found in many Type B ligands. Type C ligands have decent calculated affinity, with an unusual binding mode, and would be an interesting class of ligands for further development.

4.9 Type D ligands

The fourth types of ligands, Type D, utilized an inversed sequence of dextrorotary residues to force a parallel β strand interaction between the ligand and receptor (see Figure 4.4 D and Figure 4.4 D). Therefore while Type D ligands have some similarity to Type C Ligands, the dextrorotary nature of it's residues forces sidechain interactions that are unlike those seen in Type A, B or C. Dextrorotary versions of SG2 were starting points for the Type D series of ligands, as versions based on SG1 cannot be created without serious alterations and redesign to find an appropriate N-terminal version of SG1s constrained C-terminal (P-bA-COOH). A dextrorotary (D-) version of SG2 was the therefore the only starting point for the Type D series. Ligands designed to date have reasonable activity (see Table 4.7) and unusual binding mode, like Type C ligands, and merit further study.

Table 4.6 BHB Scores for Type D Ligand-Receptor Complexes.

Name[a]	Normalized BHB Score	Comments[b]
D [Ac-E-A-(me)F-F-(me)V-L-O-dab-NH_2]	363 (236)[c]	1st Ligand – Type D
D [Ac-E-L-(me)**L**-F-(me)**F**-L-O-dab-NH_2]	368	A→L
D [Ac-E-A-(me)**L**-F-(me)**F**-L-O-dab-NH_2	364	F→L, V→L
D [Ac-E-**L**-(me)F-F-(me)**F**-L-O-dab-NH_2]	400 (221)[c]	A→L ,V→F

[a]Unnatural amino acid glossary: O= ornithine, dab= γ diamino-butyric acid, (me)L = N-methyl Leucine, Me(F) = N-methyl-Phenylalanine, tbA= tertiary butyl Alanine, cpA= cyclopropyl Alanine, chA = cycloyhexyl Alanine.bA= beta Alanine.

[b] If the original residue in 1st ligand = X and substituted residue = Y, then substitution is shown as X→Y

[c] The self-affinity normalized BHB score for potent ligands in shown in parentheses.

4.10 Conclusion and discussion

The material in this chapter describes the design of four types of ligands to β amyloid. These types cover both anti-parallel and parallel binding modes. The ligands use both levorotary and dextrorotary residues. About a dozen ligands, in all four types have a high predicted potency as well as low self-recognition scores. While certain classes (such as Type B) were rich in high potency ligands, other classes like Type D required much more effort (not shown) to obtain a couple of high potency ligands. As previously noted, there is no immediate need to further explore Type C and D ligands unless Type A and Type B ligands hit some insurmountable roadblock. While the calculated affinities are likely to hold up in simpler assays, the effect of modifications such as N-myristoylation on ligand affinity has to be ascertained through experiments. Similarly penetration through the blood brain barrier and pharmacokinetic properties cannot be predicted with a useful degree of certainty with computational methods.

CHAPTER 5: EXPERIMENTAL CHARACTERIZATION OF NOVEL PEPTIDIC INHIBITORS

5.1 Introduction

The current chapter describes basic experimental characterization of two designed ligands (previously mentioned in Chapter 4), SG1 and SG2. The ability of these ligands to interact with, and block β amyloid oligomerization, was measured with three experimental techniques:

a] Thioflavin T (ThT) fluorescence assay[353]
b] Western Blot (WB)[354]
c] Circular Dichroism (CD) Spectroscopy[355]

An 11-mer peptide with the sequence of β amyloid (13-23), Ac-HHQKLVFFAED-NH_2, was also characterized by CD spectroscopy. It had been previously used as a surrogate receptor for β amyloid in docking experiments (Chapters 3 & 4).

5.2 Materials and Common Methods

Human sequence β amyloid (1-42) and β amyloid (1-40) peptides were purchased from both Anaspec Inc (CA, USA) and Biopeptide Inc (CA, USA). The peptidic β amyloid oligomerization inhibitors, Ac-K(me)LV(me)FF-NH_2 and Ac-LP(me)FFD-NH_2, were purchased from Anaspec Inc (CA, USA). Other inhibitors and reagents such as Doxycycline, Rifampicin, Epicatechin Gallate, Thioflavin T, PBS Buffer, Sodium Dodecyl Sulfate (SDS), tris(hydroxymethyl)aminomethane (TRIS) and DMSO were purchased from VWR Canada (AB, Canada). Plastic-ware such as spectrofluorometer cuvettes and pipette tips were also purchased from VWR Canada.

The peptidic ligands known as SG1 and SG2 were synthesized at the Core Peptide Synthesis Facility at the University of Calgary by Dr. Dennis McMaster. The 11-mer

receptor fragment, henceforth known as R1, was also synthesized at the same facility. SG1, SG2 and R1 were synthesized by solid phase methods using standard Fmoc chemistry with Rink amide HMBA/ AM resins (SG2, R1) or Wang resin (SG1). Deprotection steps (30 minutes) were completed with 20% piperidine in N-methyl pyrrolidinone (NMP). Couplings reactions (30 min) used a 4-fold excess of Fmoc-amino acids with the coupling agents: 2-(1 H benzotriazole-1-yl)-1,1,3,3-tetramethyl uroniumtetrafluoroborate (TBTU) and N-hydroxybenzotriazole (HOBT) in NMP. Later batches of these compounds were made with alternate coupling agents, 2-(1H-7-azabenzotriazol-1-yl)-1,1,3,3-tetramethyl uronium hexafluorophosphate methanaminium (HATU) and 1-hydroxy-7-azabenzotriazole (HOAT), to increase yield.[356] Their characterization by mass spectroscopy is shown in Appendix B.

Amino acid sidechains were protected with standard protection groups, viz., ornithine (Boc), γ-diaminobutryic acid (Boc) and glutamic Acid (tBu). Peptides were cleaved from the resin and simultaneously deprotected with 95% aqueous trifluoroacetic acid (TFA) in the presence of 2% triisopropylsilane (TIS) and 2% ethanedithiol for 90 min. Products were precipitated with ether, washed twice with ether, filtered, purified with established HPLC techniques, lyophilized and stored at −20 ^{o}C. The molecular mass of the products was verified with electrospray and MALDI-TOF spectrometry. The final products were white lyophilized flakes with an estimated purity of over > 95%.

Stock solutions of SG1, SG2 and R1 (1 mM) were made in purified deionized (18 mΩ) water and stored at −20 ^{o} C. Stock solutions of Doxycycline, Rifampicin, Epicatechin Gallate, Ac-K(me)LV(me)FF-NH_2 and Ac-LP(me)FFD-NH_2 were also made in purified deionized (18 mΩ) water and stored at −20 ^{o} C. β amyloid (1-40) stock solutions were made in purified deionized (18 mΩ) water adjusted to a pH of 11 with NaOH/NH_4OH. Though this method is less elaborate than older methods that utilized fluorinated alcohols/TFA for preparing monomeric β amyloid stock solutions[357], commercially available β amyloid peptide preparations can now be

reliably disaggregated. Therefore an aqueous stock solution of β amyloid (1-40) at pH 11, made from such preparations, will not oligomerize unless the pH is lowered. CD experiments described in later sections of this chapter do demonstrate that this simple method does reliably create monomeric β amyloid.

β amyloid (1-42) stock solutions were also made by dissolving pre-monomerized preparations in purified deionized (18 mΩ) water adjusted to a pH of 11. However DMSO was added to the stock solution such that it had a final DMSO concentration of 20%. Addition of DMSO was necessary as β amyloid (1-42) oligomerizes far more readily than β amyloid (1-40). The final concentration of DMSO in each assay was less than 2% (after dilution), and was determined to have no effect on fibrillization.

5.3 Thioflavin T Fluorescence Assay

The Thioflavin T (ThT) fluorescence assay measures the extent of amyloid fibril formation, or inhibition thereof by ligands. It was chosen as the initial assay for measuring the anti-fibrillization activity of SG1 and SG2 because it was the simplest, least expensive and most widely used of the three assays. Moreover activity in this assay is a good surrogate indicator for activity in more expensive and technically demanding cell-based cytotoxicity assay.[358]

Thioflavin T (ThT) is a benzothiazole dye with a high affinity for fibrillar forms of amyloid proteins, but little or no affinity for their monomeric and smaller oligomeric forms. Upon binding to larger aggregates/fibrils of amyloidogenic proteins, the fluorescence of ThT between 460-490 nm undergoes a dramatically increase. Inhibition of amyloid protein fibrillization by any compound will reduce or eliminate the increase in fluorescence. Since fibrillization is an extension of the process that initially forms soluble oligomers, compounds that block fibrillization will almost always block formation of soluble oligomers. Protocols for the Thioflavin T (ThT) fluorescence assay are available in literature. [358, 115, 111]

The ThT assay protocol used, in this thesis, was a simplified version of many existing protocols. An aliquot of β amyloid peptide (1-40 or 1-42) stock solution was added to 200 μl PBS (in a disposable 0.5 ml plastic vial), containing or not containing a known amount of inhibitor. The mixture volume was adjusted such that it was 250 μl and the final concentration of β amyloid peptide (1-40 or 1-42) was 25 μM. The mixtures were vortexed for approximately 30 seconds and incubated, without shaking, at 37 °C for 5-7 days. The incubation period has been known to vary from one batch of β amyloid to another, and therefore each new batch of β amyloid peptides was validated with appropriate positive and negative controls. The assay methodology described in this thesis gave a good reproduction of literature values for peptidic and non-peptidic inhibitors (data not shown).[359]

Fluorescence experiments were performed using a Hitachi F-2000 fluorescence spectrophotometer. The contents of each incubated vial were pipetted out into a 5 ml plastic vial containing 3.75 ml of 10 μM Thioflavin T in PBS buffer (pH 7.5). The solution was vigorously mixed, and pipetted into a disposable 4 ml spectrofluorometer cuvette. Maximum fluorescence was observed when the excitation and emission wavelengths were set to 446 and 490 nm, respectively. Fluorescence readings were averaged over 30 seconds. Data on the effect of inhibitors was obtained with four or more independent samples for each concentration point. Plastic vials, pipette tips and cuvettes were not reused.

The concentration-effect data, seen in Figure 5.1, indicates that both SG1 and SG2 were significantly more potent that the control ligand, Ac-K(me)LV(me)FF-NH_2, at causing a 50% inhibition (IC_{50}) of both β amyloid (1-40) and β amyloid (1-42) fibrillization. For the sake of brevity, Ac-K(me)LV(me)FF-NH_2 is henceforth referred to as ‘I5mer’.The IC_{50} for both designed ligands was also attained at sub-stoichiometric molar ratios of 0.2, 0.5 (SG1) and 0.4, 0.8 (SG2) respectively to β amyloid (1-40) and (1-42). I5mer required a molar excess ratio of 2 and 4 to reach the IC_{50} for β amyloid (1-40) and (1-42) respectively.

The concentration-response/binding curve of a ligand, to a receptor, is sigmoidal and the midpoint of the linear part, aka IC_{50} (or EC_{50}), is a far better measurement of a ligands affinity than its IC_0 or IC_{100}, both of which occur in the non-linear regions of concentration-response curve. Having said that, IC_0 or IC_{100} values are useful to quantify the range of concentrations required for the desired activity. The IC_{100} value corresponds to the ligand concentration required to completely block β amyloid fibrillization. The fibrillization of β amyloid (1-40) was blocked at better molar ratios (0.2,0.4 and 2), by all three ligands (SG1,SG2, I5mer), than those required (0.5, 0.8, 4) to block β amyloid (1-42) fibrillization.

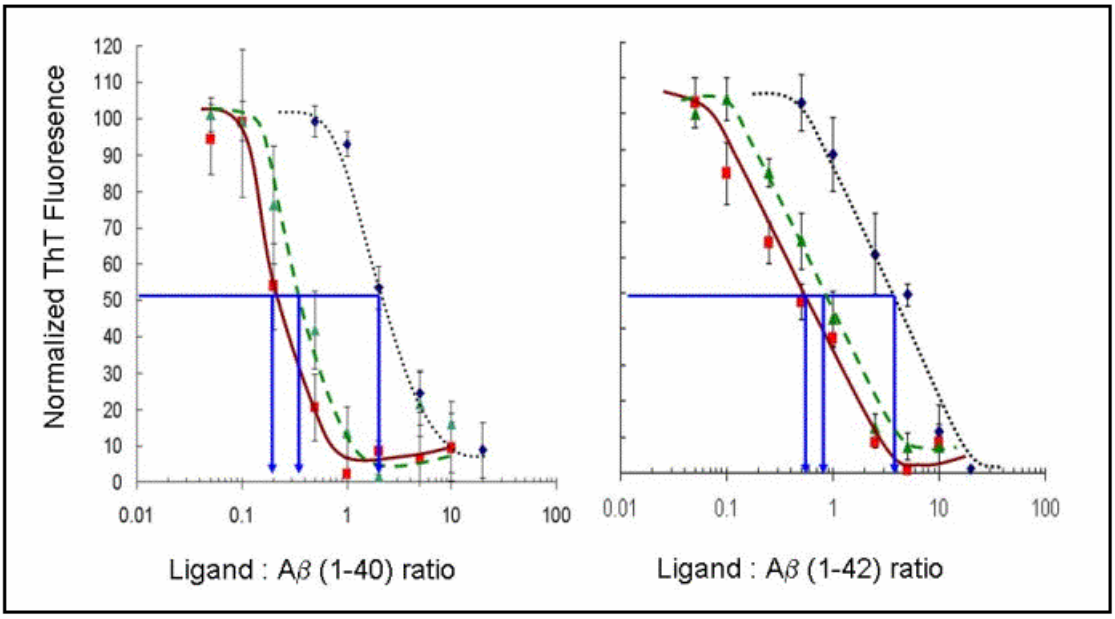

Figure 5.1 *Concentration-effect curves for the anti-fibrillization activity of SG1 (solid red line), SG2 (dashed green line) and I5mer (dotted blue line) against β amyloid (1-40) and β amyloid (1-42). The blue arrows plot the IC_{50} for each ligand to a ligand: β amyloid molar ratio. Please note that Aβ = β Amyloid.*

SG1 was somewhat more potent than SG2, and thus confirmed predictions made in Chapter 4, where SG1 (BHB score =369) was more potent than SG2 (BHB score =322). Both designed ligands were about 4-6 times more potent than I5mer

(BHB Score = 100), yet their molecular weight was only 30% higher that the standard ligand.

5.4 Western Blot Assay

The western blot assay was performed by Dave MacTavish in the lab of Dr. J. Jhamandas at University of Alberta, Edmonton Canada. It measured the effects of various molar stoichiometric ratios of SG1 and SG2 on the formation of soluble β amyloid oligomers. The β amyloid monomers and oligomers were labeled with 6E10 monoclonal antibodies.[360] The results, seen in Figure 5.2 and 5.3, demonstrated that sub-stoichiometric concentrations of SG1 and SG2 can block the formation of tetramers and larger oligomers of β amyloid (1-42). Increasing, but still sub-stoichiometric amounts of SG1 and SG2 reduced, and ultimately eliminated the formation of β amyloid trimers. The elimination of dimer formation required almost stoichiometric amounts (20 μM) of SG1 and SG2.

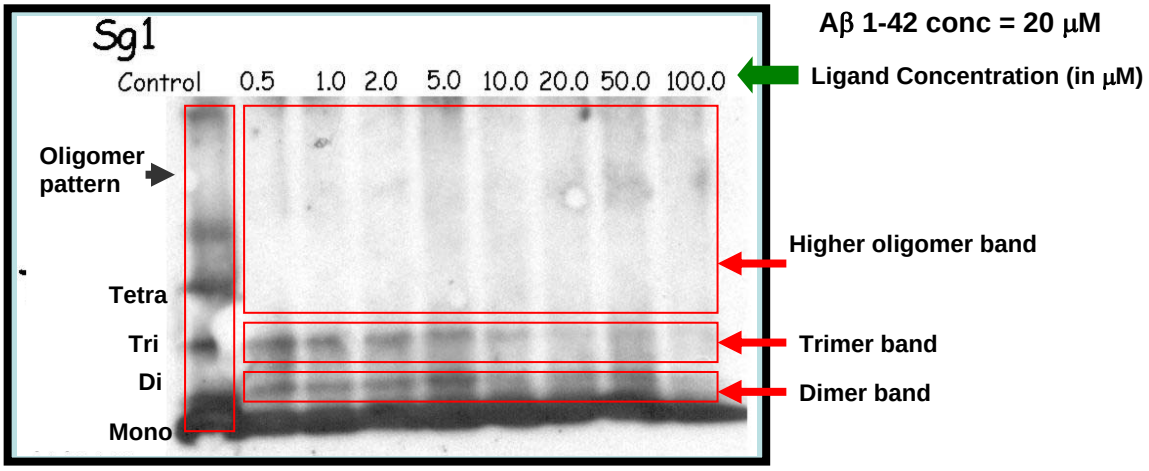

Figure 5.2 *Western blot of the concentration-dependent inhibition of β amyloid* (1-42) *oligomerization by SG1. Control (no ligand) oligomer pattern is on the far left side. SG1 eliminates the formation of tetramer and higher oligomers at very low concentrations, and causes gradual disappearance of trimers and dimers.*

Both ligands have about the same efficacy in blocking the formation of β amyloid (1-42) soluble oligomers. Since, β amyloid (1-42) was more aggregation prone than β amyloid 1-40, it is likely that the SG1 and SG2 would be more potent at inhibiting the formation of β amyloid (1-40) oligomers.

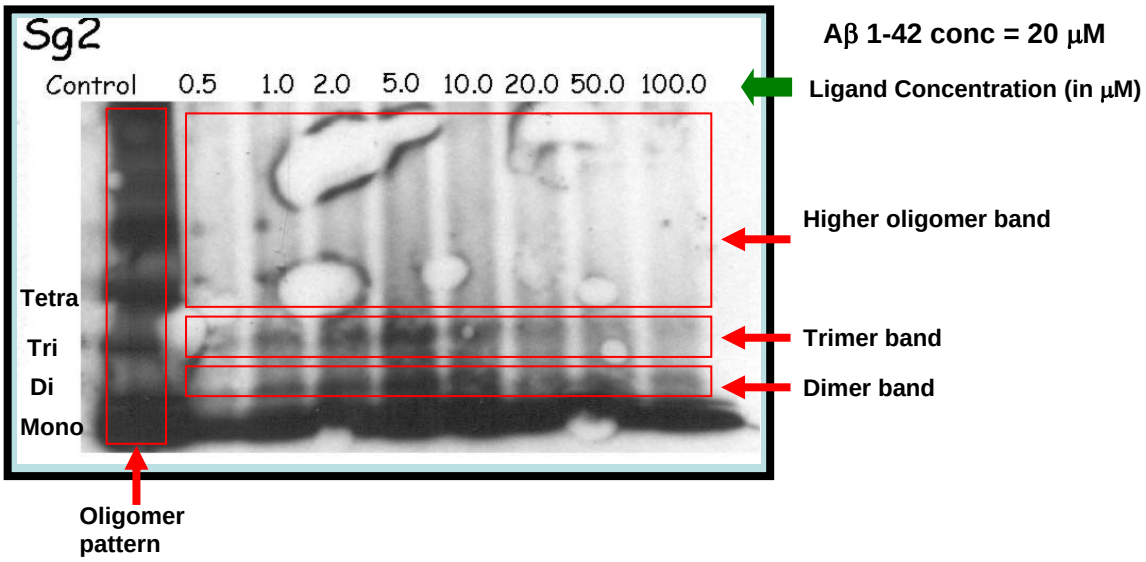

Figure 5.3 *A western blot of the concentration-dependent inhibition of β amyloid* (1-42) *oligomerization by SG2. Control (no ligand) oligomer pattern is on the far left side. SG2 also eliminates the formation of tetramer and higher oligomers at very low concentrations, and causes gradual disappearnce of trimers and then dimers.*

It would be worthwhile to repeat the assay with β amyloid (1-42) to ascertain reproducibility and with β amyloid (1-40) to compare the effects of SG1 and SG2 on oligomer formation.

5.5 Circular Dichroism Based Assays

Circular Dichroism (CD) spectroscopy is a popular technique for studying the secondary structure of proteins. Though it lacks the spatial resolution of X-ray crystallography or the information content of 2D NMR, it can be used to study proteins in systems and environments that would not be possible with X-ray

crystallography or 2D NMR (e.g. membrane bound proteins, dynamic protein-protein interactions). CD spectroscopy is especially suited to studying changes in secondary structure of proteins under physiological conditions.[361] The first CD spectroscopy studies on β amyloid peptides were performed in the early 1990s. [362, 363] These and subsequent studies suggest that nascent β amyloid peptide is predominantly random coil and its β strand content is increased by incubation.[364]

CD spectra shown in this thesis were acquired with a JASCO J-715 spectropolarimeter (UK) equipped with a thermostatted cell holder, using a quartz cell of 1-mm path length at 37°C. Spectra were collected over the wavelength range 180–260 nm with a 1 nm bandwidth. For each spectrum, ten scans were collected and averaged. The averaged data were then corrected for background using software supplied by the manufacturer. The CD values were expressed using mean residue molar ellipticity (MRE). Quantitative estimation of secondary structure was obtained by using the CONTIN deconvolution algorithm [365] on the CD deconvolution server- Dichroweb[366]

$$MRE = \frac{MRW * \theta}{10 * c * l} \qquad (5.1)$$

where MRW= Mean Residue Weight = molecular weight/ number of *chiral* backbone amide linkages. θ = machine units (mdeg), c = peptide concentration (mg/ml) and l = path length in cm. Spectra for all peptides and mixtures were obtained at pH 7.5 in 20 mM TRIS buffer. Though phosphate buffers are usually the first choice for obtaining CD spectra, the use of Cu^{2+} in some samples caused phosphate to slowly precipitate out of those samples.

5.6 Base CD Spectra of β Amyloid, R1, SG1, SG2 and I5mer.

The CD spectra of freshly prepared β amyloid (1-40), R1, SG1, SG2 and I5mer are shown in Figure 5.4. The ‘base’ CD spectra demonstrate that both nascent β

amyloid and R1[367] have no defined secondary structure, and is in agreement with the results obtained by other groups. In contrast SG1, SG2 and I5mer [368] possess some defined secondary structure (as determined by the CONTIN algorithm), which is most likely a mixture of β strand and α helix.

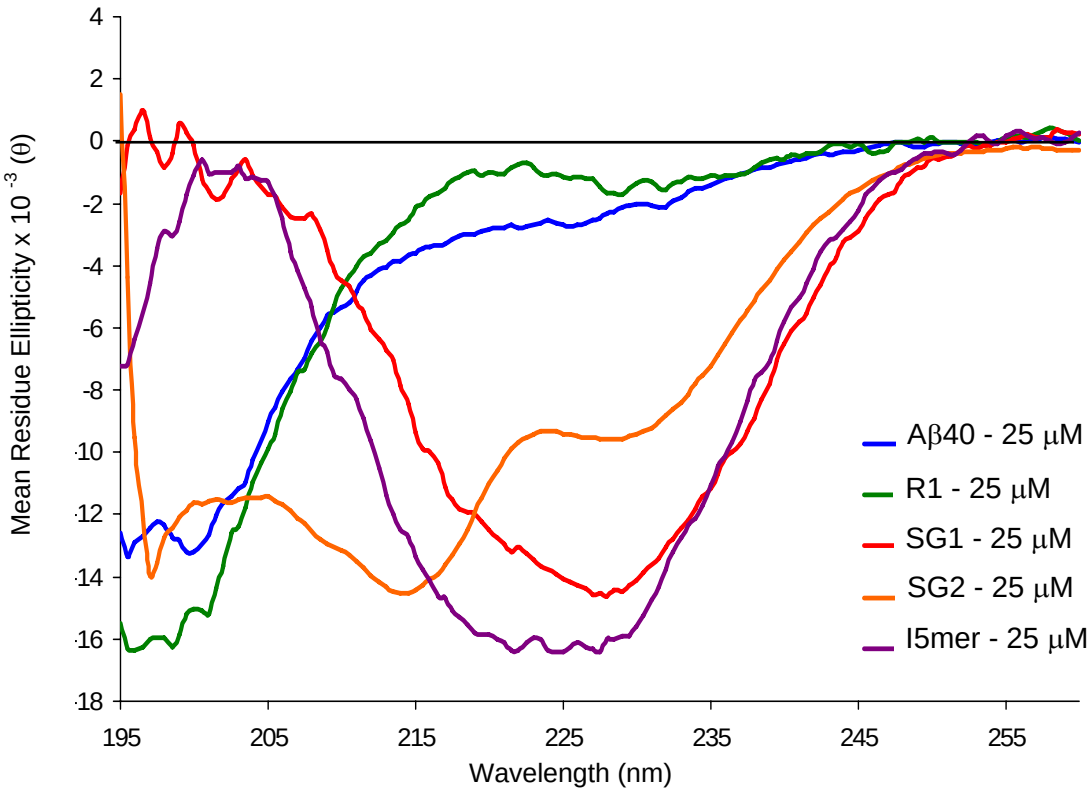

Figure 5.4 *The CD spectra of Aβ40 (blue), R1 (green), SG1 (red), SG2 (orange) and I5mer (purple) in a 20 mM TRIS buffer, at pH7.4, at 37° C. Mean Residue Ellipticity (θ) is in units of degrees cm^2 $dmol^{-1}$ $residue^{-1}$. Each CD spectrum is an average of 10 scans.*

It should be understood that all CD deconvolution algorithms were developed with large protein (100-300 residues) test sets, and therefore will suffer from limitations of accuracy when processing spectra from small peptides like R1 and the ligands. The addition of equimolar amounts of Cu^{2+} had no measurable effect on the CD spectra of R1, SG1, SG2 or I5mer (not shown). It however did cause a slight

reduction in the intensity, but not the overall shape, in the CD spectra of β amyloid (1-40).

Interaction of β amyloid with another molecule of itself (in the body) usually occurs on the surface of cell membranes, and such interactions are characterized by measurable changes in secondary structure.[369] Therefore, it was necessary to study the effects of surfactants on the CD spectra of β amyloid, R1 and the ligands. Sodium Dodecyl Sulphate (SDS) is the most commonly used surfactant to study protein/ peptide to 'membrane' interactions in cell free systems. Literature values for the Critical Micellar Concentration (CMC) of SDS in 5-40 mM TRIS buffer are between 2 and 3 mM.[370]

5.7 Effect of SDS on CD Spectra

SDS concentrations in the range of 0-10 mM had no significant effect on the CD spectra of R1, SG1, SG2 and I5mer (data not shown). Its effects on β amyloid (1-40) were both significant and concentration dependent. Many research groups have recently shown that surfactants, like SDS, have concentration dependent biphasic effects on β amyloid and other amyloidogenic peptides.[67, 68, 371, 372] It appears that concentrations of surfactants lower than their Critical Micellar Concentration (CMC), in a given solvent, promote the formation of soluble β strand rich oligomers. However, surfactant concentrations equal to or above the CMC concentration block the formation of oligomers and induce α helices in amyloidogenic peptides. The experimentally CMC of SDS, in buffers similar to those used in CD measurements, range from 2-3 mM. [371, 372]

The effect of various SDS concentrations on the CD spectra of β amyloid (1-40) is shown in Figure 5.5. SDS concentrations between 0 and 2 mM (in 20 mM TRIS) reduce the random coil component of CD spectra, and seem to increase the β strand content. However SDS concentrations approaching 3 mM or above cause an increase in α helical content at the loss of both random coil and β strand

content. A deconvolution of the CD spectra of β amyloid, with the CONTIN algorithm, as shown in Figure 5.5 (inset) showcases the effect in a graphical format.

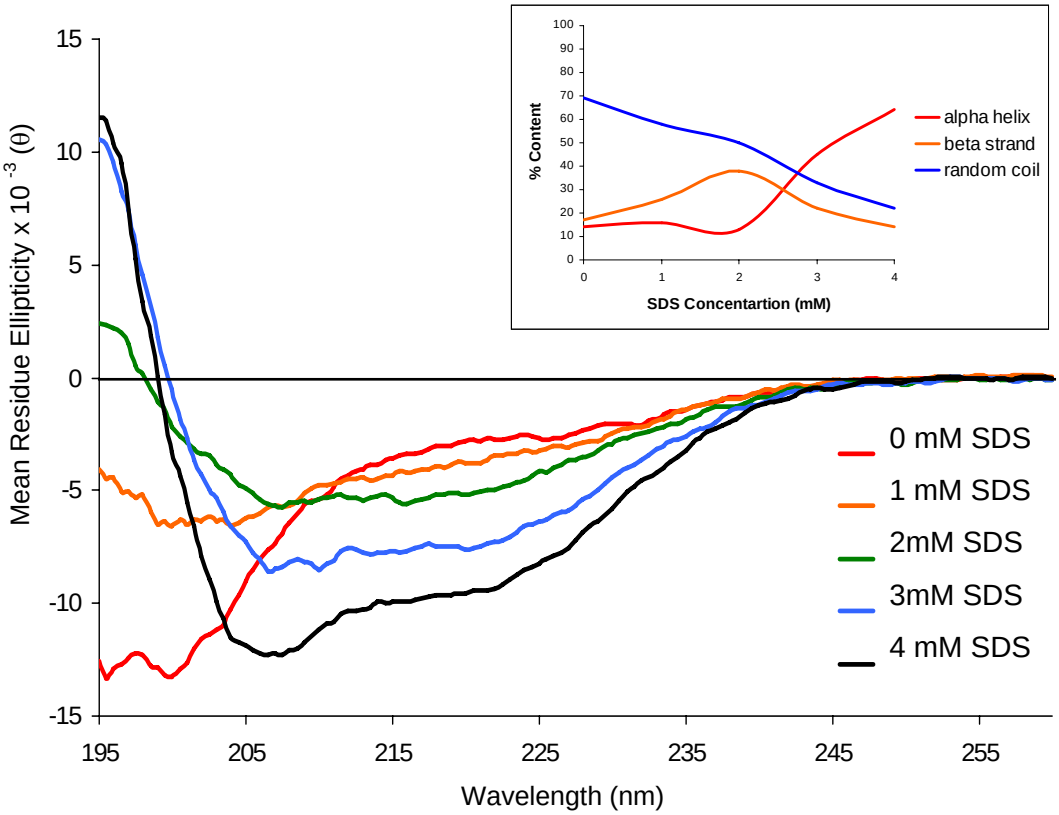

Figure 5.5 *The CD spectra of Aβ40 in TRIS 20 mM (at pH 7.5) with 0 mM (red), 1 mM (orange), 2 mM (green), 3 mM (light blue) and 4 mM SDS (black) at 37° C. Mean Residue Ellipticity (θ) is measured in units of degrees cm^2 $dmol^{-1}$ $residue^{-1}$. Each CD spectrum is an average of 10 scans. Inset graph shows changes in content of secondary structure as reported by CONTIN (Dichroweb)*

The effects of varying concentrations of SDS on the CD spectra of R1 were much less prominent than those seen in β amyloid (1-40). The effects, seen in Figure 5.6, indicate that SDS has a much smaller effect on the secondary structure of R1 as measured by CD.

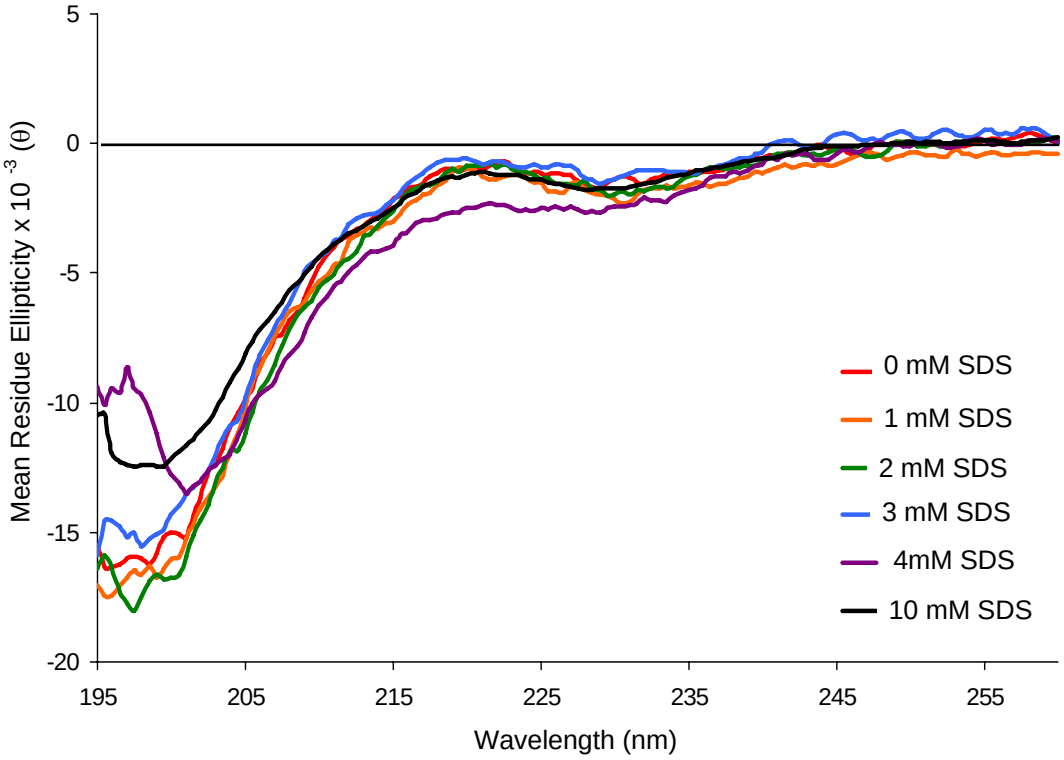

Figure 5.6 *The CD spectra of R1 in TRIS 20 mM (at pH 7.5) with 0 mM (red), 1 mM (orange), 2 mM (green), 3 mM (blue green), 4 mM SDS (purple) and 10 mM (black) at 37° C. Mean Residue Ellipticity (θ) is measured in units of- degrees cm^2 $dmol^{-1}$ $residue^{-1}$. Each CD spectrum is an average of 10 scans.*

5.8 Effects of Incubation on CD Spectra

The CD spectra of R1, SG1, SG2 and I5mer are not affected by incubation at 37° C for up to 7 days (data not shown). While there is no doubt that the 11mer peptide does undergo fibrillization, it seems to be a slower process than for β amyloid.

Incubation of β amyloid for 1, 3 and 7 days, causes change in the spectra (increased β strand content), resembling results published by other researchers. These changes have some resemblance to, but are not identical to those seen

later with submicellar SDS concentrations. The data has not been shown here because different batches of peptide show somewhat different CD spectral changes under identical conditions. In contrast, both fresh β amyloid with or without submicellar SDS has consistent CD spectra (as shown in Figure 5.5), regardless of the peptide manufacturer, batch or duration of storage as a stock solution.

5.9 Effect of Inhibitors on CD Spectra

Only SG1 and I5mer were tested in these experiments, since adequate amounts of SG2 were not available when they were performed. The effects of inhibitors on the spectra of R1 are not shown as there was no detectable effect even after 7 days of incubation at 37° C. Given the slow interaction of R1 with itself, that is not surprising. In contrast both SG1 and I5mer have an effect on the spectra of β amyloid.

Effects of these inhibitors were measured as the difference between arithmetic sums of their individual CD spectra (Sum) and the actual CD spectra of the mixture (Mix). The spectral difference indicated the nature of the secondary structure changes occurring through complex formation between the receptor and the ligand. Both possible CD 'difference' spectra (Mix-Sum and Sum-Mix), were calculated and subjected to deconvolution by CONTIN. In each case only one "difference" spectra gave a good deconvolution (RMSD <0.1), while the other possibility invariably gave a nonsensically poor deconvolution.

Though the CD spectra of inhibitor + β amyloid mixtures did show some differences from a mixture of otherwise non-interacting peptides, there was some variability in the effects (depending on the batch of peptide used). The effects of submicellar SDS on the inhibitor-β amyloid mixture in contrast, were both highly reproducible and immediate (and are discussed in section 5.9).

It appears that mixing β amyloid (1-40) and ligands (SG1/ I5mer) results in the formation of hetero-complexes with increased β strand content, which keeps increasing on incubation. While it is likely that lower molar ratios of the ligands could have an effect after incubation, the experiments chose to concentrate on ligand stoichiometries high enough to have a small but immediate effect on CD spectra (via hetero-complex formation).

5.10 Effects of Submicellar SDS and Inhibitors on CD Spectra

The literature on effects of submicellar SDS on β amyloid, repeated in a previous section of this chapter, created the possibility that the underlying process that sped up the formation of soluble oligomers (homo-complexes) could also speed up the interaction of ligands with the receptor. Therefore a reliably submicellar concentration of SDS (1mM) was added to receptor-ligand mixtures of varying molar stoichiometries.

Once again, submicellar SDS did not help the formation of a R1-ligand hetero-complex. However it was effective in speeding up formation of β amyloid(1-40)-ligand hetero-complexes. These hetero-complexes were formed almost instantaneously (within a minute) and had stable CD spectra for at least 1 hour at 37° C. Their ‘difference’ CD spectra, obtained as mentioned in the previous section, showed an increase in β strand content that was ligand concentration dependent (see Figure 5.7 and 5.8).

The CD ‘difference’ spectra of SG1 with β amyloid (1-40) as shown in Figure 5.7, show that SG1 can form complexes at substoichiometric molar ratios, indeed all ligand concentrations except the first (25 μM) are substoichiometric. In one aspect, they support the results of the western blot assays, which showed that substoichiometric concentrations of SG1 (and SG2) could block the formation of β amyloid (1-42) oligomers, and stoichiometric molar amounts blocked dimer formation.

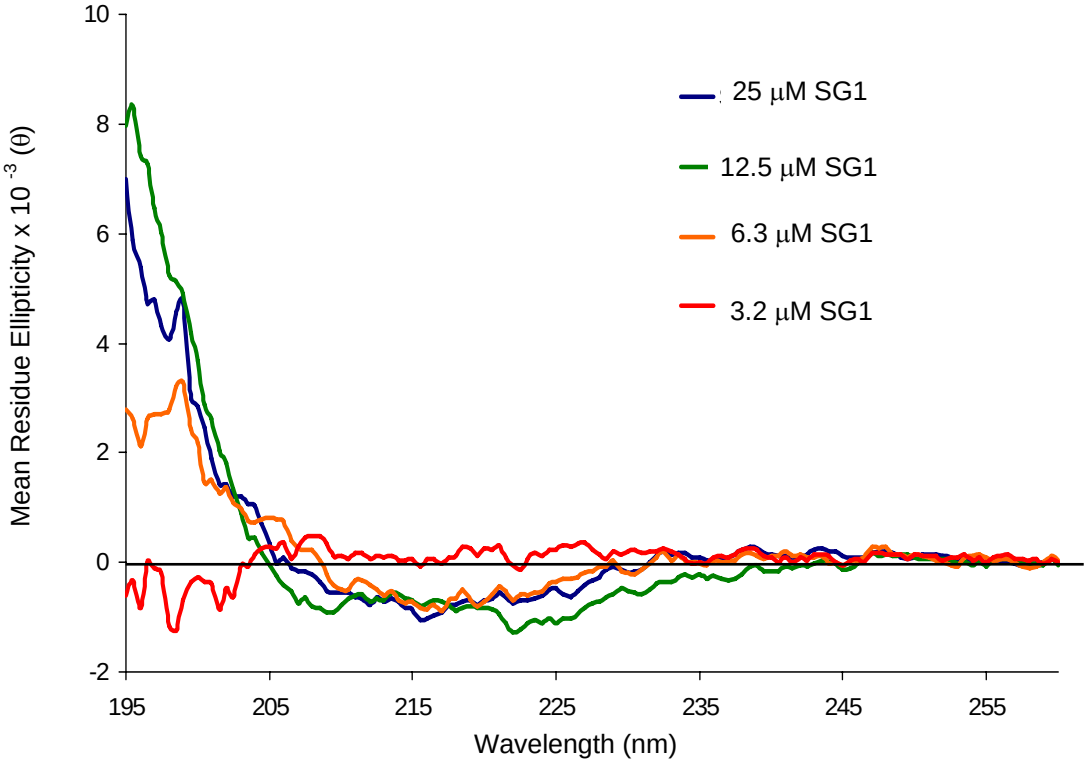

Figure 5.7 *The "mixture –sum difference" in CD spectra of β amyloid 40 (25 μM) and 1 mM SDS in TRIS 20 mM (at pH 7.5) with 25 μM SG1 (blue), 12.5 μM SG1 (green), 6.3 μM SG1 (orange), 3.2 μM SG1 (red). Mean Residue Ellipticity (θ) is measured in - degrees cm^2 $dmol^{-1}$ $residue^{-1}$. Each CD spectrum is an average of 10 scans.*

Given that β amyloid (1-42) is more amyloidogenic than β amyloid (1-40) it is likely that a significant component of the CD spectra of β amyloid by itself in submicellar amounts of SDS is due to soluble oligomers. While size-exclusion chromatography and electrophoresis have ascertained that to be the case with β amyloid (1-42) in submicellar concentrations of SDS, it has not yet been done for β amyloid (1-40). The standard ligand, I5mer, (seen in Figure 5.8) also causes the formation of hetero-complexes with a 'difference' spectra not unlike that obtained with SG1 (Figure 5.7).

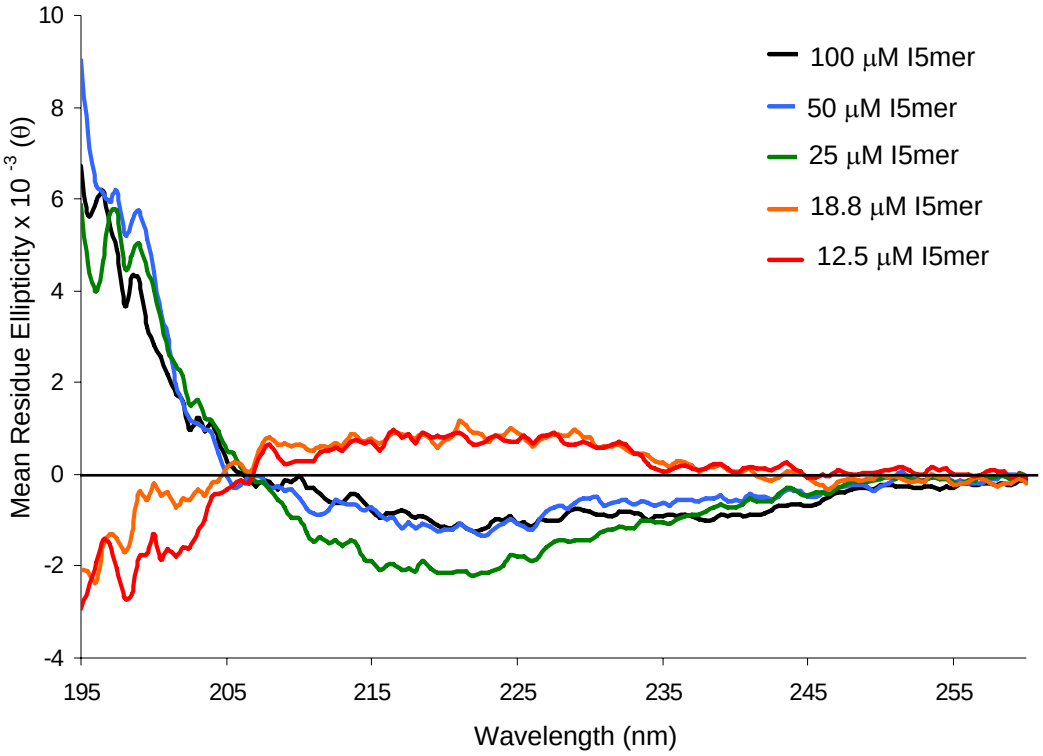

Figure 5.8 *The "mixture –sum difference" in CD spectra of β amyloid 40 (25 μM) and 1 mM SDS in TRIS 20 mM (at pH 7.5) with 100 μM I5mer (black), 50 μM I5mer (light blue), 25 μM I5mer (green), 18.8 μM I5mer (orange), and 12.5 μM I5mer (red). Mean Residue Ellipticity (θ) is measured in - degrees cm^2 $dmol^{-1}$ $residue^{-1}$. Each CD spectrum is an average of 10 scans.*

Once again the 'difference' spectra are dependent on ligand concentration, though the stoichiometric ratio required suggests that I5mer is less potent than SG1. The dropoff in the 'difference' CD spectra at lower concentration is also far sharper than for SG1.

It therefore appears that both SG1 and I5mer can form hetero-complexes with β amyloid (1-40) at molar stoichiometric ratios consistent with their activity in other assays, and is discussed in some more detail in the next section.

5.11 Conclusion and Discussion

The assays mentioned in this chapter measure three aspects of the interaction of β amyloid to ligands. The Thioflavin T (ThT) assay measures the ability to inhibit fibril formation, which is the last step in the process of β amyloid oligomerization. In that assay the designed ligands, SG1 and SG2, and I5mer inhibited fibril formation by both β amyloid (1-40) and (1-42). The molar stoichiometries required by I5mer to affect β amyloid oligomerization are within the range of activities reported for it by other groups using similar assays. Therefore, the superior potency of SG1 and SG2 as compared to I5mer, in the ThT fibrillization assay, is confirmed.

Western blots demonstrated that concentrations of β amyloid equivalent to those that block fibrillization in the ThT assay inhibit soluble β amyloid (1-42) oligomer formation, with equal stoichiometric molar amounts causing the inhibition of even dimers. The CD assay, demonstrated that ligands formed hetero-complexes with β amyloid (1-40) at molar stoichiometries similar to those required to block fibrillization in the ThT assay (and oligomer formation in the western blots).

It therefore appears that all three assays suggest that designed ligands can interact with β amyloid and block the formation of oligomers and fibrils. It also appears that they are superior to the standard ligand, I5mer, thus validating the predictions made in Chapter 4.

CHAPTER 6: FUTURE DEVELOPMENT AND EXPERIMENTS

6.1 Introduction

The last chapter of this thesis will attempt to lay out a path for future research projects to advance compounds described and developed in the current project towards their ultimate goal, namely clinical testing in AD patients. Development of potent ligands into drugs that demonstrate a therapeutic effect in human beings is an inherently risky endeavor, under the best of circumstances. The search for disease modifying treatments for AD has proved to be especially fruitless, notwithstanding the considerable amounts of money and research effort put into developing such drugs. Many promising drugs have failed in human clinical trials, even after demonstrating considerable efficacy in animal models of AD. The pre-clinical development of newer AD drugs must therefore factor both standard pharmacokinetic considerations as well as therapeutic efficacy in better (and novel) animal models of AD.

The suggested investigations are listed in the preferred chronological order starting with cell culture based assays and culminating in chronic animal AD models.

6.2 Effects in β amyloid cytotoxicity assays

Results of β amyloid aggregation, Western Blot and Circular Dichroism assays described in Chapter 5, demonstrate that the designed peptidic ligands described in Chapter 4, do indeed bind to β amyloid and block formation of soluble oligomers and fibrils. These assays also suggest that they are significantly more potent than other well characterized peptidic ligands, as previously shown in Chapter 4 and 5.

Since there is a good correlation between the ability of a ligand to block β amyloid oligomer formation and its ability to block β amyloid induced cytotoxicity, it is reasonable to believe that these designed ligands are potent and superior inhibitors of β amyloid induced cytotoxicity, which is the primary biochemical lesion

in both early-onset and mature-onset AD. However, it is necessary to validate any correlation-causation based claim with experimental data, since correlation does not imply causation.[373]

A rat PhaeoChromocytoma (PC-12) cell line is the standard cell-based assay for measuring the effects of a test compound on β amyloid induced cytotoxicity.[374] The assay quantitates the cytotoxicity of a given compound (or reversal of cytotoxicity) by measuring surrogate markers of cell viability such as normal metabolic activity or cell membrane integrity. PC-12 cells are a good surrogate for studying basic neuronal cell physiology, and are much easier to grow than primary neuronal cultures.[375] Moreover, the effects of previously known peptidic (and non-peptidic) inhibitors on β amyloid induced cytotoxicity have been well studied in PC-12 cell lines. [109, 110, 111] Therefore any useful comparison of the designed ligand's cytoprotective activity to older compounds can only be made by using PC-12 based cytotoxicity assays. The assays also measure any intrinsic toxicity of test compounds to neuronal type cells.

Testing of designed ligands in primary neuronal cultures is also desirable, if somewhat more problematic.[376, 377] The major problems with using primary neuronal cultures stem from difficulties in obtaining reproducible cell cultures and the lack of extensive experimental data for older ligands with any given primary neuronal culture type. Having said that, it would be worthwhile to study effects of designed and standard ligands in primary neuron cultures from newer murine transgenic AD models, such as 3xTgAD.[54]

6.3 Effects in β amyloid vascular assays

Literature, previously cited in Chapter 2 (section 2.7), suggests that β amyloid has adverse effects on cerebrovascular function. While the precise type of β amyloid oligomers responsible for vascular effects is unclear, the effects involve generation

of superoxide radicals. So far, there have been no reported studies of the effects of oligomerization inhibitors on β amyloid induced vascular dysfunction.

The vascular effects of β amyloid (1-40) occur at significantly lower concentrations [378] than its cytotoxic effects[379], and therefore might have an important role in the onset and pathology of late onset AD. Testing the effects of β amyloid aggregation inhibitors on β amyloid induced vascular dysfunction should be an important part of any future effort to develop inhibitors of β amyloid oligomerization.

The effects of β amyloid (and oligomerization inhibitors) on vascular function can be measured by a variety of vascular assays. These assays range from isolated vascular preparations like the rat aorta[380] to whole animal assays which measure changes in cerebral blood flow (CBF).[381] Measuring the effects of these compounds on the impaired CBF in some chronic AD models is another worthwhile option.[382]

6.4 Determination of ADME properties

The pharmacokinetic properties of a potential drug are as important as its pharmacological effects, and are commonly known as ADME properties. ADME is an acronym for **A**bsorption, **D**istribution, **M**etabolism and **E**xcretion. Poor ADME characteristics are one of major reason behind the high attrition rate of many promising compounds undergoing preclinical testing.[383]

Since compounds developed in this project will most likely be parentally administered pseudopeptidic drugs, determination of the rate and extent of oral absorption is not necessary. The metabolic stability of these compounds does however need to be experimentally validated as they are pseudopeptidic in nature. Ligand features such as the use of unnatural residues, N-methylated residues and dextrorotary residues (described in Chapter 4) should make them fairly stable to enzymatic degradation. Initially simple *in vitro* tests based on hepatic microsomes

will be useful to predict the metabolic fate of the ligands.[384] However more complex *in vivo* testing of the plasma and tissue half-lives of these drugs will be necessary, preferably in at least 3 separate animal species including rhesus monkeys (*Macaca mulatta*). Other tests such as measuring the extent of protein binding, checking for inhibition of hepatic enzymes and levels of drug metabolites in urine are also important for ligands that have passed the initial tests. ADME assays are likely to be done by Contract Research Organizations (CROs) with prior expertise in ADME profiling.

Adequate penetration of the Blood Brain Barrier (BBB) is probably the most crucial pharmacokinetic consideration for any drug used to treat diseases of the central nervous system.[385] Lipid based functionalizations and design features necessary for adequate penetration of ligands through the BBB have been previously discussed in Chapter 4. However it will be necessary to measure BBB penetration for each tested ligand in an animal assay. Unlike ADME properties, passive and most active BBB penetration for a given compound is fairly consistent across mammalian species. The assays for measuring BBB penetration [386, 387] will be also performed by CROs with prior expertise in that area.

6.5 Efficacy in Acute Animal AD Models

The intracerebral injection of β amyloid causes acute cognitive dysfunction, localized plaque buildup and inflammation in the brain.[388] Reversal of these effects with systemically administered β amyloid oligomerization inhibitors was one of the first demonstrations of therapeutic efficacy of these compounds. [389] The assay has since been refined to use stereotactic injection of β amyloid in the temporal lobes of the animal to better reproduce the effects of AD. [390]

The β amyloid intracerebral injection assay is one of the quickest animal assays for determining the efficacy of a compound for treating AD. Moreover because of the short duration of the model (a few weeks) it uses a much smaller amount of the

tested compound than chronic animal models of AD. Therefore it is usually considered to a preliminary step to testing compounds in chronic animal AD models.

6.6 Efficacy in Chronic Animal AD Models

Chronic animal models of AD along with their advantages and disadvantages have been reviewed in Chapter 1. Compounds that demonstrate efficacy in the previously mentioned assays will be tested in chronic animal models of AD. The most accurate reproduction of human pathology (albeit of early onset AD) is seen in the 3xTg-AD model, and would be the best model for testing the efficacy of new β amyloid oligomerization inhibitors. [54]

However the availability of this particular model for testing our drug candidates might be complicated by intellectual property and licensing issues. Therefore it is necessary to have a second choice of animal AD models for chronic testing of the advanced drug candidates. Double transgenic models such as APP/PSAP and APP/*tau* (see Chapter 1) are the most obvious second choice for chronic animal testing. APP/PSAP based models are best suited for studying the effect of the compounds on β amyloid induced neuronal dysfunction, inflammation and CBF changes. [44, 45] APP/*tau* based models are best suited for studying the impact of the compounds on β amyloid induced primary and secondary (*tau* induction related) damage including its impact on the overall disease process.

Regardless of which chronic AD animal model is finally chosen for testing, the compounds will have to reduce soluble/insoluble β amyloid levels and ameliorate cognitive deficits to be developed any further. Demonstration of reasonable ADME characteristics in a few non-human mammalian species and efficacy in chronic animal models of AD is one of the major pieces of evidence necessary for filing an Investigational New Drug (IND) application, with the FDA or it's equivalent outside the USA), and initiating Phase I clinical trials in human beings.

REFERENCES

[1] Brookmeyer R, Corrada MM, Curriero FC, Kawas C. (2002) Survival following a diagnosis of Alzheimer disease, *Arch Neurol,* 59(11): 1764–7.

[2] Larson EB, Shadlen MF, Wang L, McCormick WC, Bowen JD, Teri L, Kukull WA. (2004) Survival after initial diagnosis of Alzheimer disease. *Ann Intern Med*. 40(7): 501-9.

[3] US Census Bureau (1995) http://www.census.gov/population/socdemo/statbriefs/agebrief.html (accessed Nov-11-2009)

[4] US Census Bureau- 65+ in the US : (2006) http://www.census.gov/prod/2006pubs/p23-209.pdf (accessed Nov-11-2009)

[5] Bloom BS, de Pouvourville N, Straus WL. (2003) Cost of illness of Alzheimer's disease: how useful are current estimates? *Gerontologist.* 43(2):158–64.

[6] Andersen K, Launer LJ, Dewey ME, Letenneur L, Ott A, Copeland JR, Dartigues JF, Kragh-Sorensen P, Baldereschi M, Brayne C, Lobo A, Martinez-Lage JM, Stijnen T, Hofman A. (1999) Gender differences in the incidence of AD and vascular dementia: The EURODEM Studies. EURODEM Incidence Research Group. *Neurology.* 10; 53(9): 1992-7.

[7] Driscoll I, Resnick SM. (2007) Testosterone and cognition in normal aging and Alzheimer's disease: an update. *Curr Alzheimer Res.* 4(1): 33-45.

[8] Pike CJ, Rosario ER, Nguyen TV. (2006) Androgens, aging, and Alzheimer's disease. *Endocrine.* 29(2):233-41.

[9] Trinh NH, Hoblyn J, Mohanty S, Yaffe K. (2003) Efficacy of cholinesterase inhibitors in the treatment of neuropsychiatric symptoms and functional impairment in Alzheimer disease: a meta-analysis. *JAMA.* 289(2): 210–6.

[10] Stahl SM. (2000) The new cholinesterase inhibitors for Alzheimer's disease, Part 1: their similarities are different. *J Clin Psychiatry.* 61(10): 710–1.

[11] Areosa SA, Sherriff F. Memantine for dementia. (2003) *Cochrane Database Syst Rev* (3) : CD003154.

[12] Waite J. (2006) The effectiveness of atypical antipsychotics for the treatment of aggression and psychosis in Alzheimer's disease. *Cochrane Database Syst Rev.* (1):CD003476.

[13] Shenk David. (2001) *The Forgetting: Alzheimer's: Portrait of an Epidemic.* New York, NY, Doubleday, ISBN 0-385-79837-3

[14] William Shakesphere. (1999) *King Lear* (reprint) Penguin Classics, London

[15] Schoenhofen E, Wyszynski DF, Andersen S, Pennington J, Young R, Terry DF, Perls TT. (2006) Characteristics of 32 Supercentenarians *Journal of the American Geriatrics Society*. 54, 1237-1240.

[16] Rossor MN. (2001) Pick's disease: a clinical overview. *Neurology.* 56(11 Suppl 4): S3-5.

[17] Caselli RJ, Beach TG, Yaari R, Reiman EM. (2006) Alzheimer's disease a century later. *J Clin Psychiatry.* 7(11):1784-800.

[18] Ballard CG. (2004) Definition and diagnosis of dementia with Lewy bodies. *Dement Geriatr Cogn Disord.* 17 Suppl 1:15-24.

[19] Graeber MB, Kosel S, Egensperger R, Banati RB, Muller U, Bise K, Hoff P, Moller HJ, Fujisawa K, Mehraein P. (1997) Rediscovery of the case described by Alois Alzheimer in 1911: historical, histological and molecular genetic analysis. *Neurogenetics.* 1(1): 73-80.

[20] Klunemann HH, Fronhofer W, Wurster H, Fischer W, Ibach B, Klein HE. (2002) Alzheimer's second patient: Johann F. and his family. *Ann Neurol.* 52(4): 520-3.

[21] Möller HJ, Graeber MB. (1998) The case described by Alois Alzheimer in 1911. Historical and conceptual perspectives based on the clinical record and neurohistological sections*. Eur Arch Psychiatry Clin Neurosci.* 248(3):111-22.

[22] Graeber MB, Mehraein P. (1999) Reanalysis of the first case of Alzheimer's disease. *Eur Arch Psychiatry Clin Neurosci.* 249 Suppl 3: 10-3.

[23] Goedert M, Ghetti B. (2007) Alois Alzheimer: his life and times. *Brain Pathol.* 17(1): 57-62.

[24] Reisberg B. (2006) Diagnostic criteria in dementia: a comparison of current criteria, research challenges, and implications for DSM-V. *J Geriatr Psychiatry Neurol.* 19(3): 137-46.

[25] Henderson VW, Finch CE. (1989) The neurobiology of Alzheimer's disease. *J Neurosurg.* 70(3):335-53.

[26] Armstrong RA. (1998) Beta-amyloid plaques: stages in life history or independent origin*? Dement Geriatr Cogn Disord.*;9(4):227-38.

[27] Castellani RJ, Nunomura A, Lee HG, Perry G, Smith MA. (2008) Phosphorylated tau: toxic, protective, or none of the above. *J Alzheimers Dis.* 14(4):377-83.

[28] What is Alzheimer's (http://alz.org/alzheimers_disease_what_is_alzheimers.asp), (accessed Nov-01-2009)

[29] Selkoe DJ. (2000) Toward a comprehensive theory for Alzheimer's disease. Hypothesis: Alzheimer's disease is caused by the cerebral accumulation and cytotoxicity of amyloid beta-protein. *Ann N Y Acad Sci.* 924:17-25.

[30] Rankin CA, Gamblin TC. (2008) Assessing the toxicity of tau aggregation. *J Alzheimers Dis.* 14(4):411-6.

[31] Honson NS, Kuret J. (2008) Tau aggregation and toxicity in tauopathic eurodegenerative diseases. *J Alzheimers Dis.*14(4):417-22.

[32] Hardy J, Selkoe DJ. (2002) The amyloid hypothesis of Alzheimer's disease: progress and problems on the road to therapeutics. *Science.* 297(5580):353-6.

[33] LaFerla FM, Oddo S. (2005) Alzheimer's disease: Abeta, tau and synaptic dysfunction. *Trends Mol Med.* 11(4):170-6.

[34] Bertram L, Tanzi RE. (2008) Thirty years of Alzheimer's disease genetics: the implications of systematic meta-analyses. *Nat Rev Neurosci.* 9(10):768-78.

[35] Williamson J, Goldman J, Marder KS. (2009) Genetic aspects of Alzheimer disease. *Neurologist.* 15(2):80-6.

[36] Manelli AM, Stine WB, Van Eldik LJ, LaDu MJ. (2004) ApoE and Abeta1-42 interactions: effects of isoform and conformation on structure and function. *J Mol Neurosci.* 23(3):235-46

[37] Van Dam D, De Deyn PP. (2006) Drug discovery in dementia: the role of rodent models. *Nat Rev Drug Discov.* 5(11):956-70.

[38] Eriksen JL, Janus CG. (2007) Plaques, tangles, and memory loss in mouse models of neurodegeneration. *Behav Genet.* 37(1):79-100.

[39] Games D, Adams D, Alessandrini R, Barbour R, Berthelette P, Blackwell C, Carr T, Clemens J, Donaldson T, Gillespie F, et al (1995) Alzheimer-type neuropathology in transgenic mice overexpressing V717F beta-amyloid precursor protein. *Nature.* 373(6514):523-7.

[40] Hsiao K, Chapman P, Nilsen S, Eckman C, Harigaya Y, Younkin S, Yang F, Cole G. (1996) Correlative memory deficits, Abeta elevation, and amyloid plaques in transgenic mice. *Science.* 274(5284):99-102.

[41] Irizarry MC, McNamara M, Fedorchak K, Hsiao K, Hyman BT. (1997) APPSw transgenic mice develop age-related A beta deposits and neuropil abnormalities, but no neuronal loss in CA1. *J Neuropathol Exp Neurol.* 56(9):965-73.

[42] McGowan E, Eriksen J, Hutton M. (2006) A decade of modeling Alzheimer's disease in transgenic mice. *Trends Genet.* 22(5):281-9.

[43] Czech C, Masters C, Beyreuther K. (1994) Alzheimer's disease and transgenic mice. *J Neural Transm Suppl.* 44:219-30.

[44] McGowan E, Sanders S, Iwatsubo T, Takeuchi A, Saido T, Zehr C, Yu X, Uljon S, Wang R, Mann D, Dickson D, Duff K. (1999) Amyloid phenotype characterization of transgenic

mice overexpressing both mutant amyloid precursor protein and mutant presenilin 1 transgenes. *Neurobiol Dis.* 6(4):231-44.

[45] Holcomb L, Gordon MN, McGowan E, Yu X, Benkovic S, Jantzen P, Wright K, Saad I, Mueller R, Morgan D, Sanders S, Zehr C, O'Campo K, Hardy J, Prada CM, Eckman C, Younkin S, Hsiao K, Duff K. (1998) Accelerated Alzheimer-type phenotype in transgenic mice carrying both mutant amyloid precursor protein and presenilin 1 transgenes. *Nat Med.* 4(1):97-100.

[46] Götz J, Deters N, Doldissen A, Bokhari L, Ke Y, Wiesner A, Schonrock N, Ittner LM. (2007) A decade of tau transgenic animal models and beyond. *Brain Pathol.* 17(1):91-103

[47] Lewis J, McGowan E, Rockwood J, Melrose H, Nacharaju P, Van Slegtenhorst M, Gwinn-Hardy K, Paul Murphy M, Baker M, Yu X, Duff K, Hardy J, Corral A, Lin WL, Yen SH, Dickson DW, Davies P, Hutton M. (2000) Neurofibrillary tangles, amyotrophy and progressive motor disturbance in mice expressing mutant (P301L) tau protein. *Nat Genet.* 25(4):402-5.

[48] Lambourne SL, Humby T, Isles AR, Emson PC, Spillantini MG, Wilkinson (2007) Impairments in impulse control in mice transgenic for the human FTDP-17 tauV337M mutation are exacerbated by age. *Hum Mol Genet.* 16(14):1708-19.

[49] Götz J, Ittner LM. (2008) Animal models of Alzheimer's disease and frontotemporal dementia. *Nat Rev Neurosci.* 9(7):532-44.

[50] Götz J, Chen F, van Dorpe J, Nitsch RM. (2001) Formation of neurofibrillary tangles in P301l tau transgenic mice induced by Abeta 42 fibrils. *Science.* 293(5534):1491-5.

[51] Lewis J, Dickson DW, Lin WL, Chisholm L, Corral A, Jones G, Yen SH, Sahara N, Skipper L, Yager D, Eckman C, Hardy J, Hutton M, McGowan E. (2001) Enhanced neurofibrillary degeneration in transgenic mice expressing mutant tau and APP. *Science.* 293(5534):1487-91.

[52] Götz J, Schild A, Hoerndli F, Pennanen L. (2004) Amyloid-induced neurofibrillary tangle formation in Alzheimer's disease: insight from transgenic mouse and tissue-culture models. *Int J Dev Neurosci.* 22(7):453-65.

[53] Ribé EM, Pérez M, Puig B, Gich I, Lim F, Cuadrado M, Sesma T, Catena S, Sánchez B, Nieto M, Gómez-Ramos P, Morán MA, Cabodevilla F, Samaranch L, Ortiz L, Pérez A, Ferrer I, Avila J, Gómez-Isla T.(2005) Accelerated amyloid deposition, neurofibrillary degeneration and neuronal loss in double mutant APP/tau transgenic mice. *Neurobiol Dis.* 20(3):814-22.

[54] Oddo S, Caccamo A, Shepherd JD, Murphy MP, Golde TE, Kayed R, Metherate R, Mattson MP, Akbari Y, LaFerla FM. (2003) Triple-transgenic model of Alzheimer's disease with plaques and tangles: intracellular Abeta and synaptic dysfunction. *Neuron.* 39(3):409-21.

[55] Oddo S, Vasilevko V, Caccamo A, Kitazawa M, Cribbs DH, LaFerla FM. (2006)

Reduction of soluble Abeta and tau, but not soluble Abeta alone, ameliorates cognitive decline in transgenic mice with plaques and tangles. *J Biol Chem.* 281(51):39413-23.

[56] Senechal Y, Larmet Y, Dev KK. (2006) Unraveling in vivo functions of amyloid precursor protein: insights from knockout and knockdown studies. *Neurodegener Dis.* 3(3):134-47.

[57] Priller C, Bauer T, Mitteregger G, Krebs B, Kretzschmar HA, Herms J. (2006) Synapse formation and function is modulated by the amyloid precursor protein. *J Neurosci.* 26(27):7212-21

[58] Zheng H, Koo EH. (2006) The amyloid precursor protein: beyond amyloid. *Mol Neurodegener.* 1:5.

[59] Zheng H, Jiang M, Trumbauer ME, Sirinathsinghji DJ, Hopkins R, Smith DW, Heavens RP, Dawson GR, Boyce S, Conner MW, Stevens KA, Slunt HH, Sisoda SS, Chen HY, Van der Ploeg LH. (1995) beta-Amyloid precursor protein-deficient mice show reactive gliosis and decreased locomotor activity. *Cell.* 81(4):525-31.

[60] Müller U, Cristina N, Li ZW, Wolfer DP, Lipp HP, Rülicke T, Brandner S, Aguzzi A, Weissmann C. (1994) Behavioral and anatomical deficits in mice homozygous for a modified beta-amyloid precursor protein gene*. Cell. 79*(5):755-65.

[61] Lin SY, Chu HL. (2003) Fourier transform infrared spectroscopy used to evidence the prevention of beta-sheet formation of amyloid beta(1-40) peptide by a short amyloid fragment. *Int J Biol Macromol.* 32(3-5):173-7.

[62] Nichols MR, Moss MA, Reed DK, Hoh JH, Rosenberry TL. Amyloid-beta aggregates formed at polar-nonpolar interfaces differ from amyloid-beta protofibrils produced in aqueous buffers. *Microsc Res Tech.* 2005 Jul;67(3-4):164-74.

[63] Laczkó I, Vass E, Soós K, Fülöp L, Zarándi M, Penke B. (2008) Aggregation of Abeta(1-42) in the presence of short peptides: conformational studies.
J Pept Sci. 14(6):731-41.

[64] Sgarbossa A, Buselli D, Lenci F. (2008) In vitro perturbation of aggregation processes in beta-amyloid peptides: a spectroscopic study. *FEBS Letters.* 582(23 – 24):3288 – 3292.

[65] Sciarretta KL, Gordon DJ, Petkova AT, Tycko R, Meredith SC. (2005) Abeta40-Lactam(D23/K28) models a conformation highly favorable for nucleation of amyloid. *Biochemistry.* 44(16):6003-14.

[66] Rangachari V, Moore BD, Reed DK, Sonoda LK, Bridges AW, Conboy E, Hartigan D, Rosenberry TL. (2007) Amyloid-beta(1-42) rapidly forms protofibrils and oligomers by distinct pathways in low concentrations of sodium dodecylsulfate. *Biochemistry.* 46(43):12451-62.

[67] Rangachari V, Reed DK, Moore BD, Rosenberry TL. (2006) Secondary structure and interfacial aggregation of amyloid-beta(1-40) on sodium dodecyl sulfate micelles. *Biochemistry.* 45(28):8639-48.

[68] Tew DJ, Bottomley SP, Smith DP, Ciccotosto GD, Babon J, Hinds MG, Masters CL, Cappai R, Barnham KJ. (2008) Stabilization of neurotoxic soluble beta-sheet-rich conformations of the Alzheimer's disease amyloid-beta peptide. *Biophys J.* 94(7):2752-66.

[69] Aleshkov S, Abraham CR, Zannis VI. (1997) Interaction of nascent ApoE2, ApoE3, and ApoE4 isoforms expressed in mammalian cells with amyloid peptide beta (1-40). Relevance to Alzheimer's disease. *Biochemistry.* 36(34):10571-80.

[70] Mastrangelo IA, Ahmed M, Sato T, Liu W, Wang C, Hough P, Smith SO. (2006) High-resolution atomic force microscopy of soluble Abeta42 oligomers. *J Mol Biol.* 358(1):106-19.

[71] Ono K, Condron MM, Teplow DB. (2009) Structure-neurotoxicity relationships of amyloid {beta}-protein oligomers. *Proc Natl Acad Sci U S A.* 106(35): 14745-14750

[72] Cerf E, Sarroukh R, Tamamizu-Kato S, Breydo L, Derclaye S, Dufrêne YF, Narayanaswami V, Goormaghtigh E, Ruysschaert JM, Raussens V. (2009) Antiparallel beta-sheet: a signature structure of the oligomeric amyloid beta-peptide. *Biochem J.* 421(3):415-23.

[73] Huang TH, Yang DS, Plaskos NP, Go S, Yip CM, Fraser PE, Chakrabartty A. (2000) Structural studies of soluble oligomers of the Alzheimer beta-amyloid peptide. *J Mol Biol.* 297(1):73-87.

[74] Ward RV, Jennings KH, Jepras R, Neville W, Owen DE, Hawkins J, Christie G, Davis JB, George A, Karran EH, Howlett DR. (2000) Fractionation and characterization of oligomeric, protofibrillar and fibrillar forms of beta-amyloid peptide. *Biochem J.* 348 Pt 1:137-44.

[75] Lal R, Lin H, Quist AP. (2007) Amyloid beta ion channel: 3D structure and relevance to amyloid channel paradigm. *Biochim Biophys Acta.* 1768(8):1966-75.

[76] Klyubin I, Betts V, Welzel AT, Blennow K, Zetterberg H, Wallin A, Lemere CA, Cullen WK, Peng Y, Wisniewski T, Selkoe DJ, Anwyl R, Walsh DM, Rowan MJ. (2008) Amyloid beta protein dimer-containing human CSF disrupts synaptic plasticity: prevention by systemic passive immunization. *J Neurosci.* 28(16):4231-7.

[77] Townsend M, Shankar GM, Mehta T, Walsh DM, Selkoe DJ. (2006) The role of cell-derived oligomers of Abeta in Alzheimer's disease and avenues for therapeutic intervention. *J Physiol.* 572(Pt 2):477-92.

[78] Lesné S, Koh MT, Kotilinek L, Kayed R, Glabe CG, Yang A, Gallagher M, Ashe KH. (2006) A specific amyloid-beta protein assembly in the brain impairs memory. *Nature.* 440(7082):352-7.

[79] Dineley KT. (2007) Beta-amyloid peptide--nicotinic acetylcholine receptor interaction: the two faces of health and disease. *Front Biosci.* 12:5030-8.

[80] Walsh DM, Klyubin I, Fadeeva JV, Rowan MJ, Selkoe DJ. (2002)

Naturally secreted oligomers of amyloid beta protein potently inhibit hippocampal long-term potentiation in vivo. *Biochem Soc Trans.* 30(4):552-7.

[81] McLean CA, Cherny RA, Fraser FW, Fuller SJ, Smith MJ, Beyreuther K, Bush AI, Masters CL. (1999) Soluble pool of Abeta amyloid as a determinant of severity of neurodegeneration in Alzheimer's disease. *Ann Neurol.* 46(6):860-6.

[82] Tycko R. (2006) Solid-state NMR as a probe of amyloid structure. *Protein Pept Lett.* 13(3):229-34.

[83] Kheterpal I, Zhou S, Cook KD, Wetzel R. (2000) Abeta amyloid fibrils possess a core structure highly resistant to hydrogen exchange. *Proc Natl Acad Sci U S A.* 97(25):13597-601.

[84] Whittemore NA, Mishra R, Kheterpal I, Williams AD, Wetzel R, Serpersu EH. (2005) Hydrogen-deuterium (H/D) exchange mapping of Abeta 1-40 amyloid fibril secondary structure using nuclear magnetic resonance spectroscopy. *Biochemistry.* 44(11):4434-41.

[85] Williams AD, Portelius E, Kheterpal I, Guo JT, Cook KD, Xu Y, Wetzel R. (2004) Mapping abeta amyloid fibril secondary structure using scanning proline mutagenesis. *J Mol Biol.* 335(3):833-42.

[86] Morimoto A, Irie K, Murakami K, Masuda Y, Ohigashi H, Nagao M, Fukuda H, Shimizu T, Shirasawa T. (2004) Analysis of the secondary structure of beta-amyloid (Abeta42) fibrils by systematic proline replacement. *J Biol Chem.* 279(50):52781-8.

[87] Lynch T, Cherny RA, Bush AI. (2000) Oxidative processes in Alzheimer's disease: the role of abeta-metal interactions. *Exp Gerontol.* 35(4):445-51.

[88] Smith DG, Cappai R, Barnham KJ. (2007) The redox chemistry of the Alzheimer's disease amyloid beta peptide. *Biochim Biophys Acta.* 1768(8):1976-90.

[89] Rauk A. (2008) Why is the amyloid beta peptide of Alzheimer's disease neurotoxic? *Dalton Trans.* 14;(10):1273-82.

[90] Rauk A. (2009) The chemistry of Alzheimer's disease. *Chem Soc Rev.* 38(9):2698-715.

[91] Hewitt N, Rauk A. (2009) Mechanism of hydrogen peroxide production by copper-bound amyloid beta peptide: a theoretical study. *J Phys Chem B.* 113(4):1202-9.

[92] Raffa DF, Rickard GA, Rauk A. (2007) Ab initio modelling of the structure and redox behaviour of copper(I) bound to a His-His model peptide: relevance to the beta-amyloid peptide of Alzheimer's disease. *J Biol Inorg Chem.* 12(2):147-64.

[93] Findeis MA. (2000) Approaches to discovery and characterization of inhibitors of amyloid beta-peptide polymerization. *Biochim Biophys Acta.* 1502(1):76-84

[94] Findeis, MA, Lee JJ, Kelley M; Wakefield J, Chin J, Kubasek W, Zhang MH, Molineaux SM. (2001) Characterization of cholyl-leu-val-phe-phe-ala-OH as an inhibitor of amyloid beta-peptide polymerization. *Amyloid,* 8; 231-241.

[95] Findeis MA. (2002) Peptide inhibitors of beta amyloid aggregation. *Curr Top Med Chem.* 2(4): 417-23.

[96] Levine H (2002) The challenge of inhibiting Abeta polymerization. *Curr Med Chem.* 9(11): 1121-33.

[97] LeVine H 3rd. (2007) Small molecule inhibitors of Abeta assembly. *Amyloid.* 14(3):185-97.

[98] Doig AJ. (2007) Peptide inhibitors of beta-amyloid aggregation. *Curr Opin Drug Discov Devel.* 10(5):533-9.

[99] Tjernberg LO, Näslund J, Lindqvist F, Johansson J, Karlström AR, Thyberg J, Terenius L, Nordstedt C. (1996) Arrest of beta-amyloid fibril formation by a pentapeptide ligand. *J Biol Chem.* 271(15): 8545-8.

[100] Jarrett JT, Berger EP, Lansbury PT Jr. (1993) The C-terminus of the beta protein is critical in amyloidogenesis. *Ann N Y Acad Sci.* 695:144-8

[101] Soto C, Brañes MC, Alvarez J, Inestrosa NC. (1994) Structural determinants of the Alzheimer's amyloid beta-peptide. *J Neurochem.*63(4):1191-8.

[102] Tjernberg LO, Lilliehöök C, Callaway DJ, Näslund J, Hahne S, Thyberg J, Terenius L, Nordstedt C. (1997) Controlling amyloid beta-peptide fibril formation with protease-stable ligands. *J Biol Chem.* 272(19): 12601-5.

[103] Balbach JJ, Ishii Y, Antzutkin ON, Leapman RD, Rizzo NW, Dyda F, Reed J, Tycko R. (2000) Amyloid fibril formation by A beta 16-22, a seven-residue fragment of the Alzheimer's beta-amyloid peptide, and structural characterization by solid state NMR. *Biochemistry.* 39(45): 13748-59.

[104] Klimov DK, Thirumalai D. (2003) Dissecting the assembly of Abeta16-22 amyloid peptides into antiparallel beta sheets. *Structure.* 11(3):295-307.

[105] Favrin G, Irback A, Mohanty S. (2004) Oligomerization of amyloid Abeta16-22 peptides using hydrogen bonds and hydrophobicity forces. *Biophys J.* 87(6): 3657-64.

[106] Soto C, Kindy MS, Baumann M, Frangione B. (1996). Inhibition of Alzheimer's amyloidosis by peptides that prevent beta-sheet conformation.*Biochem Biophys Res Commun.* 226(3): 672-80.

[107] Soto C, Sigurdsson EM, Morelli L, Kumar RA, Castano EM, Frangione B. (1998) Beta-sheet breaker peptides inhibit fibrillogenesis in a rat brain model of amyloidosis: implications for Alzheimer's therapy. *Nat Med.* 4(7): 822-6.

[108] Poduslo JF, Curran GL, Kumar A, Frangione B, Soto C. (1999) Beta-sheet breaker peptide inhibitor of Alzheimer's amyloidogenesis with increased blood-brain barrier permeability and resistance to proteolytic degradation in plasma. *J Neurobiol* 39(3): 371-82.

[109] Adessi C, Frossard MJ, Boissard C, Fraga S, Bieler S, Ruckle T, Vilbois F, Robinson SM, Mutter M, Banks WA, Soto C. (2003) Pharmacological profiles of peptide drug candidates for the treatment of Alzheimer's disease. *J Biol Chem.* 278(16): 13905-11.

[110] US patent # 7,175,828 (2007) Modulators of β-amyloid peptide aggregation comprising D-amino acids, Findeis MA et al, Praecis Pharmaceuticals, Inc. Waltham, MA, US

[111] Kokkoni N, Stott K, Amijee H, Mason JM, Doig AJ. (2006) N-Methylated peptide inhibitors of beta-amyloid aggregation and toxicity. Optimization of the inhibitor structure. *Biochemistry.* 45(32):9906-18.

[112] Praecis Pharmaceuticals Incorporated (PRCS) Announces Strategic Restructuring And Refocusing Of Company Operations; Cuts Work Force By 60 Percent To Reduce Costs, Halts Plenaxis Cancer Drug Promotion; Suspend Ongoing Clinical Development Of Apan http://www.biospace.com/news_story.aspx?NewsEntityId=20143120 (Accessed 9-Sep-2009)

[113] Satori Pharmaceuticals Inc. (http://www.satoripharma.com/about.html) (accessed 9-Sep-2009)

[114] Gordon DJ, Tappe R, Meredith SC. (2002) Design and characterization of a membrane permeable N-methyl amino acid-containing peptide that inhibits Abeta1-40 fibrillogenesis. *J Pept Res.* 60(1): 37-55.

[115] Gordon DJ, Sciarretta KL, Meredith SC. (2001) Inhibition of beta-amyloid(40) fibrillogenesis and disassembly of beta-amyloid(40) fibrils by short beta-amyloid congeners containing N-methyl amino acids at alternate residues. *Biochemistry.* 40(28): 8237-45.

[116] Chalifour RJ, McLaughlin RW, Lavoie L, Morissette C, Tremblay N, Boule M, Sarazin P, Stea D, Lacombe D, Tremblay P, Gervais F. (2003) Stereoselective interactions of peptide inhibitors with the beta-amyloid peptide. *J Biol Chem.* 278(37): 34874-81.

[117] US patent # 7,060,670, (2006), Stereoselective antifibrillogenic peptides and peptidomimetics thereof, Chalifour R et al, Neurochem Limited, Montreal, Lausanne, CH

[118] Senexis Inc. News Release http://www.senexis.com/downloads/Senexis%2017%20Jan%2008%20Release.pdf (accessed 9-Sep-2009)

[119] Christensen H, Maltby N, Jorm AF, Creasey H, Broe GA. (1992) Cholinergic 'blockade' as a model of the cognitive deficits in Alzheimer's disease.*Brain.* 115 (Pt 6):1681-99.

[120] Patel S, Tariot PN. (1991) Pharmacologic models of Alzheimer's disease. *Psychiatr Clin North Am.* 14(2):287-308.

[121] De La Lande IS, Porter RB (1963) The actions of tacrine and amiphenazole on acetylcholine metabolism in the guinea pig ileum. *Aust J Exp Biol Med Sci.* 41:149-61.

[122] Mendelson G. (1975) Central anticholinergic syndrome reversed by tetrahydroaminacrine (tha). *Med J Aust.* 2(24):906-9.

[123] Rupniak NM, Field MJ, Samson NA, Steventon MJ, Iversen SD. (1990) Direct comparison of cognitive facilitation by physostigmine and tetrahydroaminoacridine in two primate models. *Neurobiol Aging.* 11(6):609-13.

[124] Murray TK, Cross AJ, Green AR. (1991) Reversal by tetrahydroaminoacridine of scopolamine-induced memory and performance deficits in rats. *Psychopharmacology (Berl).* 105(1):134-6.

[125] Levy R. (1989) Tacrine in Alzheimer's disease. *Lancet.* 2(8658):329.

[126] Summers WK, Tachiki KH, Kling A. (1989) Tacrine in the treatment of Alzheimer's disease. A clinical update and recent pharmacologic studies. *Eur Neurol.* 29 Suppl 3:28-32.

[127] Crismon ML. (1994) Tacrine: first drug approved for Alzheimer's disease. *Ann Pharmacother.* 28(6):744-51

[128] Qizilbash N, Birks J, Lopez Arrieta J, Lewington S, Szeto S. (2007) WITHDRAWN: Tacrine for Alzheimer's disease. *Cochrane Database Syst Rev.* (3):CD000202

[129] Sugimoto H, Iimura Y, Yamanishi Y, Yamatsu K. (1995) Synthesis and structure-activity relationships of acetylcholinesterase inhibitors: 1-benzyl-4-(2-phthalimidoethyl)piperidine and related derivatives. *J Med Chem.* 38(24):4821-9.

[130] Ohnishi A, Mihara M, Kamakura H, Tomono Y, Hasegawa J, Yamazaki K, Morishita N, Tanaka T. (1993) Comparison of the pharmacokinetics of E2020, a new compound for Alzheimer's disease, in healthy young and elderly subjects. *J Clin Pharmacol.* 33(11): 1086-91.

[131] Polinsky RJ. (1998) Clinical pharmacology of rivastigmine: a new-generation acetylcholinesterase inhibitor for the treatment of Alzheimer's disease. *Clin Ther.* 20(4):634-47.

[132] Rösler M, Retz W, Retz-Junginger P, Dennler HJ. (1998) Effects of two-year treatment with the cholinesterase inhibitor rivastigmine on behavioural symptoms in Alzheimer's disease. *Behav Neurol.* 11(4):211-216.

[133] McKeith IG, Grace JB, Walker Z, Byrne EJ, Wilkinson D, Stevens T, Perry EK Rivastigmine in the treatment of dementia with Lewy bodies: preliminary findings from an open trial. *Int J Geriatr Psychiatry.* 15(5):387-92.

[134] Poewe W, Gauthier S, Aarsland D, Leverenz JB, Barone P, Weintraub D, Tolosa E, Dubois B. (2008) Diagnosis and management of Parkinson's disease dementia. *Int J Clin Pract.* 2008 62(10):1581-7.

[135] Marco L, do Carmo Carreiras M. (2006) Galanthamine, a natural product for the treatment of Alzheimer's disease. *Recent Patents CNS Drug Discov.* 1(1):105-11.

[136] Franco M, Catucci G. (1962) Nivaline (galanthamine bromhydrate) in the prevention and treatment of postoperative paralytic ileus *Minerva Chir.* 17:1261-4.

[137] Gujral VV. (1965) Nivalin in the treatment of residual post-polio paralysis and pseudo-hypertrophic muscular dystrophy. *Indian Pediatr.* 2(3):89-93.

[138] Nordberg A, Svensson AL. (1998) Cholinesterase inhibitors in the treatment of Alzheimer's disease: a comparison of tolerability and pharmacology. *Drug Saf.* 19(6):465-80.

[139] Paoletti P, Neyton J. (2007) NMDA receptor subunits: function and pharmacology. *Curr Opin Pharmacol.* 7(1):39-47.

[140] Johnson JW, Kotermanski SE. (2006) Mechanism of action of memantine. *Curr Opin Pharmacol.* 6(1):61-7.

[141] Aisen PS, Gauthier S, Vellas B, Briand R, Saumier D, Laurin J, Garceau D. (2007) Alzhemed: a potential treatment for Alzheimer's disease. *Curr Alzheimer Res.* 4(4):473-8.

[142] Carlsson CM. (2008) Lessons learned from failed and discontinued clinical trials for the treatment of Alzheimer's disease: future directions. *J Alzheimers Dis.* 15(2):327-38.

[143] Townsend M, Cleary JP, Mehta T, Hofmeister J, Lesne S, O'Hare E, Walsh DM, Selkoe DJ. (2006) Orally available compound prevents deficits in memory caused by the Alzheimer amyloid-beta oligomers. *Ann Neurol.* 60(6):668-76.

[144] Nitz M, Fenili D, Darabie AA, Wu L, Cousins JE, McLaurin J. (2008) Modulation of amyloid-beta aggregation and toxicity by inosose stereoisomers. *FEBS J.*275(8):1663-74.

[145] Lundkvist J, Näslund J. (2007) Gamma-secretase: a complex target for Alzheimer's disease. *Curr Opin Pharmacol.* 7(1):112-8

[146] Imbimbo BP. (2008) Therapeutic potential of gamma-secretase inhibitors and modulators. *Curr Top Med Chem.* 8(1):54-61.

[147] Ghosh AK, Kumaragurubaran N, Hong L, Kulkarni SS, Xu X, Chang W, Weerasena V, Turner R, Koelsch G, Bilcer G, Tang J. (2007) Design, synthesis, and X-ray structure of potent memapsin 2 (beta-secretase) inhibitors with isophthalamide derivatives as the P2-P3-ligands. *J Med Chem.* 50(10):2399-407.

[148] Hunt CE, Turner AJ. (2009) Cell biology, regulation and inhibition of beta-secretase (BACE-1). *FEBS J.* 276(7):1845-59.

[149] Siemers ER, Quinn JF, Kaye J, Farlow MR, Porsteinsson A, Tariot P, Zoulnouni P, Galvin JE, Holtzman DM, Knopman DS, Satterwhite J, Gonzales C, Dean RA, May PC. (2006) Effects of a gamma-secretase inhibitor in a randomized study of patients with Alzheimer disease. *Neurology.* 66(4):602-4.

[150] Eriksen JL, Sagi SA, Smith TE, Weggen S, Das P, McLendon DC, Ozols VV, Jessing KW, Zavitz KH, Koo EH, Golde TE. (2003) NSAIDs and enantiomers of flurbiprofen target gamma-secretase and lower Abeta 42 in vivo. *J Clin Invest.* 112(3):440-9.

[151] Imbimbo BP. (2009) Why Did Tarenflurbil Fail in Alzheimer's Disease? *J Alzheimers Dis.* 17(4): 757-760

[152] Schenk D. (2002) Amyloid-beta immunotherapy for Alzheimer's disease: the end of the beginning. *Nat Rev Neurosci.* 3(10):824-8.

[153] Vellas B, Black R, Thal LJ, Fox NC, Daniels M, McLennan G, Tompkins C, Leibman C, Pomfret M, Grundman M; AN1792 (QS-21)-251 Study Team. (2009) Long-term follow-up of patients immunized with AN1792: reduced functional decline in antibody responders. *Curr Alzheimer Res.* 6(2):144-51.

[154] Pride M, Seubert P, Grundman M, Hagen M, Eldridge J, Black RS. (2008) Progress in the active immunotherapeutic approach to Alzheimer's disease: clinical investigations into AN1792-associated meningoencephalitis. *Neurodegener Dis.* 5(3-4):194-6.

[155] Pride M, Seubert P, Grundman M, Hagen M, Eldridge J, Black RS. (2008) Progress in the active immunotherapeutic approach to Alzheimer's disease: clinical investigations into AN1792-associated meningoencephalitis. *Neurodegener Dis.* 5(3-4):194-6.

[156] Melnikova I. (2007) Therapies for Alzheimer's disease. *Nat Rev Drug Discov.* 6(5):341-2.

[157] Lermontova NN, Lukoyanov NV, Serkova TP, Lukoyanova EA, Bachurin SO. (2000) Dimebon improves learning in animals with experimental Alzheimer's disease. *Bull Exp Biol Med.* 129(6):544-6.

[158] Doody RS, Gavrilova SI, Sano M, Thomas RG, Aisen PS, Bachurin SO, Seely L, Hung D (2008). Effect of dimebon on cognition, activities of daily living, behaviour, and global function in patients with mild-to-moderate Alzheimer's disease: a randomised, double-blind, placebo-controlled study. *Lancet.* 372(9634):207-15.

[159] Roy S, Rauk A. (2005) Alzheimer's disease and the 'ABSENT' hypothesis: mechanism for amyloid beta endothelial and neuronal toxicity. *Med Hypotheses.* 65(1):123-37.

[160] Geerlings MI, den Heijer T, Koudstaal PJ, Hofman A, Breteler MM. (2008) History of depression, depressive symptoms, and medial temporal lobe atrophy and the risk of Alzheimer disease. *Neurology.* 70(15):1258-64.

[161] Robert PH, Berr C, Volteau M, Bertogliati-Fileau C, Benoit M, Guerin O, Sarazin M, Legrain S, Dubois B; PréAL Study Group. (2008) Importance of lack of interest in patients with mild cognitive impairment. *Am J Geriatr Psychiatry*. 16(9):770-6.

[162] Irie F, Fitzpatrick AL, Lopez OL, Kuller LH, Peila R, Newman AB, Launer LJ. (2008)

Enhanced risk for Alzheimer disease in persons with type 2 diabetes and APOE epsilon4: the Cardiovascular Health Study Cognition Study. *Arch Neurol.* 65(1):89-93.

[163] Kloppenborg RP, van den Berg E, Kappelle LJ, Biessels GJ. (2008) Diabetes and other vascular risk factors for dementia: which factor matters most? A systematic review. *Eur J Pharmacol.* 585(1):97-108.

[164] Geddes JW, Tekirian TL, Soultanian NS, Ashford JW, Davis DG, Markesbery WR. (1997) Comparison of neuropathologic criteria for the diagnosis of Alzheimer's disease. *Neurobiol Aging.* 18(4 Suppl):S99-105.

[165] Giannakopoulos P, Gold G, Kövari E, von Gunten A, Imhof A, Bouras C, Hof PR. (2007) Assessing the cognitive impact of Alzheimer disease pathology and vascular burden in the aging brain: the Geneva experience. *Acta Neuropathol.* 113(1):1-12.

[166] Bennett DA, Wilson RS, Schneider JA, Evans DA, Mendes de Leon CF, Arnold SE, Barnes LL, Bienias JL (2003) Education modifies the relation of AD pathology to level of cognitive function in older persons.*Neurology.* 60(12):1909-15.

[167] Kalaria RN. (1996) Cerebral vessels in ageing and Alzheimer's disease. *Pharmacol Ther.* 72(3):193–214.

[168] Kalaria RN. (2002) Similarities between Alzheimer's disease and vascular dementia. *J Neurol Sci.* 203–204:29–34.

[169] de la Torre JC. (2000) Critically attained threshold of cerebral hypoperfusion: the CATCH hypothesis of Alzheimer's pathogenesis. *Neurobiol Aging.* 21(2):331–42.

[170] de la Torre JC. (2000) Impaired cerebromicrovascular perfusion. Summary of evidence in support of its causality in Alzheimer's disease. *Ann NYAcad Sci.* 903:424–36.

[171] de la Torre JC. (2002) Alzheimer disease as a vascular disorder: nosological evidence. *Stroke.* 33(4):1152–62.

[172] Nagga K, Radberg C, Marcusson J. (2004) CT brain findings in clinical dementia investigation--underestimation of mixed dementia. *Dement Geriatr Cogn Disord.*18(1):59–66.

[173] Attems J, Jellinger KA. (2004) Only cerebral capillary amyloid angiopathy correlates with Alzheimer pathology--a pilot study. *Acta Neuropathol (Berl).* 107(2):83–90.

[174] Jellinger KA. (2002) Incidence of cerebrovascular lesions in Alzheimer's disease: a postmortem study. *J Neural Transm.*109(5-6):813–36.

[175] Attems J, Lintner F, Jellinger KA. (2004) Amyloid beta peptide 1-42 highly correlates with capillary cerebral amyloid angiopathy and Alzheimer disease pathology. *Acta Neuropathol (Berl).* 107(4):283–91.

[176] Haglund M, Sjobeck M, Englund E. (2004) Severe cerebral amyloid angiopathy characterizes an underestimated variant of vascular dementia. *Dement Geriatr Cogn Disord.*18(2):132–7.

[177] Coimbra A, Williams DS, Hostetler ED. (2006) The role of MRI and PET/SPECT in Alzheimer's disease. *Curr Top Med Chem.* 6(6):629-47.

[178] Whitwell JL, Shiung MM, Przybelski SA, Weigand SD, Knopman DS, Boeve BF, Petersen RC, Jack CR Jr. (2008) MRI patterns of atrophy associated with progression to AD in amnestic mild cognitive impairment. *Neurology.* 70(7):512-20.

[179] Kuller LH, Lopez OL, Newman A, Beauchamp NJ, Burke G, Dulberg C, Fitzpatrick A, Fried L, Haan MN.(2003) Risk factors for dementia in the cardiovascular health cognition study. *Neuroepidemiology.* 22(1):13-22.

[180] Amouyel P, Richard F, Berr C, David-Fromentin I, Helbecque N. (2000) The renin angiotensin system and Alzheimer's disease. *Ann NY Acad Sci.* 903:437–41.

[181] Roman GC, Royall DR. (2004) A diagnostic dilemma: is "Alzheimer's dementia" Alzheimer's disease, vascular dementia, or both? *Lancet Neurol.* 3(3):141.

[182] Honig LS, Tang MX, Albert S, Costa R, Luchsinger J, Manly J et al. (2003) Stroke and the risk of Alzheimer disease. *Arch Neurol.* 60(12):1707–12.

[183] Forette F, Seux ML, Staessen JA, Thijs L, Babarskiene MR, Babeanu S et al. (2002) The prevention of dementia with antihypertensive treatment: new evidence from the Systolic Hypertension in Europe (Syst-Eur) study. *Arch Intern Med*.162(18):2046–52.

[184] Hanon O, Seux ML, Lenoir H, Rigaud AS, Forette F.(2004) Prevention of dementia and cerebroprotection with antihypertensive drugs. *Curr Hypertens Rep.* 6(3):201–7.

[185] Zamrini E, McGwin G, Roseman JM. (2004) Association between statin use and Alzheimer's disease. *Neuroepidemiology.* 23(1-2):94–8.

[186] Skoog I, Gustafson D. (2006) Update on hypertension and Alzheimer's disease. *Neurol Res.* 28(6):605-11.

[187] Goldsmith HS. (2002) Treatment of Alzheimer's disease by transposition of the omentum. *Ann NY Acad Sci.* 977:454–67.

[188] Goldsmith HS, Wu W, Zhong J, Edgar M. (2003) Role of the omentum in the treatment of Alzheimer's disease. *Neurol Res.* 25(6):625–34.

[189] Borchelt DR, Thinakaran G, Eckman CB, Lee MK, Davenport F, Ratovitsky T et al. (1996) Familial Alzheimer's disease-linked presenilin 1 variants elevate Abeta1-42/1-40 ratio in vitro and in vivo. *Neuron.*17(5):1005–13.

[190] Odetti P, Angelini G, Dapino D, Zaccheo D, Garibaldi S, Dagna-Bricarelli F et al. (1998) Early glycoxidation damage in brains from Down's syndrome. *Biochem Biophys Res Commun.* 243(3):849–51.

[191] Cecchi C, Fiorillo C, Sorbi S, Latorraca S, Nacmias B, Bagnoli S et al. (2002) Oxidative stress and reduced antioxidant defenses in peripheral cells from familial Alzheimer's patients. *Free Radic Biol Med.* 33(10):1372–9.

[192] Lovell MA, Markesbery WR. (2007) Oxidative damage in mild cognitive impairment and early Alzheimer's disease. *J Neurosci Res.* 85(14):3036-40.

[193] Butterfield DA. (2002) Amyloid beta-peptide (1-42)-induced oxidative stress and neurotoxicity: implications for neurodegeneration in Alzheimer's disease brain. *Free Radic Res.* 36(12):1307–13.

[194] Mufson EJ, Chen EY, Cochran EJ, Beckett LA, Bennett DA, Kordower JH. (1999) Entorhinal cortex beta-amyloid load in individuals with mild cognitive impairment. *Exp Neurol.* 158(2):469–90.

[195] Fonte J, Miklossy J, Atwood C, Martins R. (2001) The severity of cortical Alzheimer's type changes is positively correlated with increased amyloid-beta Levels: Resolubilization of amyloid-beta with transition metal ion chelators.*J Alzheimers Dis.*3(2):209–19.

[196] Zekry D, Duyckaerts C, Moulias R, Belmin J, Geoffre C, Herrmann F et al. (2002) Degenerative and vascular lesions of the brain have synergistic effects in dementia of the elderly. *Acta Neuropathol (Berl).*103(5):481–7.

[197] Hogervorst E, Bandelow S, Combrinck M, Irani S, Smith AD. (2003) The validity and reliability of 6 sets of clinical criteria to classify Alzheimer's disease and vascular dementia in cases confirmed post-mortem: added value of a decision tree approach. *Dement Geriatr Cogn Disord.*16(3):170–80.

[198] Borroni B, Akkawi N, Martini G, Colciaghi F, Prometti P, Rozzini L et al. (2002) Microvascular damage and platelet abnormalities in early Alzheimer's disease. *J Neurol Sci.* 203–204:189–93.

[199] Bugiani O. (2004) A beta-related cerebral amyloid angiopathy. *Neurol Sci.* 25(Suppl 1):S1–2.

[200] Nicoll JA, Yamada M, Frackowiak J, Mazur-Kolecka B, Weller RO. (2004) Cerebral amyloid angiopathy plays a direct role in the pathogenesis of Alzheimer's disease. Pro-CAA position statement. *Neurobiol Aging.* 25(5): 589–97.

[201] Thomas T, Thomas G, McLendon C, Sutton T, Mullan M. (1996) beta-Amyloid-mediated vasoactivity and vascular endothelial damage. *Nature.* 380(6570):168–71.

[202] Sutton ET, Hellermann GR, Thomas T. (1997) beta-amyloid-induced endothelial necrosis and inhibition of nitric oxide production. *Exp Cell Res.* 230(2):368–76.

[203] Jahroudi N, Kitney J, Greenberger JS, Bowser R. (1998) Endothelial cell dysfunction in response to intracellular overexpression of amyloid precursor protein. *J Neurosci Res*. 4(6):828–39.

[204] Said SI, Raza S, Berisha HI. (1998) Enhancement of systemic and pulmonary vasoconstriction by beta-amyloid peptides and its suppression by vasoactive intestinal peptide. *Ann NY Acad Sci.* 865:582–5.

[205] Iadecola C, Zhang F, Niwa K, Eckman C, Turner SK, Fischer E et al. (1999) SOD1 rescues cerebral endothelial dysfunction in mice overexpressing amyloid precursor protein.*Nat Neurosci.* 2(2):157–61.

[206] Niwa K, Younkin L, Ebeling C, Turner SK, Westaway D, Younkin S et al. (2000) Abeta 1-40-related reduction in functional hyperemia in mouse neocortex during somatosensory activation. *Proc Natl Acad Sci USA.* 97(17): 9735–40.

[207] Niwa K, Carlson GA, Iadecola C (2000) Exogenous A beta1-40 reproduces cerebrovascular alterations resulting from amyloid precursor protein overexpression in mice. *J Cereb Blood Flow Metab.* 20(12): 1659–68.

[208] Townsend KP, Obregon D, Quadros A, Patel N, Volmar C, Paris D et al. (2002) Proinflammatory and vasoactive effects of Abeta in the cerebrovasculature. *Ann NY Acad Sci.* 977:65–76.

[209] Blanc EM, Toborek M, Mark RJ, Hennig B, Mattson MP. (1997) Amyloid beta-peptide induces cell monolayer albumin permeability, impairs glucose transport, and induces apoptosis in vascular endothelial cells. *J Neurochem*. 68(5):1870–81.

[210] Jancso G, Domoki F, Santha P, Varga J, Fischer J, Orosz K et al. (1998) Beta-amyloid (1-42) peptide impairs blood-brain barrier function after intracarotid infusion in rats. *Neurosci Lett.* 253(2):139–41.

[211] Niwa K, Kazama K, Younkin SG, Carlson GA, Iadecola C. (2002) Alterations in cerebral blood flow and glucose utilization in mice overexpressing the amyloid precursor protein. *Neurobiol Dis.* 9(1):61–8.

[212] Niwa K, Kazama K, Younkin L, Younkin SG, Carlson GA, Iadecola C. (2002) Cerebrovascular autoregulation is profoundly impaired in mice overexpressing amyloid precursor protein. *Am J Physiol Heart Circ Physiol.* 283(1):H315–23.

[213] Milton NG. (1999) Amyloid-beta binds catalase with high affinity and inhibits hydrogen peroxide breakdown. *Biochem J.* 344(Pt 2):293–6.

[214] Curtain CC, Ali F, Volitakis I, Cherny RA, Norton RS, Beyreuther K et al. (2001) Alzheimer's disease amyloid-beta binds copper and zinc to generate an allosterically ordered membrane-penetrating structure containing superoxide dismutase-like subunits. *J Biol Chem.* 276(23):20466–73.

[215] Zhang Z, Rydel RE, Drzewiecki GJ, Fuson K, Wright S, Wogulis M et al. (1996) Amyloid beta-mediated oxidative and metabolic stress in rat cortical neurons: no direct evidence for a role for H2O2 generation. *J Neurochem.* 67(4):1595–606.

[216] Atkinson J. (2001) Cerebrovascular structure and dementia: new drug targets. *Trends Pharmacol Sci.* 22(12):630–5

[217] Sorond FA, Schnyer DM, Serrador JM, Milberg WP, Lipsitz LA. (2008) Cerebral blood flow regulation during cognitive tasks: effects of healthy aging. *Cortex.* 44(2):179-84.

[218] Wollner L, McCarthy ST, Soper ND, Macy DJ. (1979) Failure of cerebral autoregulation as a cause of brain dysfunction in the elderly.*Br Med J.* 1(6171):1117–8.

[219] Kalaria RN. (2000) The role of cerebral ischemia in Alzheimer's disease. *Neurobiology of Aging.* 21:321–30.

[220] Tkac I, Troscak M, Javorsky M, Petrik R, Tomcova M. (2001) Increased intracranial arterial resistance in patients with type 2 diabetes mellitus. *Wien Klin Wochenschr.* 113(22):870–3.

[221] Iadecola C, Gorelick PB. (2003) Converging pathogenic mechanisms in vascular and neurodegenerative dementia. *Stroke.* 34(2):335–7.

[222] Iadecola C. (2003) Cerebrovascular effects of amyloid-beta peptides: mechanisms and implications for Alzheimer's dementia. *Cell Mol Neurobiol.* 23(4-5):681–9.

[223] Iadecola C. (2003) Atherosclerosis and neurodegeneration: unexpected conspirators in Alzheimer's dementia. *Arterioscler Thromb Vasc Biol.* 23(11):1951–3.

[224] Iadecola C. (2004) Neurovascular regulation in the normal brain and in Alzheimer's disease. *Nat Rev Neurosci 2004*;5(5): 347–60.

[225] Crawford F, Suo Z, Fang C, Mullan M. (1998) Characteristics of the in vitro vasoactivity of beta-amyloid peptides. *Exp Neurol.* 150(1):159–68.

[226] Suo Z, Su G, Placzek A, Kundtz A, Humphrey J, Crawford F et al. (2000) A beta vasoactivity in vivo. *Ann NY Acad Sci.* 903:156–63.

[227] Niwa K, Porter VA, Kazama K, Cornfield D, Carlson GA, Iadecola C. (2001) A beta-peptides enhance vasoconstriction in cerebral circulation. *Am J Physiol Heart Circ Physiol.* 281(6):H2417–24.

[228] Price JM, Chi X, Hellermann G, Sutton ET. (2001) Physiological levels of beta-amyloid induce cerebral vessel dysfunction and reduce endothelial nitric oxide production. *Neurol Res.* 23(5):506–12.

[229] Paris D, Humphrey J, Quadros A, Patel N, Crescentini R, Crawford F et al. (2003) Vasoactive effects of A beta in isolated human cerebrovessels and in a transgenic mouse model of Alzheimer's disease: role of inflammation. *Neurol Res.* 25(6):642–51.

[230] Price JM, Hellermann A, Hellermann G, Sutton ET. (2004) Aging enhances vascular dysfunction induced by the Alzheimer's peptide beta-amyloid. *Neurol Res.* 26(3):305–11.

[231] Plaschke K, Ranneberg T, Bauer J, Weigand M, Hoyer S, Bardenheuer HJ. (1997)

The effect of stepwise cerebral hypoperfusion on energy metabolism and amyloid precursor protein (APP) in cerebral cortex and hippocampus in the adult rat. *Ann NY Acad Sci.* 826:502–6.

[232] Bennett SA, Pappas BA, Stevens WD, Davidson CM, Fortin J, Chen J. (2000) Cleavage of amyloid precursor protein elicited by chronic cerebral hypoperfusion. *Neurobiol Aging.* 21(2):207–14.

[233] Shi J, Yang SH, Stubley L, Day AL, Simpkins JW. (2000) Hypoperfusion induces overexpression of beta-amyloid precursor protein mRNA in a focal ischemic rodent model. *Brain Res.* 53(1):1-4.

[234] Huang X, Cuajungco MP, Atwood CS, Hartshorn MA, Tyndall JD, Hanson GR, Stokes KC, Leopold M, Multhaup G, Goldstein LE, Scarpa RC, Saunders AJ, Lim J, Moir RD, Glabe C, Bowden EF, Masters CL, Fairlie DP, Tanzi RE, Bush AI. (1999) Cu(II) potentiation of alzheimer abeta neurotoxicity. Correlation with cell-free hydrogen peroxide production and metal reduction. *J Biol Chem.* 274(52):37111-6.

[235] Curtain CC, Ali F, Volitakis I, Cherny RA, Norton RS, Beyreuther K, Barrow CJ, Masters CL, Bush AI, Barnham KJ. (2001) Alzheimer's disease amyloid-beta binds copper and zinc to generate an allosterically ordered membrane-penetrating structure containing superoxide dismutase-like subunits. *J Biol Chem .*276(23):20466-73.

[236] Opazo C, Huang X, Cherny RA, Moir RD, Roher AE, White AR, Cappai R, Masters CL, Tanzi RE, Inestrosa NC, Bush AI. (2002) Metalloenzyme-like activity of Alzheimer's disease beta-amyloid. Cu-dependent catalytic conversion of dopamine, cholesterol, and biological reducing agents to neurotoxic H(2)O(2). *J Biol Chem.*;277(43):40302-8.

[237] Lue LF, Kuo YM, Roher AE, Brachova L, Shen Y, Sue L, Beach T, Kurth JH, Rydel RE, Rogers J. (1999) Soluble amyloid beta peptide concentration as a predictor of synaptic change in Alzheimer's disease. *Am J Pathol.* 155(3): 853-62.

[238] Rauk A, Armstrong DA, Fairlie DP. (2000) Is Oxidative Damage By Beta Amyloid and Prion Peptides Mediated by HydrogenAtom Transfer from Glycine Alpha-Carbon to Methionine Sulfur within Beta-Sheets. *J Am Chem Soc. 122: 9761–7.*

[239] Rauk A, Armstrong DA. (2000) Influence of the b-sheet structure on the susceptibility of proteins to backbone oxidative damage: preference for alpha-C centered radical formation at glycine in anti-parallel b-sheets. *J Am Chem Soc. 122:4185–92.*

[240] Brunelle P, Rauk A.(2002) The radical model of Alzheimer’s disease: specific recognition of Gly29 and Gly33 by Met35 in a b-sheet model of Abeta:an ONIOM study. *J Alzheimer’s Dis. 2002;4(4):283–9.*

[241] Harrigan MR, Kunkel DD, Nguyen LB, Malouf AT. (1995) Beta amyloid is neurotoxic in hippocampal slice cultures. *Neurobiol Aging.* 16(5):779–89.

[242] Brera B, Serrano A, de Ceballos ML. (2000) b-amyloid peptides are cytotoxic to astrocytes in culture: a role for oxidative stress. *Neurobiol Dis.* 7(4):395–405.

[243] Rensink AA, Verbeek MM, Otte-Holler I, ten Donkelaar HT,de Waal RM, Kremer B. (2002) Inhibition of amyloid-b-induced cell death in human brain pericytes in vitro. *Brain Res.* 952(1):111–21.

[244] Barnham KJ, Ciccotosto GD, Tickler AK, Ali FE, Smith DG, Williamson NA et al. (2003) Neurotoxic, redox-competent Alzheimer's b-amyloid is released from lipid membrane by methionine oxidation. *J Biol Chem.* 278(44): 42959–42965.

[245] Milton NG. (1999) Amyloid-b binds catalase with high affinity and inhibits hydrogen peroxide breakdown. *Biochem J*. 1999;344(Pt 2):293–6.

[246] Zhang Z, Rydel RE, Drzewiecki GJ, Fuson K, Wright S, Wogulis M et al. (1996) Amyloid b-mediated oxidative and metabolic stress in rat cortical neurons: no direct evidence for a role for H2O2 generation. *J Neurochem*. 1996;67(4):1595–606.

[247] Brzyska M, Bacia A, Elbaum D. (2001) Oxidative and hydrolytic properties of b-amyloid. *Eur J Biochem.* 268(12): 3443–54.

[248] Dikalov SI, Vitek MP, Mason RP.(2004) Cupric-amyloid bpeptide complex stimulates oxidation of ascorbate and generation of hydroxyl radical. Free Radic Biol Med. 36(3): 340–7.

[249] Curtain CC, Ali F, Volitakis I, Cherny RA, Norton RS, Beyreuther K et al. (2001) Alzheimer's disease amyloid-b binds copper and zinc to generate an allosterically ordered membrane-penetrating structure containing superoxide dismutase-like subunits. *J Biol Chem.* 276(23):20466–73.

[250] Opazo C, Huang X, Cherny RA, Moir RD, Roher AE, White AR et al. (2002) Metalloenzyme-like activity of Alzheimer's disease b-amyloid. Cu-dependent catalytic conversion of dopamine, cholesterol, and biological reducing agents to neurotoxic H(2)O(2). *J Biol Chem.* 277(43): 40302–8.

[251] Vapaatalo H, Mervaala E. (2001) Clinically important factors influencing endothelial function. *Med Sci Monitor.* 7(5):1075–85.

[252] Csiszar A, Ungvari Z, Edwards JG, Kaminski P, Wolin MS, Koller A et al. (2002) Aging-induced phenotypic changes and oxidative stress impair coronary arteriolar function. *Circ Res.* 90(11):1159–66.

[253] Schnackenberg CG, Wilcox CS. (2001) The SOD mimetic tempol restores vasodilation in afferent arterioles of experimental diabetes. *Kidney Int.* 59(5):1859–64.

[254] Nassar T, Kadery B, Lotan C, Da'as N, Kleinman Y, Haj-Yehia A. (2002) Effects of the superoxide dismutase-mimetic compound tempol on endothelial dysfunction in streptozotocin-induced diabetic rats. *Eur J Pharmacol* . 436(1-2):111–8.

[255] Tatchum-Talom R, Martin DS. (2004) Tempol improves vascular function in the mesenteric vascular bed of senescent rats. *Can J Physiol Pharmacol*. 82(3):200–7.

[256] Carubelli R, Schneider Jr JE, Pye QN, Floyd RA. (1995) Cytotoxic effects of autoxidative glycation. *Free Radic Biol Med.* 18(2):265–9.

[257] Ortwerth BJ, James H, Simpson G, Linetsky M. (1998) The generation of superoxide anions in glycation reactions with sugars, osones, and 3- deoxyosones. *Biochem Biophys Res Commun.* 245(1):161–5.

[258] Mossine VV, Linetsky M, Glinsky GV, Ortwerth BJ, Feather MS. (1999) Superoxide free radical generation by Amadori compounds: the role of acyclic forms and metal ions. *Chem Res Toxicol.* 12(3):230–6.

[259] Rodriguez-Manas L, Angulo J, Vallejo S, Peiro C, Sanchez-Ferrer A, Cercas E et al. (2003) Early and intermediate Amadori glycosylation adducts, oxidative stress, and endothelial dysfunction in the streptozotocin-induced diabetic rats vasculature. *Diabetologia.* 46(4):556–66.

[260] Vlassara H, Palace MR. (2003) Glycoxidation:the menace of diabetes and aging. *Mt Sinai J Med.* 70(4):232–41

[261] Rodriguez-Manas L, Arribas S, Giron C, Villamor J, Sanchez-Ferrer CF, Marin J. (1993) Interference of glycosylated human hemoglobin with endothelium-dependent responses. *Circulation.* 88(5 Pt 1):2111–6.

[262] Angulo J, Rodriguez-Manas L, Peiro C, Vallejo S, Sanchez- Ferrer A, Sanchez-Ferrer CF. (1999) Impairment of endothelial relaxations by glycosylated human oxyhemoglobin depends on the oxidative state of the heme group. *Gen Pharmacol*. 32(4):475–81.

[263] Stanger O, Herrmann W, Pietrzik K, Fowler B, Geisel J, Dierkes J et al. (2004) Clinical use and rational management of homocysteine, folic acid, and B vitamins in cardiovascular and thrombotic diseases. *Z Kardiol*. 93(6):439–53.

[264] Lang D, Kredan MB, Moat SJ, Hussain SA, Powell CA, Bellamy MF et al.(2000) Homocysteine-induced inhibition of endothelium-dependent relaxation in rabbit aorta:role for superoxide anions. *Arterioscler Thromb Vasc Biol.* 20(2):422–7.

[265] Shukla N, Thompson CS, Angelini GD, Mikhailidis DP, Jeremy JY. (2002) Homocysteine enhances impairment of endothelium- dependent relaxation and guanosine cyclic monophosphate formation in aortae from diabetic rabbits.*Diabetologia.* ;45(9):1325–31.

[266] Ungvari Z, Csiszar A, Edwards JG, Kaminski PM, Wolin MS, Kaley G et al. (2003) Increased superoxide production in coronary arteries in hyperhomocysteinemia: role of tumor necrosis factor-alpha, NAD (P)H oxidase, and inducible nitric oxide synthase. *Arterioscler Thromb Vasc Biol.* 23(3):418–24.

[267] Hucks D, Thuraisingham RC, Raftery MJ, Yaqoob MM. (2004) Homocysteine induced impairment of nitric oxide-dependent vasorelaxation is reversible by the superoxide dismutase mimetic TEMPOL. *Nephrol Dial Transplant.* 19(8):1999–2005.

[268] Emsley AM, Jeremy JY, Gomes GN, Angelini GD, Plane F.(1999) Investigation of the inhibitory effects of homocysteine and copper on nitric oxide-mediated relaxation of rat isolated aorta. *Br J Pharmacol.* 126(4): 1034–40.

[269] Khan MA, Thompson CS, Emsley AM, Mumtaz FH, Mikhailidis DP, Angelini GD et al. (1999) The interaction of homocysteine and copper markedly inhibits the relaxation of rabbit corpus cavernosum: new risk factors for angiopathic erectile dysfunction. *BJU Int*. 84(6): 720–4.

[270] Rafii MS, Aisen PS. (2009) Recent developments in Alzheimer's disease therapeutics. *BMC Medicine.* 7:7

[271] Kroemer RT. (2007) Structure-based drug design: docking and scoring.*Curr Protein Pept Sci.* 8(4):312-28

[272] Ekins S, Mestres J, Testa B. (2007) In silico pharmacology for drug discovery: methods for virtual ligand screening and profiling. *Br J Pharmacol.* 152(1):9-20

[273] Gray JJ. (2006) High-resolution protein-protein docking. *Curr Opin Struct Biol.* 6(2):183-93

[274] Rubinstein M, Niv MY. (2009) Peptidic modulators of protein-protein interactions: Progress and challenges in computational design. *Biopolymers.* 91(7):505-13

[275] Lyskov S, Gray JJ. (2008) The RosettaDock server for local protein-protein docking. *Nucleic Acids Res.* 36 (Web Server issue):W233-8.

[276] Stephen R. Comeau1, David W. Gatchell2, Sandor Vajda1, Carlos J. Camacho1 (2004) ClusPro: an automated docking and discrimination method for the prediction of protein complexes. *Bioinformatics.* 20(1):45–50

[277] Chini MG, Scrima M, D'Ursi AM, Bifulco G. (2009) Fibril aggregation inhibitory activity of the beta-sheet breaker peptides: a molecular docking approach. *J Pept Sci.* 15(3):229-34.

[278] Mothana B, Roy S, Rauk A. (2009) Molecular dynamics study of the interaction of Aβ(13-23) with β-sheet inhibitors. *ARKIVOC* (v) 116-134

[279] Müller BA. (2009) Imatinib and its successors--how modern chemistry has changed drug development. *Curr Pharm Des.* 15(2):120-33.

[280] Gubernator K, Böhm HJ (1998). Structure-Based Ligand Design, Methods and Principles in Medicinal Chemistry. Weinheim: Wiley-VCH.

[281] Andrew R. Leach (2001) *Molecular Modelling: Principles and Applications* (2nd Edition) Publisher: Prentice Hall

[282] Sun H. (2008)Pharmacophore-based virtual screening. *Curr Med Chem.* 15(10):1018-24.

[283] McInnes C.(2007) Virtual screening strategies in drug discovery. *Curr Opin Chem Biol.* 11(5):494-502.

[284] Tuccinardi T. (2009) Docking-based virtual screening: recent developments. *Comb Chem High Throughput Screen.* 12(3):303-14.

[285] GOLD 3.0. (2009) Cambridge Crystallographic Data Centre, Cambridge, U.K.

[286] Glide 5.0. (2009) Schrodinger Inc. Portland, OR.

[287] FRED 2.2. (2009) OpenEye Scientific Software, Santa Fe, NM.

[288] Feher M. (2006) Consensus scoring for protein-ligand interactions. *Drug Discoverv Today.* 11(9-10): 421-8.

[289] Eldridge, M. D.; Murray, C. W.; Auton, T. R.; Paolini, G. V.; Mee, R. P. (1997) Empirical scoring functions: I. The development of a fast empirical scoring function to estimate the binding affinity of ligands in receptor complexes. *J. Comput.-Aided Mol. Des.* 11: 425-45.

.

[290] Gohlke, H.; Hendlich, M.; Klebe, G. (2000) Knowledge-based scoring function to predict protein-ligand interactions. *J. Mol. Biol.* 295:337-356.

[291] Muegge, I.; Martin, Y. C. (1999) A general and fast scoring function for protein-ligand interactions; a simplified potential approach. *J. Med.Chem.* 42:791-804.

[292] Rognan, D.; Lauemoller, S. L.; Holm, A.; Buus, S.; Tschinke, V. (1999) Predicting binding affinities of protein ligands from three-dimensional models: application to peptide binding to class I major histocompatibility proteins. *J. Med. Chem.* 42: 4650-4658.

[293] Böhm, H. J. (1994) The development of a single empirical scoring function to estimate the binding constant for a protein-ligand complex of known three-dimensional structure. *J. Comput.-Aided Mol. Des.* 8, 243-256

[294] GoldMine 1.1. (2009) Cambridge Crystallographic Data Centre: Cambridge, U.K.

[295] Cavasotto CN, Orry AJ. (2007) Ligand docking and structure-based virtual screening in drug discovery. *Curr Top Med Chem.* 2007; 7(10):1006-14.

[296] Mohan V, Gibbs AC, Cummings MD, Jaeger EP, DesJarlais RL. Docking: successes and challenges. *Curr Pharm Des.* 2005 ;11(3):323-33.

[297] Feher M, Deretey E, Roy S. (2003) BHB: a simple knowledge-based scoring function to improve the efficiency of database screening. *J Chem Inf Comput Sci.* 43(4):1316-27.

[298] Finder VH, Glockshuber R. (2007) Amyloid-beta aggregation. *Neurodegener Dis.* 4(1):13-27.

[299] Roychaudhuri R, Yang M, Hoshi MM, Teplow DB (2009) Amyloid β-Protein Assembly and Alzheimer Disease. *J. Biol. Chem.* 284 (8), 4749-4753

[300] Nichols MR, Moss MA, Reed DK, Hoh JH, Rosenberry TL. (2005) Amyloid-beta aggregates formed at polar-nonpolar interfaces differ from amyloid-beta protofibrils produced in aqueous buffers. *Microsc Res Tech.* 67(3-4):164-74.

[301]Raffa DF, Rauk A. (2007) Molecular dynamics study of the beta amyloid peptide of Alzheimer's disease and its divalent copper complexes. *J Phys Chem B.* 12;111(14):3789-99.

[302] Cerf E, Sarroukh R, Tamamizu-Kato S, Breydo L, Derclaye S, Dufrêne Y, Narayanaswami V, Goormaghtigh E, Ruysschaert JM, Raussens V. (2009) Anti-parallel beta-sheet - a signature structure of the oligomeric amyloid-beta peptide. *Biochem J.* 421(3):415-23.

[303] S.R. Comeau, C.J. Camacho.(2005) Predicting oligomeric assemblies: N-mers as a primer. *J. Struct. Biol.* 150(3):233-44

[304] Ferrão-Gonzales AD, Robbs BK, Moreau VH, Ferreira A, Juliano L, Valente AP, Almeida FC, Silva JL, Foguel D. (2005) Controlling beta-amyloid oligomerization by the use of naphthalene sulfonates: trapping low molecular weight oligomeric species. *J Biol Chem.* 280(41):34747-54.

[305] Sciarretta KL, Gordon DJ, Petkova AT, Tycko R, Meredith SC. Abeta40-Lactam(D23/K28) models a conformation highly favorable for nucleation of amyloid. (2004) *Biochemistry.* 44(16):6003-14.

[306] Reddy G, Straub JE, Thirumalai D. (2009) Influence of preformed Asp23-Lys28 salt bridge on the conformational fluctuations of monomers and dimers of Abeta peptides with implications for rates of fibril formation. *J Phys Chem B.* 113(4):1162-72.

[307] Nilsson MR. (2004) Techniques to study amyloid fibril formation in vitro. *Methods.* 34(1):151-60.

[308] Rangachari V, Moore BD, Reed DK, Sonoda LK, Bridges AW, Conboy E, Hartigan D, Rosenberry TL. (2007) Amyloid-beta(1-42) rapidly forms protofibrils and oligomers by distinct pathways in low concentrations of sodium dodecylsulfate. *Biochemistry.* 46(43): 12451-62.

[309] Bitan G, Kirkitadze MD, Lomakin A, Vollers SS, Benedek GB, Teplow DB. (2003) Amyloid beta -protein (Abeta) assembly: Abeta 40 and Abeta 42 oligomerize through distinct pathways. *Proc Natl Acad Sci U S A.* 100(1):330-5.

[310] Tjernberg LO, Callaway DJ, Tjernberg A, Hahne S, Lilliehöök C, Terenius L, Thyberg J, Nordstedt C. (1999) A molecular model of Alzheimer amyloid beta-peptide fibril formation. *J Biol Chem.* 274(18): 12619-25.

[311] Yu L, Edalji R, Harlan JE, Holzman TF, Lopez AP, Labkovsky B, Hillen H, Barghorn S, Ebert U, Richardson PL, Miesbauer L, Solomon L, Bartley D, Walter K, Johnson RW, Hajduk PJ, Olejniczak ET. (2009) Structural characterization of a soluble amyloid beta-peptide oligomer. *Biochemistry.* 48(9):1870-7.

.

[312] Bu Z, Shi Y, Callaway DJ, Tycko R. (2007) Molecular alignment within beta-sheets in Abeta(14-23) fibrils: solid-state NMR experiments and theoretical predictions. *Biophys J.* 92(2):594-602.

[313] Tjernberg LO, Tjernberg A, Bark N, Shi Y, Ruzsicska BP, Bu Z, Thyberg J, Callaway DJ. (2002) Assembling amyloid fibrils from designed structures containing a significant amyloid beta-peptide fragment. *Biochem J.* 366(Pt 1): 343-51

[314] Shi Y, Stouten PF, Pillalamarri N, Barile L, Rosal RV, Teichberg S, Bu Z, Callaway DJ. (2006) Quantitative determination of the topological propensities of amyloidogenic peptides. *Biophys Chem.* 120(1): 55-61.

[315] Cornell WD, Cieplak P, Bayly CI, Gould IR, Merz KM Jr, Ferguson DM, Spellmeyer DC, Fox T, Caldwell JW, Kollman PA (1995). A Second Generation Force Field for the Simulation of Proteins, Nucleic Acids, and Organic Molecules. *J. Am. Chem. Soc.* 117: 5179-5197.

[316] Jorgensen WL, Tirado-Rives J (1988). The OPLS Force Field for Proteins. Energy Minimizations for Crystals of Cyclic Peptides and Crambin. *J. Am. Chem. Soc.* 110: 1657-1666.

[317] Halgren, TA. (1996) Merck molecular force field. I. Basis, form, scope, parameterization, and performance of MMFF94. *J. Comp. Chem.* 17(5-6): 490-519

[318] Van Der Spoel D, Lindahl E, Hess B, Groenhof G, Mark AE, Berendsen HJ (2005). GROMACS: fast, flexible, and free. *J Comput Chem* 26 (16): 1701–18.

[319] Wojciechowski, M., Lesyng, B. (2004) Generalized Born Model: Analysis, Refinement and Applications to Proteins J*. Phys. Chem. B* 108: 18368–18376.

[320] Molecular Operating Environment, version 2004.03-2007.09. Chemical Computing Group Inc.: Montreal, PQ.

[321] Still, W. C.; Tempczyk, A.; Hawley, R. C.; Hendrickson, T. Semianalytical (1990) Treatment of Solvation for Molecular Mechanics and Dynamics. *J. Am. Chem. Soc.* 112: 6127-6129.

[322] Qiu, D, Shenkin, PS., Hollinger, FP, Still WC. (1997)The GB/SA Continuum Model for Solvation. A Fast Analytical Method for the Calculation of Approximate Born Radii. *J. Phys. Chem. A* 101: 3005-3114.

[323] Metropolis, N., Rosenbluth, A.W., Rosenbluth, M.N., Teller, A.H. (1953) Equation of State Calculations by Fast Computing Machines. *Journal of Chem. Phys.* 21, 1087-1092.

[324] Schmidt JM, Mercure J, Tremblay GB, Pagé M, Kalbakji A, Feher M, Dunn-Dufault R, Peter MG, Redden PR. (2003) De novo design, synthesis, and evaluation of novel nonsteroidal phenanthrene ligands for the estrogen receptor. *J Med Chem.* 46(8):1408-18.

[325] Williams CI, Feher M. (2008) The effect of numerical error on the reproducibility of molecular geometry optimizations.*J Comput Aided Mol Des.* 22(1):39-51.

[326] Sciarretta KL, Gordon DJ, Meredith SC. (2006) Peptide-based inhibitors of amyloid assembly. *Methods Enzymol.* 413:273-312.

[327] Porat Y, Mazor Y, Efrat S, Gazit E. (2004) Inhibition of islet amyloid polypeptide fibril formation: a potential role for heteroaromatic interactions. *Biochemistry.* 43(45):14454-62.

[328] Ma B, Nussinov R. (2007) Trp/Met/Phe hot spots in protein-protein interactions: potential targets in drug design. *Curr Top Med Chem.* 7(10):999-1005.

[329] Vedani A, Dobler M, Lill MA. (2006) The challenge of predicting drug toxicity in silico. *Basic Clin Pharmacol Toxicol.* 99(3):195-208.

[330] Alavijeh MS, Palmer AM. (2004) The pivotal role of drug metabolism and pharmacokinetics in the discovery and development of new medicines. *IDrugs.* 7(8):755-63

[331] Kazmierski WM. (1999) *Peptidomimetic protocols: Methods in Molecular Medicine.* Volume 23, Humana: Totowa, NJ (ISBN-13: 9780896035171).

[332] Abel A. (1999) *Advances in Amino Acid Mimetics and Peptidomimetics.* JAI: Stamford, Vol. 2. (ISBN 13: 9780762306145)

[333] Witkowska E, Orowska A, Sagan B, Smoluch M, Izdebski J (2001) Tryptic hydrolysis of hGH-RH(1-29)-NH2 analogues containing Lys or Orn in positions 12 and 21. *J. Pep. Sci.* 7(3): 166 – 172

[334] Allen MC, wade R (1988) Synthesis of somatostatin analogs resistant to the action of trypsin. *Int. J. Pep. Pro.Res.* 32(2): 89-97

[335] Parham P. (2005) Putting a face to MHC restriction. *J Immunol.* 174(1):3-5.

[336] Sela M, Zisman E. (1997) Different roles of D-amino acids in immune phenomena. *FASEB J.* 11(6):449-56.

[337] Kim SI, Yi JS, Ko YG. (2006) Amyloid beta oligomerization is induced by brain lipid rafts. *J Cell Biochem.* 99(3):878-89

[338] Banks WA (2008) Delivery of peptides to the brain: emphasis on therapeutic development. *Biopolymers.* 90(5):589-94.

[339] Girardin F. (2006) Membrane transporter proteins: a challenge for CNS drug development. *Dialogues Clin Neurosci.* 8(3):311-21.

[340] Mora AL, Tam JP. (1998) Controlled lipidation and encapsulation of peptides as a useful approach to mucosal immunizations. *J Immunol.* 161(7):3616-23.

[341] Pakalns T, Haverstick KL, Fields GB, McCarthy JB, Mooradian DL, Tirrell M. (1999)

Cellular recognition of synthetic peptide amphiphiles in self-assembled monolayer films. *Biomaterials.* 20(23-24):2265-79.

[342] Stickney JT, Booden MA, Buss JE. (2001) Targeting proteins to membranes, using signal sequences for lipid modifications. *Methods Enzymol.* 332:64-77.

[343] Wang TY, Leventis R, Silvius JR. (2001) Partitioning of lipidated peptide sequences into liquid-ordered lipid domains in model and biological membranes. *Biochemistry.* 40(43):13031-40.

[344] Rijkers DT, den Hartog JA, Liskamp RM. (2004) Synthesis and biological activity of N-terminal lipidated and/or fluorescently labeled conjugates of astressin as corticotropin releasing factor antagonists. *Bioorg Med Chem.* 12(19):5099-106.

[345] Hamilton JA, Brunaldi K. (2007) A model for fatty acid transport into the brain. *J Mol Neurosci.* 33(1):12-7

[346] Edmond J. (2001) Essential polyunsaturated fatty acids and the barrier to the brain: the components of a model for transport. *J Mol Neurosci.* 16(2-3):181-93

[347] Ouellet M, Emond V, Chen CT, Julien C, Bourasset F, Oddo S, Laferla F, Bazinet RP, Calon F. (2009) Diffusion of docosahexaenoic and eicosapentaenoic acids through the blood-brain barrier: An in situ cerebral perfusion study. *Neurochem Int.* 2009 May 12. [Epub]

[348] Petkova AT, Buntkowsky G, Dyda F, Leapman RD, Yau WM, Tycko R. (2004) Solid state NMR reveals a pH-dependent antiparallel beta-sheet registry in fibrils formed by a beta-amyloid peptide. *J Mol Biol.* 335(1):247-60.

[349] Yu L, Edalji R, Harlan JE, Holzman TF, Lopez AP, Labkovsky B, Hillen H, Barghorn S, Ebert U, Richardson PL, Miesbauer L, Solomon L, Bartley D, Walter K, Johnson RW, Hajduk PJ, Olejniczak ET. (2009) Structural characterization of a soluble amyloid beta-peptide oligomer. *Biochemistry.* 48(9):1870-7.

[350] Petkova AT, Yau WM, Tycko R. (2006) Experimental constraints on quaternary structure in Alzheimer's beta-amyloid fibrils. *Biochemistry.* 45(2):498-512.

[351] Fischer PM. (2003) The design, synthesis and application of stereochemical and directional peptide isomers: a critical review. *Curr Protein Pept Sci.* 4(5):339-56.

[352] Knowles SE, Ballard FJ.(1978) Effects of amino acid analogues on protein synthesis and degradation in isolated cells. *Br J Nutr.* 40(2):275-87.

[353] LeVine H 3rd. (1993) Thioflavine T interaction with synthetic Alzheimer's disease beta-amyloid peptides: detection of amyloid aggregation in solution. *Protein Sci.* 2(3):404-10.

[354] Sian AK, Frears ER, El-Agnaf OM, Patel BP, Manca MF, Siligardi G, Hussain R, Austen BM. (2000) Oligomerization of beta-amyloid of the Alzheimer's and the Dutch-cerebral-haemorrhage types. *Biochem J.* 349(Pt 1):299-308.

[355] Soto C, Castaño EM, Kumar RA, Beavis RC, Frangione B. (1995) Fibrillogenesis of synthetic amyloid-beta peptides is dependent on their initial secondary structure. *Neurosci Lett.* 200(2):105-8.

[356] Bozsó1 Z, Tóth1 G, Murphy1 R, Lovas S. (2000) Difficulties in coupling to conformationally constrained aromatic amino acids. *Int. J. Pep. Res. Therapeutics.* 7(3). 157-163

[357] Zagorski MG, Yang J, Shao H, Ma K, Zeng H, Hong A. (1999) Methodological and chemical factors affecting amyloid beta peptide amyloidogenicity. *Methods Enzymol.* 309:189-204

[358] Findeis MA, Musso GM, Arico-Muendel CC, Benjamin HW, Hundal AM, Lee JJ, Chin J, Kelley M, Wakefield J, Haywa (1999) Modified-peptide inhibitors of amyloid beta-peptide polymerization. *Biochemistry.* 38(21):6791-800.

[359] Findeis MA. (2000) Approaches to discovery and characterization of inhibitors of amyloid beta-peptide polymerization. *Biochim Biophys Acta.* 1502(1):76-84.

[360] Pirttila T, Kim KS, Mehta PD, Frey H, Wisniewski HM. (1994) Soluble amyloid beta-protein in the cerebrospinal fluid from patients with Alzheimer's disease, vascular dementia and controls. *J Neurol Sci.* 127(1):90-5.

[361] Kelly SM, Jess TJ, Price NC. (2005) How to study proteins by circular dichroism. *Biochim Biophys Acta.* 10;1751(2):119-39.

[362] Barrow CJ, Zagorski MG. (1991) Solution structures of beta peptide and its constituent fragments: relation to amyloid deposition. *Science.* 253(5016):179-82.

[363] Otvos L Jr, Szendrei GI, Lee VM, Mantsch HH. (1993) Human and rodent Alzheimer beta-amyloid peptides acquire distinct conformations in membrane-mimicking solvents. *Eur J Biochem.* 211(1-2):249-57.

[364] Nichols MR, Moss MA, Reed DK, Cratic-McDaniel S, Hoh JH, Rosenberry TL. (2005) Amyloid-beta protofibrils differ from amyloid-beta aggregates induced in dilute hexafluoroisopropanol in stability and morphology. *J Biol Chem.* 280(4):2471-80.

[365] Provencher, S.W. and Glockner, J. (1981) Estimation of globular protein secondary structure from circular dichroism. *Biochemistry* 20, 33-37.

[366] Whitmore, L. and Wallace, B.A. (2008) Protein Secondary Structure Analyses from Circular Dichroism Spectroscopy: Methods and Reference Databases. *Biopolymers* 89, 392-400.

[367] Ferrão-Gonzales AD, Robbs BK, Moreau VH, Ferreira A, Juliano L, Valente AP, Almeida FC, Silva JL, Foguel D. (2005) Controlling {beta}-amyloid oligomerization by the use of naphthalene sulfonates: trapping low molecular weight oligomeric species. *J Biol Chem.* 280(41):34747-54.

[368] Gordon DJ, Tappe R, Meredith SC. (2002) Design and characterization of a membrane permeable N-methyl amino acid-containing peptide that inhibits Abeta1-40 fibrillogenesis. *J Pept Res.* 60(1):37-55.

[369]Aisenbrey C, Borowik T, Byström R, Bokvist M, Lindström F, Misiak H, Sani MA, Gröbner G. (2008) How is protein aggregation in amyloidogenic diseases modulated by biological membranes? *Eur Biophys J.* 37(3):247-55.

[370] Esposito C., Colicchio P., Facchiano A., Ragone R. (1998) Effect of a weak electrolyte on the critical micellar concentration of sodium dodecyl sulfate. *Journal of Colloid and Interface Science.* 200 (2), 310-312

[371] Sureshbabu N, Kirubagaran R, Jayakumar R. (2009) Surfactant-induced conformational transition of amyloid beta-peptide. *Eur Biophys J.* 38(4):355-67.

[372] Wahlström A, Hugonin L, Perálvarez-Marín A, Jarvet J, Gräslund A. (2008) Secondary structure conversions of Alzheimer's Abeta(1-40) peptide induced by membrane-mimicking detergents. *FEBS J.* 275(20):5117-28.

[373] Johnson SR (2008) The Trouble with QSAR (or How I Learned To Stop Worrying and Embrace Fallacy) J. *Chem. Inf. Model.* 48 (1), pp 25–26

[374] Shearman MS, Ragan CI, Iversen LL. (1994) Inhibition of PC12 cell redox activity is a specific, early indicator of the mechanism of beta-amyloid-mediated cell death. *PNAS.* 91(4):1470-4.

[375] L A Greene and A S Tischler (1976) Establishment of a noradrenergic clonal line of rat adrenal pheochromocytoma cells which respond to nerve growth factor. *PNAS.* 73(7): 2424–2428.

[376] Hong HS, Maezawa I, Yao N, Xu B, Diaz-Avalos R, Rana S, Hua DH, Cheng RH, Lam KS, Jin LW. (2007) Combining the rapid MTT formazan exocytosis assay and the MC65 protection assay led to the discovery of carbazole analogs as small molecule inhibitors of Abeta oligomer-induced cytotoxicity. *Brain Res.* 1130(1):223-34.

[377] Qin XY, Cheng Y, Cui J, Zhang Y, Yu LC. (2009) Potential protection of curcumin against amyloid beta-induced toxicity on cultured rat prefrontal cortical neurons. *Neurosci Lett.* 463(2):158-61.

[378] Arendash GW, Su GC, Crawford FC, Bjugstad KB, Mullan M. (1999) Intravascular beta-amyloid infusion increases blood pressure: implications for a vasoactive role of beta-amyloid in the pathogenesis of Alzheimer's disease. *Neurosci Lett.* 268(1):17-20.

[379] Matharu B, Gibson G, Parsons R, Huckerby TN, Moore SA, Cooper LJ, Millichamp R, Allsop D, Austen B. (2009) Galantamine inhibits beta-amyloid aggregation and cytotoxicity. *J Neurol Sci.* 280(1-2):49-58.

[380] Paris D, Town T, Parker TA, Humphrey J, Mullan M. (1998) Isoform-specific vasoconstriction induced by apolipoprotein E and modulation of this effect by Alzheimer's beta-amyloid peptide. *Neurosci Lett.* 256(2):73-6.

[381] Luo F, Seifert TR, Edalji R, Loebbert RW, Hradil VP, Harlan J, Schmidt M, Nimmrich V, Cox BF, Fox GB. (2008) Non-invasive characterization of beta-amyloid(1-40) vasoactivity by functional magnetic resonance imaging in mice. *Neuroscience.* 155(1):263-9.

[382] Shin HK, Jones PB, Garcia-Alloza M, Borrelli L, Greenberg SM, Bacskai BJ, Frosch MP, Hyman BT, Moskowitz MA, Ayata C. (2007) Age-dependent cerebrovascular dysfunction in a transgenic mouse model of cerebral amyloid angiopathy. *Brain.* 130(Pt 9):2310-9.

[383] Roberts SA. (2003) Drug metabolism and pharmacokinetics in drug discovery. *Curr Opin Drug Discov Devel.* 6(1):66-80.

[384] Houston JB, Galetin A. (2008) Methods for predicting in vivo pharmacokinetics using data from in vitro assays. *Curr Drug Metab.* 9(9):940-51.

[385] Tsaioun K, Bottlaender M, Mabondzo A; Alzheimer's Drug Discovery Foundation. (2009) ADDME--Avoiding Drug Development Mistakes Early: central nervous system drug discovery perspective. *BMC Neurol.* 9 Suppl 1:S1.

[386] Abbott NJ, Dolman DE, Patabendige AK. (2008) Assays to predict drug permeation across the blood-brain barrier, and distribution to brain. *Curr Drug Metab.* 9(9):901-10.

[387] Nicolazzo JA, Charman SA, Charman WN. (2006) Methods to assess drug permeability across the blood-brain barrier. *J Pharm Pharmacol.* 58(3):281-93.

[388] Harkany T, Hortobágyi T, Sasvári M, Kónya C, Penke B, Luiten PG, Nyakas C. (1999) Neuroprotective approaches in experimental models of beta-amyloid neurotoxicity: relevance to Alzheimer's disease. *Prog Neuropsychopharmacol Biol Psychiatry.* 23(6):963-1008.

[389] Sigurdsson EM, Permanne B, Soto C, Wisniewski T, Frangione B. (2000) In vivo reversal of amyloid-beta lesions in rat brain. *J Neuropathol Exp Neurol.* 59(1):11-7

[390] Zhong SZ, Ge QH, Li Q, Qu R, Ma SP. (2009) Peoniflorin attentuates Abeta((1-42))-mediated neurotoxicity by regulating calcium homeostasis and ameliorating oxidative stress in hippocampus of rats. *J Neurol Sci.* 280(1-2):71-8.

APPENDIX A

The following is a description of the protocols used to dock and score peptidic ligands to β amyloid, as previously mentioned in Chapter 3 and 4.

Docking peptidic ligands to β amyloid is performed in three stages. The first stage of ligand docking utilizes a MOE script called ‘dock.svl’. The next two stages of ligand docking utilize a script called ‘analysis.dock.svl’. Text files with the source code of both scripts are included in the attached CD.

The second script, ‘analysis_dock.svl’, is also used to score docked ligands and its use for that purpose is also described towards the end this Appendix.

To use the script ‘dock.svl’:

1. Open a fresh instance of an interactive mode of MOE or use *File>Close* to remove all molecules in the workspace.

2. Open previously created receptor and ligand files. Check if their atoms have correct partial charges or use *Compute>Partial* Charges to recalculate them. Set a Current Working Directory (*CWD*)

3. Select the ligand chain through the ‘Sequence Editor’ interface in MOE and use *Selection> Atoms> Of Selected Chains* to confirm selection.

4. Press *Shift+Alt* keys and use the middle button/ wheel of your mouse to move the ligand relative to the receptor.

5. Position the ligand next to receptor such that it is close to the expected final docked position. Use *Render>Draw>Hydrogen Bonds* and *VDV Contacts* to make sure that the ligand forms a few backbone hydrogen

bonds with the receptor. The VDV Contacts map should allow the user to simultaneously position the ligand such that there is minimum clash between sidechains of the receptor and ligand. Sidechain clashes can be eliminated by changing the dihedral angles around α and β carbon in the affected residues, by using the *Edit>Build>Molecule* interface.

6. Check state of solvation by using the *Window>Potential Setup* menu. For the first stage of ligand docking, *Solvation* is set as *Born.* Fix Hydrogens and Charges if required.

7. Use the *File>New>Text Editor* interface to search and load 'dock.svl'.

8. In the GUI generated by the 'save and load' command, change the generic output database file name to a more suitable one. Turn *Open Database Viewer* - ON and *Random Start* and *Use Potential Grids* – OFF. Select *Simulated Annealing* as the method of choice. *Total Runs* can be kept at the default number of 25 or increased to 100.

9. Use the *Docking Box* button to access another submenu for positioning the docking box such that it encompasses the ligand and the relevant part of the receptor. Please make sure that the box size is appropriate and gives a fairly tight fit for the complex without cutting out any part of the ligand or relevant parts of the receptor.

10. Start the docking calculation. One series of docking calculations takes about 4-24 hours depending upon the size of the ligand and number of runs used.

The output of the first stage of docking should be a *.mdb format database with a list of the best ligand poses from each of the specified number of runs.

The next two stages of ligand docking involve the use of the versatile multifunctional script known as ‘analysis_dock.svl’.

To use the script, ‘analysis_dock.svl’, for the second part of the ligand docking process:

1. Open a fresh instance of an interactive mode of MOE or use *File>Close* to remove all molecules in the workspace.

2. Open previously created receptor and docked ligand database files. Check if ligand atoms have correct partial charges or use *Compute>Partial* Charges to recalculate them. Set a Current Working Directory (*CWD*)

3. Check state of solvation by using the *Window>Potential Setup* menu. For the second (and third stage) of ligand docking, *Solvation* is set as *Distance.* Fix Hydrogens and Charges if required.

4. Use the *File>New>Text Editor* interface to search and load ‘analysis.svl’

5. Make sure that script recognizes the correct database as the one to operate on.

6. The script’s GUI is modular, consisting of menus and corresponding action buttons.

7. Check and set *Molecular Fieldname* from the dropdown menu. Set *Energy Calculation* as *binding energy using local minimum*. The *Optimization Options* are set as *optimize hydrogen and ligand*. The *Save Structure* option is set to *ligand*.

8. *Conf. Search Iterations* is set at *10,000*, as is *Number of Failures*. *Number of MM steps* is set at *5,000*. *Solvation* is turned OFF. Force Field should be set at MMFF94x.

9. Start the Energy Calculations with the *Energy* button at the bottom of the script invoked GUI.

The third stage of the ligand docking process is identical to the second except the following differences.

1. Change the names of the new database fields created by the second stage such that the field ‘dock’ is renamed as field ‘dock_mol_01’. This step will prevent the script from overwriting previous outputs.

2. Apply the following changes to Step 7 from the second stage:
   Check and set *Molecular Fieldname* to the new one (dock_mol_01).
   The *Optimization Options* are now set as *optimize pocket with protocol*.
   The *Save Structure* option is set to *ligand and receptor*.

3. The rest remains unchanged from the second stage.

4. Once again, start the Energy Calculations with the *Energy* button at the bottom of the script invoked GUI.

The next stage of the ligand docking process involves scoring the docked and optimized ligand poses.

1. Open database created by the third stage of the docking process and rename the newly created fields to prevent accidental overwriting.

2. Calculate E_bind_normalized by multiplying the E_bind_app field created by stage 3 by –0.05. The result is the normalized binding energy component ‘B’ used in the BHB function, described in Chapter 3.

3. Hydrogen Bonds can either be calculated using the last module of the ‘analysis_dock’ invoked GUI, or can be filled in after visual observation (make sure hydrogen bond display is turned on). For a small number of ligand poses visual observation is preferred to automated scripts. Each hydrogen bond (salt bridge) between charged residues is assigned a value of 5 if present and 0 if absent. The combined values for each ligand pose are the ‘H‘component of BHB. It is necessary to perform this operation only on the most energetically favorable pose, and those within 1 kcal/mol of that value.

4. Buriedness is the third component of the BHB score. It can be calculated through a series of steps that start with creation of new and separate database field to accommodate receptor and the ligand obtained from the energetically most favored docking pose or within 1 kcal/mol of the top pose.

5. The receptor is then loaded into a clean MOE workspace. The *Sequence Editor* is used to select all atoms of the hydrophobic residues, LVFF in this case.

6. Each ligand pose to be evaluated in individually selected in the database viewer, and GUI of the script is used to set *Selected Entries Only*.

7. *Receptor Buriedness*, *Ligand Buriedness* and *Hydrophobic Contact Surface* are turned ON. Receptor Buriedness is set *from selected receptor atoms*. The *Surfaces* button on the Script GUI is used to initiate the

calculation. The process is repeated for each selected pose of the ligand receptor complex. Buriedness (RB) is used in BHB as $20*(RB+RB^3)$.

APPENDIX B

Peptide = R1

Sequence = Ac-HHQKLVFFAED-NH_2

Number of Amino Acids = 11

Molecular Weight = 1411.58 (average); 1410.70 (monoisotopic)

Purity by analytical HPLC = approx. 97% (single peak)

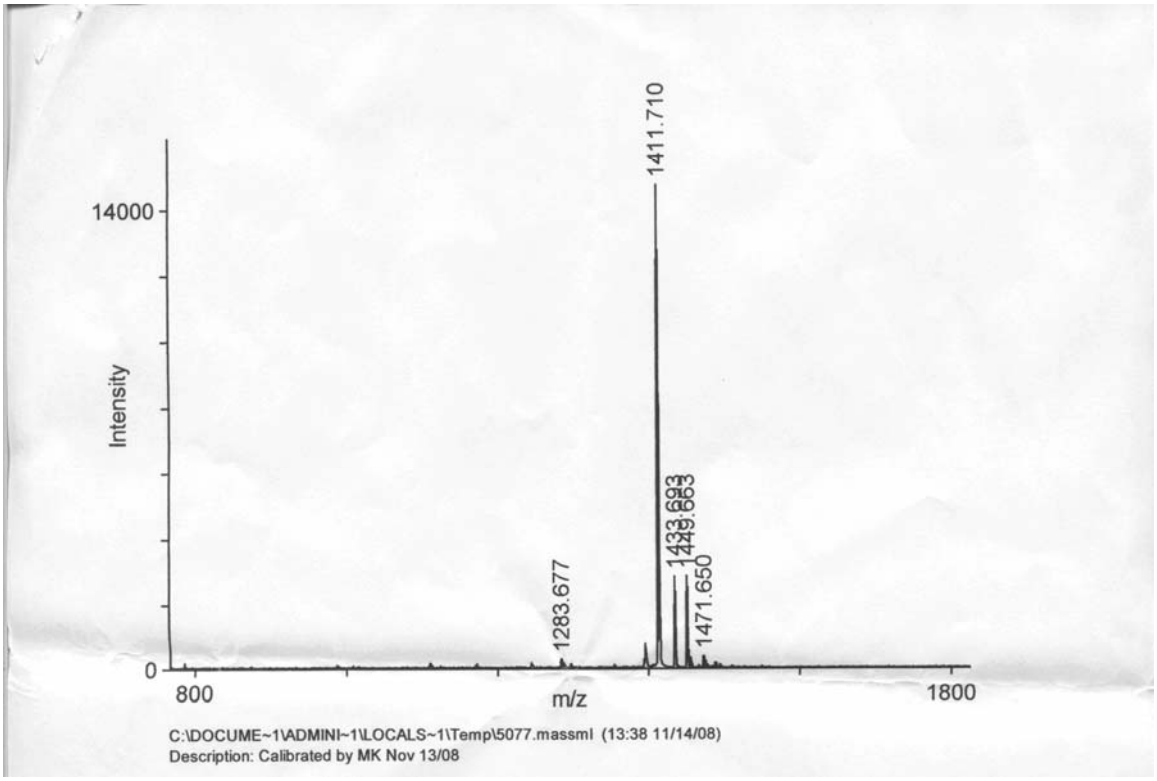

MALDI-TOF Spectra of R1

R1 + H^+ = 1411.70 (calculated); 1411.71 (measured).

R1 + Na^+ = 1433.68 (calculated); 1433.69 (measured).

R1 + K^+ = 1449.80 (calculated); 1449.66 (measured).

Peptide = SG1

Sequence = Ac-dab-O-(me)L-F-(me)F-L-P-bA-COOH

Number of Amino Acids = 8

Molecular Weight = 991.24 (average); 990.59 (monoisotopic)

Purity by analytical HPLC = approx. 95% (single peak)

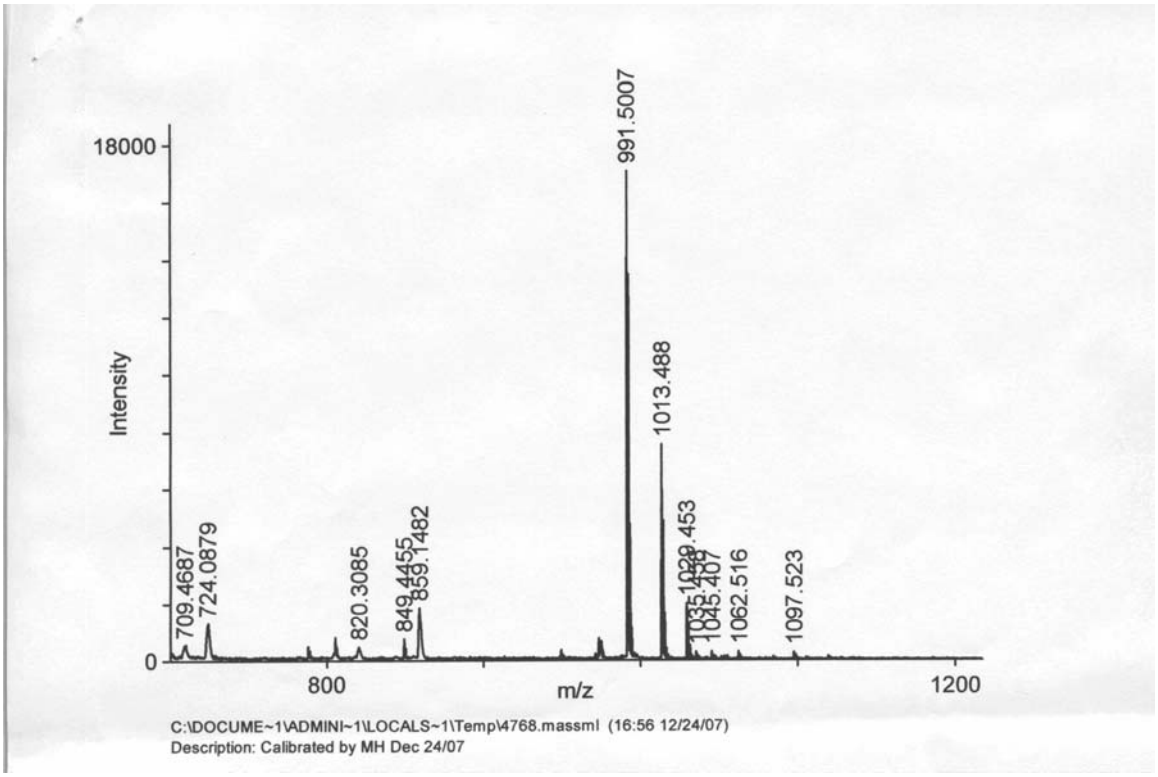

MALDI-TOF Spectra of SG1

SG1 + H^+ = 991.60 (calculated); 991.50 (measured).

SG1 + Na^+ = 1013.57 (calculated); 1013.49 (measured).

SG1 + K^+ = 1029.59 (calculated); 1029.45 (measured).

Peptide = SG2

Sequence = Ac-dab-O-(me)L-V-(me)F-F-A-E-NH_2

Number of Amino Acids = 8

Molecular Weight = 1008.23 (average); 1007.58 (monoisotopic)

Purity by analytical HPLC = approx. 95% (single peak)

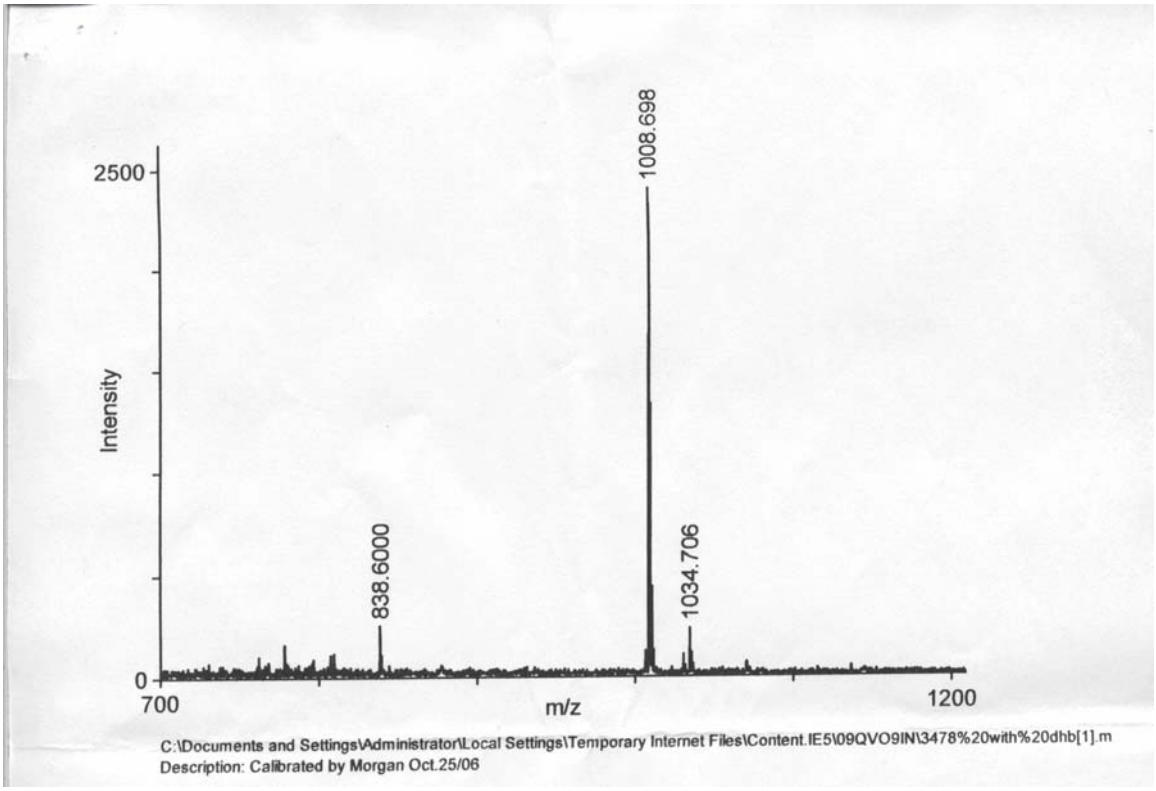

MALDI-TOF Spectra of SG2

SG2 + H^+ = 1008.59 (calculated); 1008.70 (measured).

The identity of the minor impurity at 1034.70 is unknown.